AD A135 466 NAVY TACTICAL APPLICATIONS GUIDE OPERATIONAL ENVIRONMENTAL SATELLITES POL..(U) BOHAN (WALTER A) CO PARK RIDGE IL R W FETT ET AL. JUN 83 NEPRF-TR-83-02 1/2

UNCLASSIFIED N00228-82-C-6222 F/G 22/2 NL

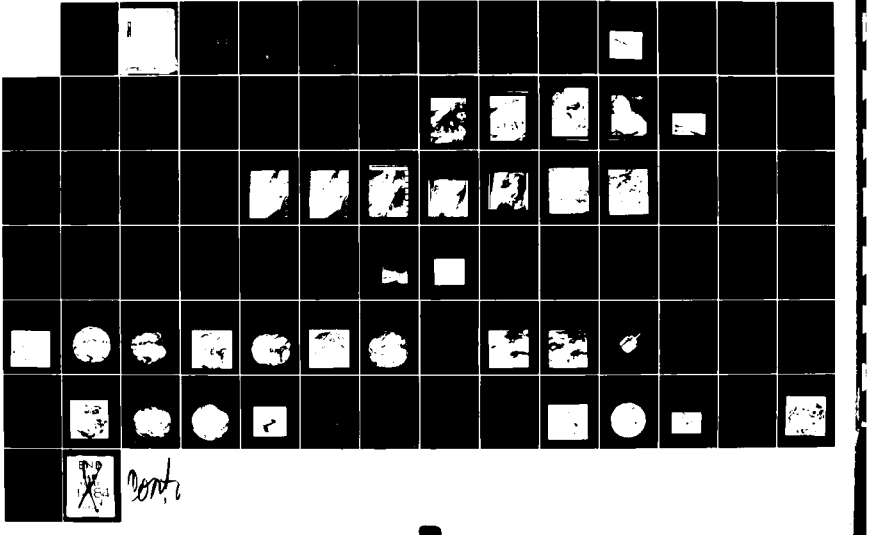

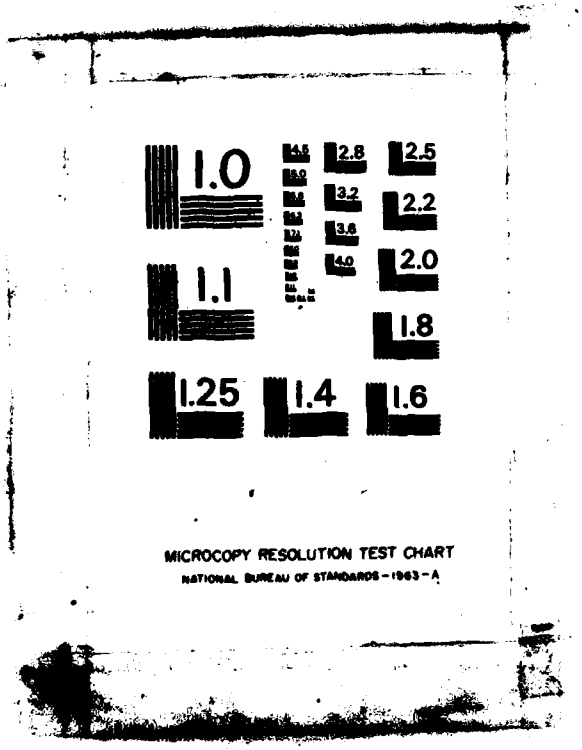
1.0
1.1
1.25
1.4
1.6
2.8
3.2
3.6
4.0
2.5
2.2
2.0
1.8
MICROCOPY RESOLUTION TEST CHART
NATIONAL BUREAU OF STANDARDS - 1963 - A

UNCLASSIFIED

SECURITY CLASSIFICATION OF THIS PAGE (When Data Entered)

REPORT DOCUMENTATION PAGE	READ INSTRUCTIONS BEFORE COMPLETING FORM
1. REPORT NUMBER: NAVENVPREDRSCHFAC Technical Report 83-02	2. GOVT ACCESSION NO.: AD-A135 466
	3. RECIPIENT'S CATALOG NUMBER
4. TITLE (and Subtitle): Navy Tactical Applications Guide Operational Environmental Satellites	5. TYPE OF REPORT & PERIOD COVERED
	6. PERFORMING ORG. REPORT NUMBER
7. AUTHOR(s): Robert W. Fett, Walter A. Bohan, John J. Bates, Sherree L. Tipton	8. CONTRACT OR GRANT NUMBER(s): The Walter A. Bohan Company N00228-82-C-6222
9. PERFORMING ORGANIZATION NAME AND ADDRESS: The Walter A. Bohan Company 2026 Oakton Street Park Ridge, IL 60068	10. PROGRAM ELEMENT, PROJECT, TASK AREA & WORK UNIT NUMBERS: 62759N. WF 59-553. NEPRF WU: 6.3-18
11. CONTROLLING OFFICE NAME AND ADDRESS: Naval Air Systems Command Department of the Navy Washington, D.C. 20361	12. REPORT DATE: June 1983
	13. NUMBER OF PAGES: 70
14. MONITORING AGENCY NAME & ADDRESS(if different from Controlling Office): Naval Environmental Prediction Research Facility Monterey, California 93940	15. SECURITY CLASS. (of this report): Unclassified
	15a. DECLASSIFICATION/DOWNGRADING SCHEDULE
16. DISTRIBUTION STATEMENT (of this Report): Approved for Public Release Distribution Unlimited	DTIC ELECTE DEC 7 1983 B
17. DISTRIBUTION STATEMENT (of the abstract entered in Block 20, if different from Report)	
18. SUPPLEMENTARY NOTES	
19. KEY WORDS (Continue on reverse side if necessary and identify by block number): Meteorological Satellite Systems; Defense Meteorological Satellite Program (DMSP); National Oceanic and Atmospheric Administration (NOAA) satellites; Geostationary satellites; Polar-orbiting satellites; METEOSAT, GOES, GMS, INSAT, and Meteor, and GOMS satellites	
20. ABSTRACT (Continue on reverse side if necessary and identify by block number): This volume contains user oriented sections on current operational satellite systems that describe imagery acquisition and distribution, sensor systems, and spectral characteristics. In addition, sample imagery is included for each of the meteorological satellite systems.	

DD FORM 1 JAN 73 1473 EDITION OF 1 NOV 65 IS OBSOLETE S/N 0102-014-6601

UNCLASSIFIED

SECURITY CLASSIFICATION OF THIS PAGE (When Data Entered)

NAVY TACTICAL APPLICATIONS GUIDE

OPERATIONAL ENVIRONMENTAL SATELLITES

POLAR-ORBITING SATELLITES
GEOSTATIONARY SATELLITES

SPACECRAFT - SENSORS - IMAGERY

Prepared under the direction of
Robert W. Fett
Tactical Applications Department
Naval Environmental Prediction Research Facility

Scientific Coordinator
Walter A. Bohan
The Walter A. Bohan Company

1983

THE WALTER A. BOHAN COMPANY
2086 OAKTON STREET, PARK RIDGE, ILLINOIS 60068
APPLIED RESEARCH IN SATELLITE METEOROLOGY AND OCEANOGRAPHY

Foreword

This volume on Operational Environmental Satellites has been developed as an update to and an expansion of material originally printed in Section 1 of Navy Tactical Applications Guide, Volume 3, "North Atlantic and Mediterranean Weather Analysis and Forecast Applications." The volume provides an extensive discussion pertaining to operational satellite systems including U.S. and foreign satellites. The material is intended to provide a background of primary interest to the operational meteorologist as opposed to the engineering or electronic specialist. Topics of major concern are the satellite description, orbital characteristics, data acquisition system, sensor system description, spectral characteristics, and examples of typical visible, infrared, and water vapor data.

Comments on the usefulness of this volume or suggestions for further additions are solicited to insure user needs for such information are fully addressed.

Kenneth L. Van Sickle

KENNETH VAN SICKLE
Captain, U.S. Navy
Commanding Officer, NEPRF

Acknowledgements

The assistance of AG1 Rudy Schaar, AG2 Michael Dodge, AG2 Darryl Wagoner, AG3 Robert Bonaly, AG3 John Benvick, and AG3 Brian Kenthack in developing the documentation for many of the case studies in this volume is gratefully acknowledged. PH1 Albert Matthews processed many of the original photographs used in this publication. The correlative meteorological and oceanographic data used in the case studies were provided by the Fleet Numerical Oceanography Center, Monterey, CA, and the U.S. Naval Oceanographic Command Detachment, Asheville, NC. Appreciation is also extended to the personnel of the DMSP sites at Rota, Spain and San Diego, CA; and aboard the aircraft carriers USS *Constellation*, USS *Kitty Hawk*, USS *John F. Kennedy*, USS *Enterprise*, USS *Independence*, and USS *Midway*.

Additional satellite imagery was supplied by the National Earth Satellite, Data, and Information Service (NESDIS) of the National Oceanic and Atmospheric Administration (NOAA), the European Space Agency (ESA), and the Japan Weather Association (JWA).

The assistance of the staff of The Walter A. Bohan Company is acknowledged; in particular, Lido A. Andreoni for design of the format of the publication and layouts of the case studies. Gregory E. Terhune for his assistance in the preparation of case study graphics and participation in the editing and formatting of the text. The high quality of the reproduction of the satellite imagery used in the case studies and the excellent printing of the publication are due to the combined efforts of Peter M. Samorez and Michael E. Brock.

Contents

Introduction

Technical information concerning the orbital characteristics, means of data acquisition, sensor characteristics, spectral response, etc., of various satellite systems is of great interest to the satellite meteorologist and is important for image interpretation. Most of this type of information appears in a variety of reports, often not particularly well designed for the professional meteorologist. The Navy meteorologist, especially, needs information on a variety of foreign as well as domestic satellite systems, as the region of operations shifts on a global basis.

This volume has been designed to fill that need and will be periodically updated as time passes and satellite systems, sensors and data types evolve.

Section 1

Polar-orbiting Satellites

Sun-synchronous Polar-orbiting Satellites

Both the DMSP and TIROS-N/NOAA satellites are launched with an inclination such that the orbit is sun-synchronous. This means that the orbital plane of the satellite precesses 360° in 365 days. Precession of the orbital plane at this rate keeps it always in the same orientation with respect to the sun, day to day and revolution to revolution. Thus, an individual satellite may be termed to be in a morning, noon, or afternoon orbit (pass) depending on this orientation.

The combination of precession of the orbital plane and the rotation of the Earth produces an apparent westward motion of the satellite subtracks on the Earth (1-1a). At a near-circular orbital altitude of 835 km, these satellites have an orbital period of about 102 minutes. Subtracting the orbital precession, the longitude of the ascending node increases about 25° per revolution. Since the orbital period is about 102 minutes, there are 14 revolutions in approximately 24 hours. This means that the first revolution occurs about five degrees further east each day.

The U.S.S.R. is the only other government maintaining polar-orbiting satellites. Meteor 1 (experimental series) is in a low, sun-synchronous orbit with an inclination angle of about 97°. The orbital period for satellites in this series is about 98 minutes. Meteor 2 (operational series) has an orbit that is not sun-synchronous. This series of satellites has an inclination angle of 81°. Meteor 2 satellites orbit at an altitude of 900 km, with an orbital period of approximately 102 minutes which produces 14 revolutions per day (similar to TIROS-N).

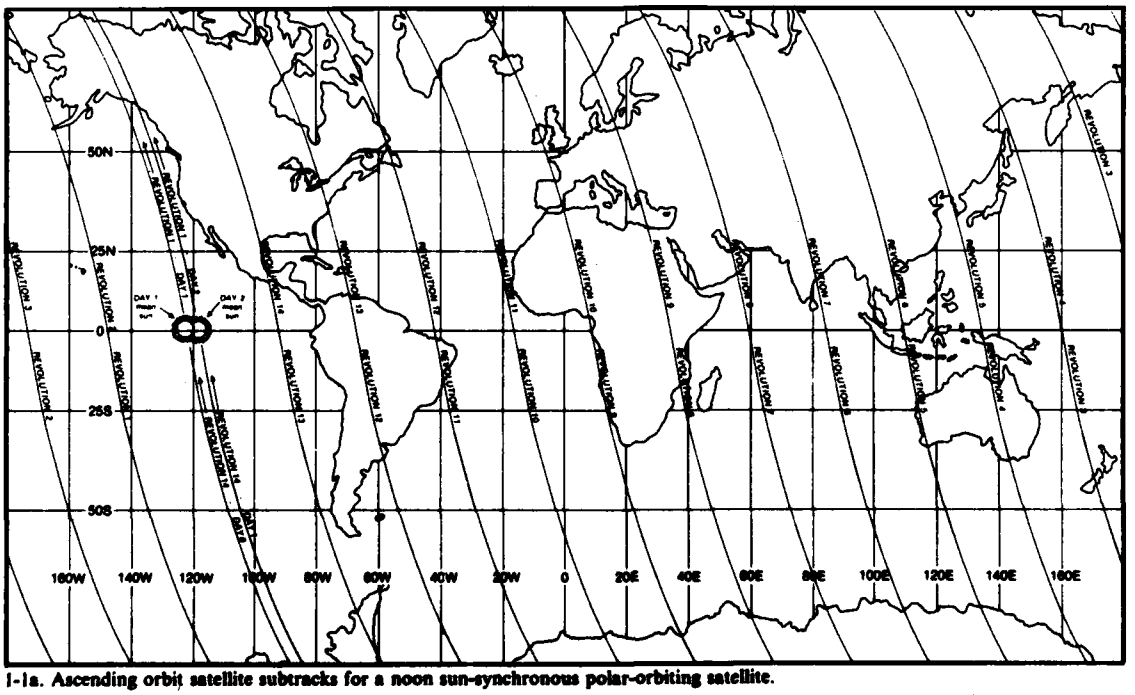

1-1a. Ascending orbit satellite subtracks for a noon sun-synchronous polar-orbiting satellite.

Defense Meteorological Satellite Program
(DMSP)

The Block 5D-2 satellite is the second generation polar-orbiting satellite developed to support operations of the Department of Defense (DOD). The spacecraft is in a near-polar, sun-synchronous orbit at an altitude of approximately 835 km (450 n mi). The orbital period is 101.4 minutes which produces 14.2 orbits per day. The operational system includes two satellites; one in a morning orbit (0730 LST descending node), and one in a noon orbit (1200 LST ascending node).

Presently, the only operational satellites are F-3 (Block 5D-1) and F-6 (Block 5D-2): refer to Table 2 (1A-9). It should be noted that on 20 December 1982, the United States initiated the Block 5D-2 program with the launch of the F-6 satellite. This section describes some aspects of the Block 5D-2 spacecraft pertinent to the image data received by direct read-out tactical sites throughout the world.

1A-1a. The Block 5D satellite is an integrated spacecraft in that the launch vehicle upper stage remains attached to and provides support for the satellite in orbit. The satellite itself is a five-sided box-like structure (the prototype for TIROS-N) in which four of the five sides are equal in size and contain thermal control louvers, while the fifth side is wider and contains the Earth-viewing sensors. A large solar power panel is attached to one end of the spacecraft; it rotates once each orbit so that it is always oriented toward the sun during the daylight portions of the orbit.

Image Acquisition

The Operational Linescan System (OLS) is the primary image acquisition system on the DMSP Block 5D-2 spacecraft. The system is designed to gather data in the visible (L-data) and infrared (T-data) spectral channels from Earth scenes, and to transmit such data in real-time or to store multi-orbit data for later transmission to a central receiving facility. The OLS data processing subsystem performs command, control, data manipulation, storage, and management functions. Commands are received from the ground through the spacecraft communications system, stored, and processed according to time codes. The OLS executes commands, accomplishes smoothing of fine resolution data, derives gain commands from orbital parameters for normalization of visible data and dynamic signal control, and outputs the data to the spacecraft communications system. All data are processed, stored and transmitted in encrypted (direct readout) or clear (stored) digital form.

Three S-band transmitters are provided on the Block 5D-2 spacecraft for data transmission. Two of these may be operated simultaneously for stored data playback. The third is used for real-time data transmission to direct readout tactical sites. A combination of one channel fine (F) resolution data (0.3 n mi resolution) and the complimentary smoothed (S) resolution data (1.5 n mi resolution) are provided in the real-time data transmission mode.

The stored data may consist of either fine resolution or smoothed resolution data. Tape recorder capacity and transmission constraints limit the quantity of fine resolution data which can be stored to a total of 40 minutes per central ground station readout. Data smoothing permits global coverage in both the infrared and visible spectrum to be stored on tape recorders. A total of up to 400 minutes of smoothed resolution data may be transmitted to the central ground station at the Air Force Global Weather Center (AFGWC), Offutt, Nebraska.

Sensor System Description

Two spectral channels are used in the OLS. One channel responds to reflected solar or lunar radiation in the 0.4–1.1 μm range, chosen so as to provide maximum contrast between earth, sea, and cloud elements of the image field, and is termed the visible light or L-band. Two different detectors are used for collection of L-band data; one is a silicon diode detector for collection of fine resolution (0.3 n mi) data (LF) during daytime, the other is a photomultiplier tube (PMT) for collection of low resolution (1.5 n mi) data (LS) under quarter moonlight or brighter nighttime conditions. The other channel of the OLS responds to emitted Earth, atmosphere, and cloud radiation in the 8.0–13.0 μm range, chosen to minimize ozone and water vapor absorption while still maintaining an acceptable signal-to-noise ratio, and is called the thermal infrared or T-band. On F-4 and subsequent vehicles, the infrared channel was narrowed to 10.8–12.5 μm.

To achieve global coverage, the DMSP spacecraft has a scanning optical telescope system driven in sinusoidal motion by counter-reacting coiled springs and a pulsed motor. This motion moves the instantaneous field-of-view (IFOV) of the detectors across the satellite subtrack with maximum scanning velocity at nadir. The scanning velocity slows as the telescope reaches the end of scan (active data swath) and reverses direction during the overscan period. Contiguous along-track scanning is accomplished by the motion of the satellite in its orbit. The sinusoidal scan motion causes the surface velocity of the detector IFOV (i.e., the scene temporal resolution) to be nearly constant. Since the geometric resolution of a sensing system is related to the product of the scene spatial

resolution and scene temporal resolution, the sinusoidal motion (along with detector switching, discussed later) permits nearly-constant geometric resolution.

The OLS optical system is divided into two portions, the oscillating telescope assembly and the relay optics. The oscillating telescope assembly consists of a Cassegrain telescope and three additional mirrors which redirect the incident radiant energy to the relay optics. One of these mirrors also provides image motion compensation. Compensation is required because the telescope reverses scan direction on alternate scans. Figure 1A-3a shows the path of the IFOV of the telescope on the ground with and without image motion compensation.

The relay optics are the stationary portion of the OLS which deliver focused Earth scene energy to each of three detectors (silicon diode, PMT, and trimetal). They consist of beam splitters which divide the radiant energy into discrete spectral bands and lenses which focus the energy onto the focal plane of each of the detectors.

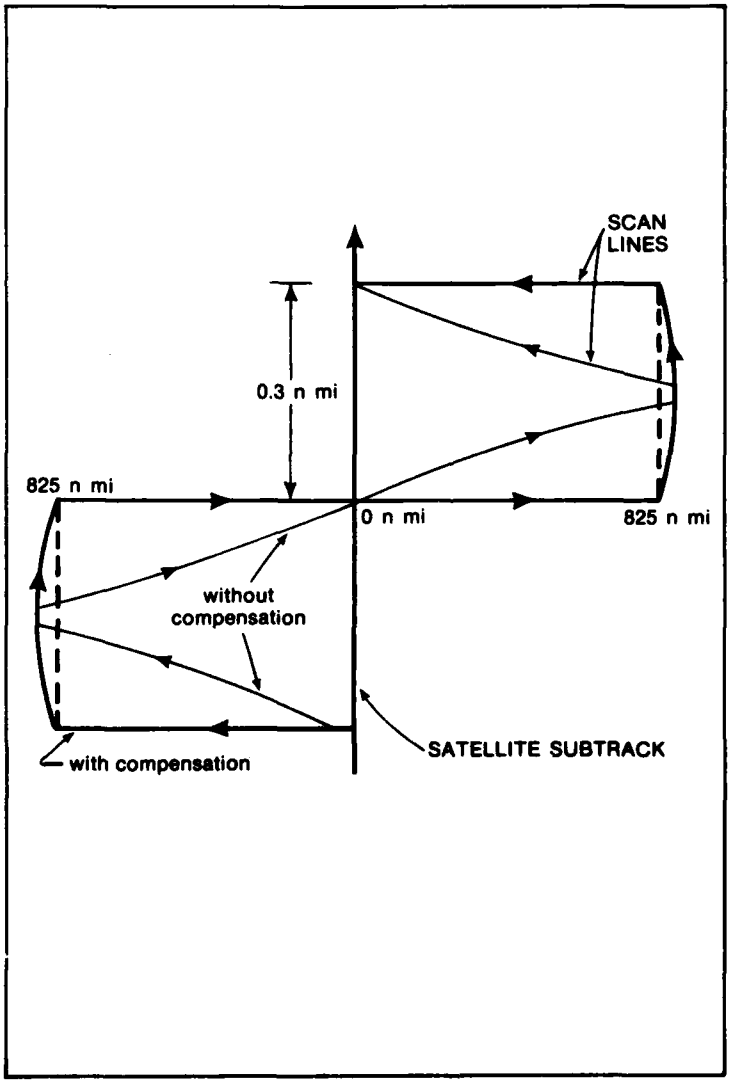

1A-3a. OLS scan line projection on the ground with and without image motion compensation.

At the fine mode visible detector, composed of three silicon diode segments, detector geometry and segment switching compensate for the enlargement and rotation of the IFOV projection on the Earth scene as scan angle increases. Figure 1A-4a illustrates the concept of IFOV rotation and switching. Four scan positions are depicted via the projection of the detector IFOV on the ground. The circled dot indicates the centroid of the nadir IFOV in each view and the shaded area indicates the IFOV segment which is on. The dashed lines indicate the two IFOV portions which may be used selectively with increase of scan angle. This selectable portion of the detector is the full IFOV in one direction and one third the full IFOV in the other.

At nadir (0 n mi), the IFOV has the nearly diamond shape of the detector. From nadir to 400 n mi, all three segments of the detector are used. As the surface distance increases from 0 to 400 n mi the IFOV projection on the ground both rotates and enlarges. The diamond-shaped orientation at nadir becomes a more rectangular shape at 400 n mi with the along-scan dimension minimized by the rotation. After 400 n mi the IFOV is switched to the section at the right side of the nadir IFOV. When scanning the left side of nadir, the IFOV rotation causes the left section to be the proper one to use. At 490 n mi the IFOV projection becomes purely rectangular, with the enlargement in the along-scan dimension just about compensated for by the reduction due to switching. Near the end of scan (800 n mi), more rotation and significant enlargement of the IFOV have occurred and its projection on the ground becomes nearly square. It can

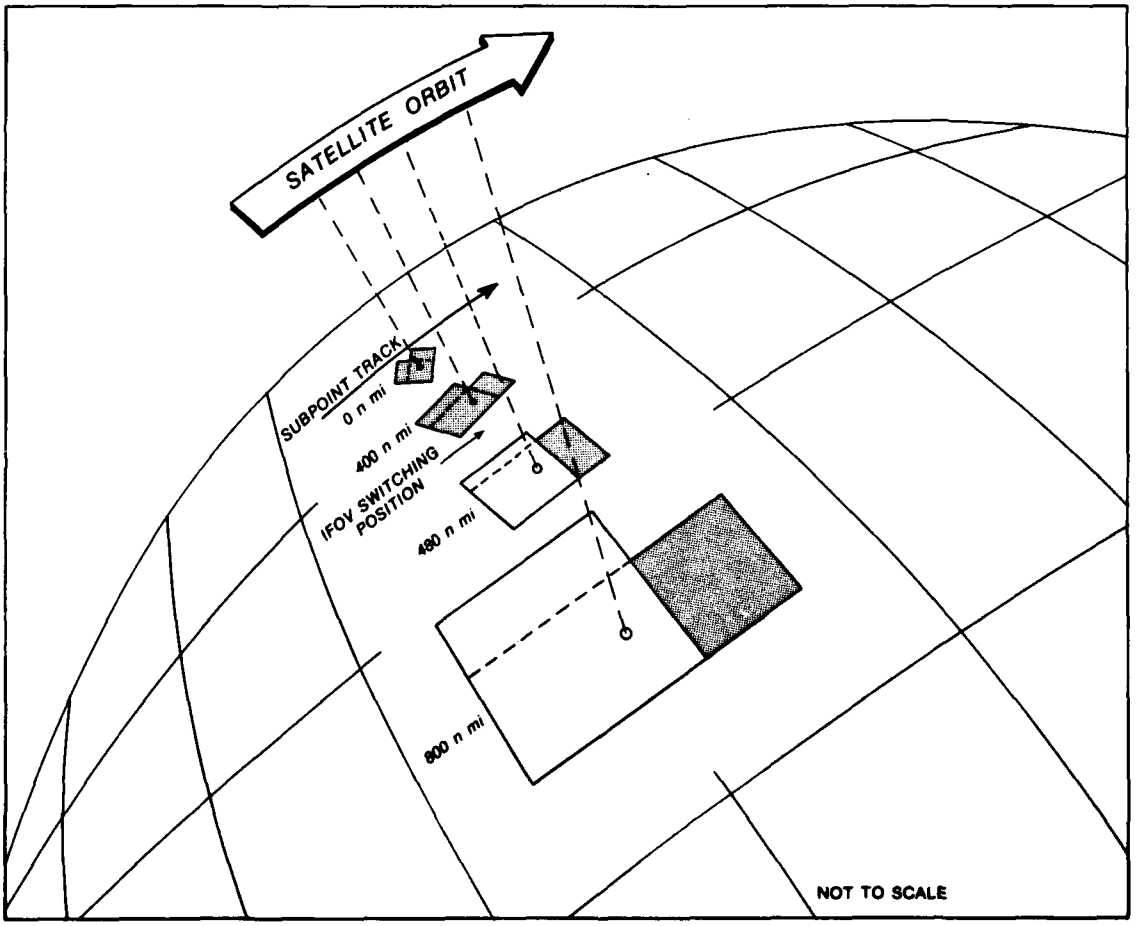

1A-4a. Segmented silicon diode detector field-of-view projection on the ground.

be seen that through the use of rotation and switching of the detector IFOV, the scene spatial resolution uniformity along scan has been significantly increased. The ground resolution along scan for all channels of the OLS is summarized in 1A-5a.

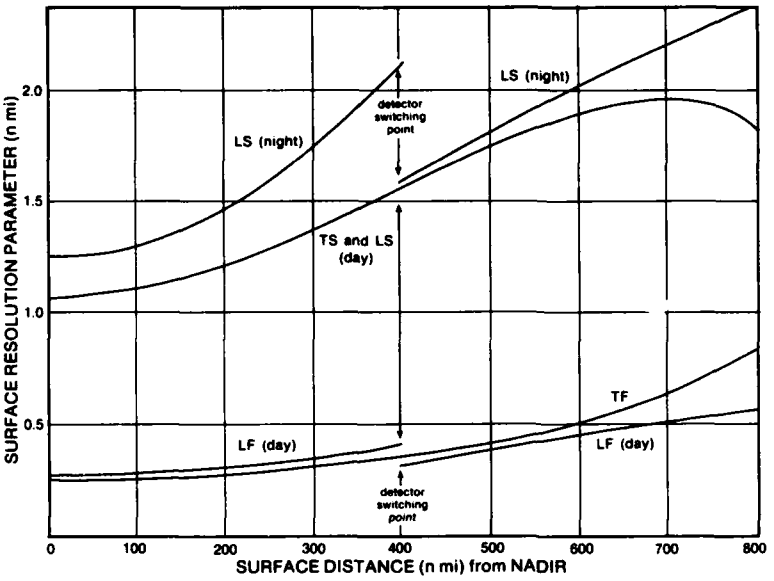

1A-5a. DMSP Block 5D OLS surface resolution.

To obtain smooth mode visible data (LS) during daytime, the sensor resolution is reduced from 0.3 n mi to 1.5 n mi by averaging five samples at every fifth sample in the along-scan direction, then averaging five such 0.3 by 1.5 n mi samples in the along-track direction.

A photomultiplier tube (PMT) is used to collect low resolution visible data (1.5 n mi resolution) under quarter moonlight or brighter nighttime conditions. It is important to note that the nighttime Block 5D-2 LS data are not obtained from the segmented silicon detector, but from the PMT which has different spectral characteristics. Nearly constant image resolution in the along-scan direction for the PMT is produced electronically. At 420 n mi from the subpoint, the IFOV projection on the ground is reduced and the PMT receives only one third the amount of energy the full IFOV would receive. Because of this, a noticeable degradation of the imagery occurs from 420 n mi to the end of scan in LS nighttime imagery. In addition to nighttime use, there is an option to use the PMT detector in terminator areas where scene illumination is too low for the silicon diode detector.

The OLS infrared detector is a trimetal (HgCdTe) that is passively cooled to an operating temperature of 105° K. The detector itself consists of two segments which are positioned in the same sense as the two selectable portions of the silicon diode detector. At nadir, the sampling switches from one segment to the other. This provides approximately constant field-of-view projection on the ground. Detector switching may sometimes cause a thermal change at nadir in the imagery due to calibration differences between the two detectors. Data smoothing for TS (1.5 n mi resolution) data is accomplished in the same manner as for daytime LS data.

The infrared sensor output is normalized in terms of the equivalent blackbody temperature of the radiating object. Output voltage is a linear function of scene temperature. The detector temperature sensitivity is 1.56° K in the temperature range 210–310° K (enlarged to range from 190° to 310° K on F-6 and later spacecraft). The net equivalent temperature difference (NETD) of the infrared system is 1° K in this same range.

Channel Characteristics

The visible channel normalized sensor response curves of the PMT and silicon diode are shown in 1A-6a. Two different PMT detector response

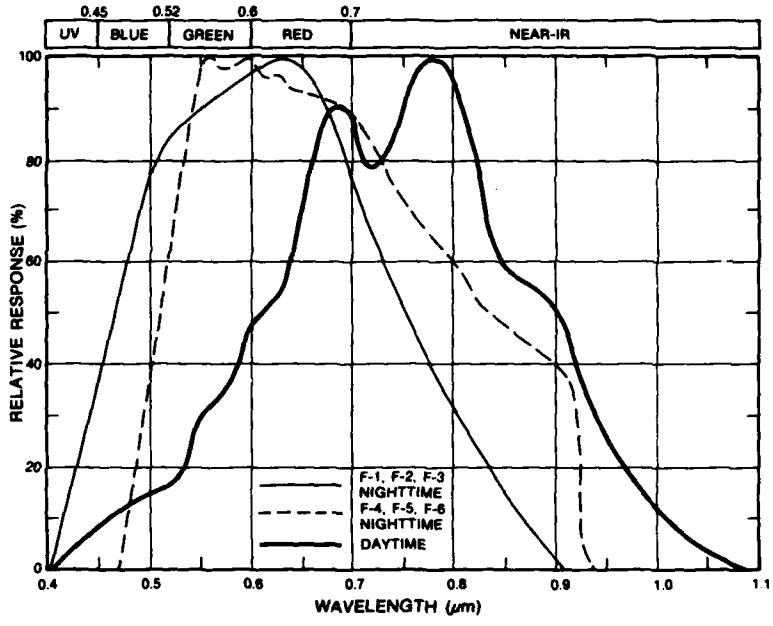

1A-6a. DMSP Block 5D visible channel normalized sensor response curves.

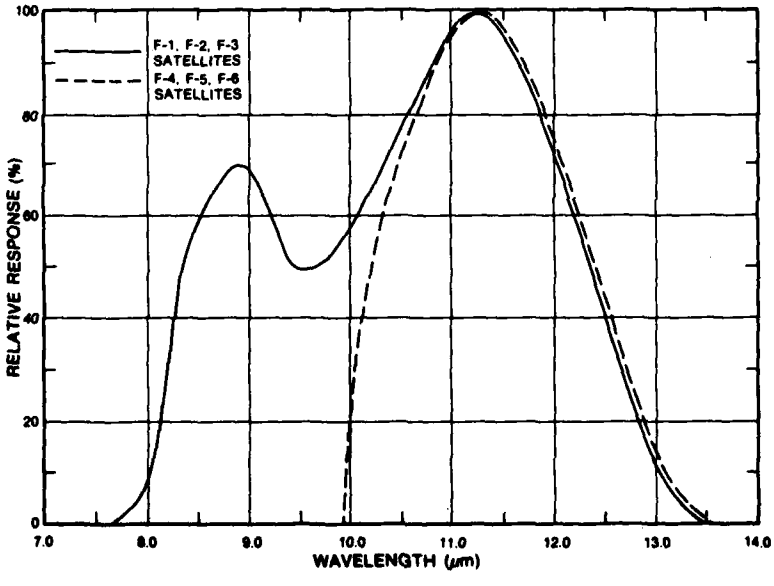

1A-6b. DMSP Block 5D infrared channel normalized sensor response curves.

curves are included. The curves for the F-1, F-2, and F-3 spacecraft have a peak response near 0.6 μm. The response has been modified for the F-4, F-5, F-6 and later spacecraft in the Block 5D-2 program to provide a broader spectral interval extending into the near infrared. The silicon diode detector response extends into and peaks in the near infrared wavelengths. This provides excellent land/water contrast and enhances haze detection capabilities.

The OLS infrared channel for F-1 through F-3 (1A-6b) senses the 8.0–13.0 μm range. This range contains the peak radiations emitted by the Earth and its atmosphere, and is an atmospheric window region largely transparent to outgoing radiation except for appreciable water vapor absorption in moist atmospheres and for an ozone absorption peak at about 0.96 μm (see NTAG, Vol. 2, Sec. 3A, Case 6). This broad spectral range was initially selected to permit fine spatial resolution while still maintaining an acceptable signal-to-noise ratio at the detector.

On the F-4 and subsequent spacecraft, refinements in the infrared detector have permitted the spectral range of the sensor to be narrowed to 10.8–12.5 μm (1A-6b), while still maintaining an acceptable signal-to-noise ratio. This new, narrower spectral range, unlike the previous range, is not appreciably affected by ozone absorption and is less affected by water vapor absorption. For operations at direct readout sites this means that new correction factors are required to accurately determine surface temperatures and cloud top temperatures and heights. Through experimentation, a combination of surface temperatures and atmospheric sounding profiles was selected from which to derive a base correction for these determinations. These surface temperatures and atmospheric sounding profiles are listed in Table 1.

TABLE 1

SURFACE TEMPERATURE (K)	PROFILE (AFGWC)
310-300	TROPICAL
290-270	U.S. STANDARD
270-250	SUBARCTIC WINTER
250-210	ARCTIC WINTER

The AFGWC has developed several theoretical temperature bias correction curves for the new infrared spectral range. Although these curves were developed for surface temperatures, they can be used to approximate the corrections required for cloud top temperatures by using one of the standard profiles.

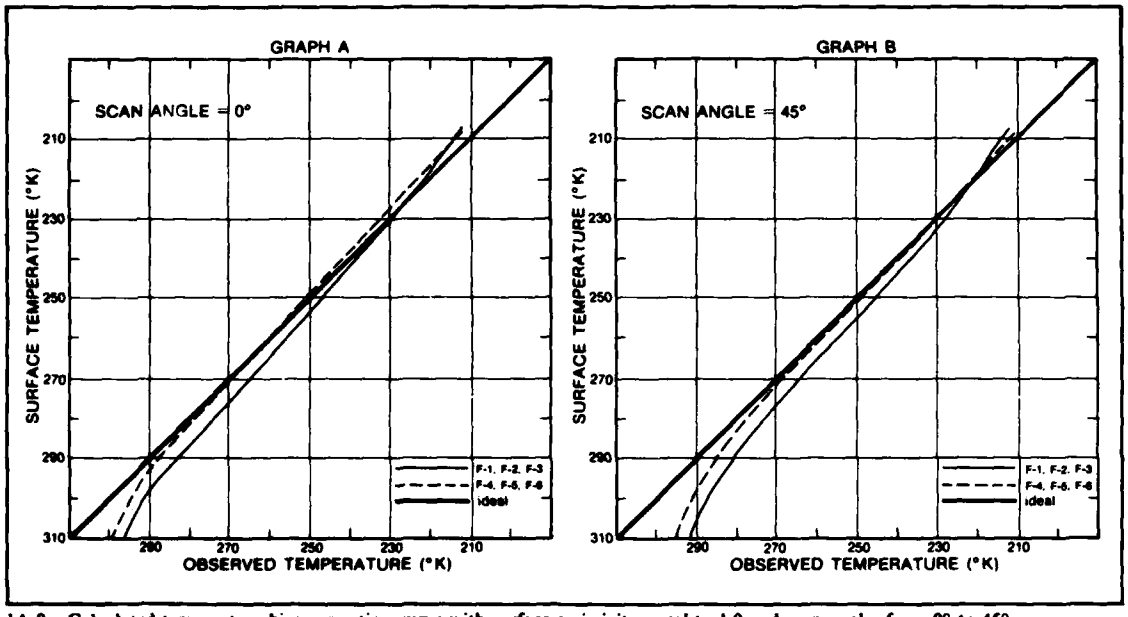

1A-8a. Calculated temperature bias correction curve with surface emissivity equal to 1.0 and scan angles from 0° to 45° (0 to 490 n mi from the satellite subtrack) and scan angle 45° (490 n mi from satellite subtrack) or greater.

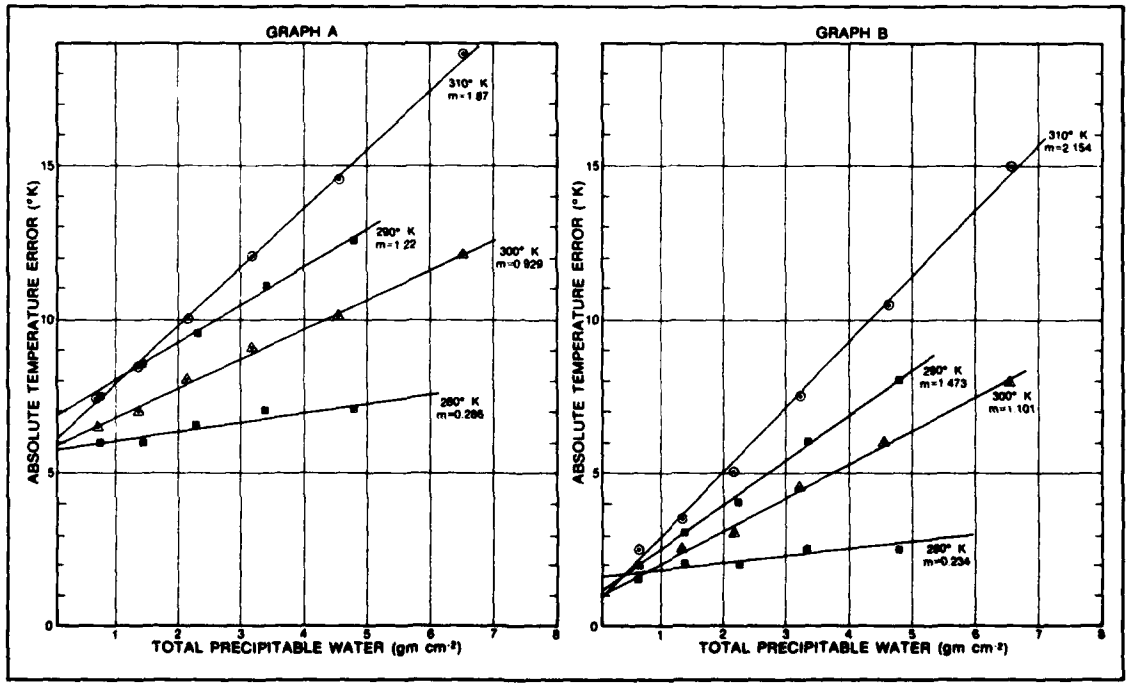

1A-8b. (A) F-1, F-2, and F-3; and (B) F-4, F-5, and F-6 absolute temperature error (ΔT) for the indicated surface temperatures as a function of atmospheric water vapor content.

Temperature bias correction values should be interpolated using 1A-8a. For scan angles between 0° and 45° (0 to 490 n mi from the satellite subtrack) use Graph A. Use Graph B as an approximation for scan angles greater than 45° (greater than 490 n mi from the satellite subtrack). It can be seen that the absolute temperature error for the F-4, F-5, and F-6 sensors is less than the error for the F-1, F-2, and F-3 sensors.

Corrections for atmospheric water vapor content (total precipitable water) should be made using 1A-8b. For the F-1, F-2, and F-3 spacecraft use Graph A; for the F-4 and subsequent spacecraft use Graph B. These curves show that the correction for water vapor attenuation is important for surface temperatures greater than 280° K.

Special Sensors

The OLS has the data management capability for acquiring, processing, recording and outputting data from up to 12 special meteorological sensors. There are eight supplementary sensors (other than those mentioned in NTAG, Vol. I, Sec. 1) on the DMSP Block 5D-2 spacecraft. Table 2, as shown below, itemizes which sensor is flown on any particular vehicle.

Special Sensor H-2 (SSH-2) is a 16-spectral channel infrared temperature, water vapor, and ozone sounder. It contains a scanning radiometer that provides soundings of temperature and water vapor, and a single measurement of ozone for vertical and slant paths under and to the side of the satellite subtrack.

Special Sensor J/4 (SSJ/4) is the precipitating proton electron spectrometer which measures the accumulated radiation dose in a semiconductor due to electrons (1 to 10 MeV), protons (>20 MeV) and the effects of nuclear interactions on a solid state detector encountered on a satellite. This spectrometer measures the Earth's trapped radiation to determine its effects on the spacecraft.

Special Sensor IE (SSIE) is a topside ionosphere plasma monitor system to characterize space plasma above the peak of the F-region with four electrostatic (electron and ion) probes. The electron sensor measures

TABLE 2 DMSP SPACECRAFT SUMMARY

	BLOCK 5D-1					BLOCK 5D-2				
primary sensor	F1 OLS	F2 OLS	F3 OLS	F4 OLS	F5 OLS	F6 OLS	F7(S7) OLS	F8(S8) OLS	F9(S9) OLS	F10(S10) OLS
mission sensors	SSH SSJ SSB	SSH SSJ SSB SSIE SSIP	SSH SSJ SSB	SSH SSM/T SSJ SSIE SSIP SSC SSD	SSH SSJ SSB SSIE SSR	SSH SSJ/4 SSB/A SSIE	SSH or SSM/T SSJ/4 SSB/S SSIE *SSJ **SSM	SSH or SSM/T SSJ/4 SSB SSIES	SSM/T SSJ/4 SSB SSIES SSM/I	SSM/T SSJ/4 SSB SSIES SSM/I
launch date	11 Sep 76	9 Jun 77	1 May 78	6 Jun 79	14 Jul 80	22 Dec 82	4th quarter 83	1st quarter 84	4th quarter 85	3rd quarter 86
design life (months)	18	18	18	18	18	36	36	36	36	36
non-operational date	16 Sep 79	24 Feb 80	operational	9 Aug 80	failed on launch	operational				

* Experimental Dosimeter to measure and indicate amount of satellite radioactivity absorption.
**Experimental Triaxial Magnetometer for precision measurement of the earth's magnetic field.

the ambient electron density and temperature and the electrostatic potential of the vehicle, while the ion sensor measures the densities of the major ion species present, the average ion temperature, the average ion mass, and the vehicle potential.

Special Sensor B/A (SSB/A) is a scanning gamma and x-ray sensor designed to measure x-ray intensity as a function of energy from approximately 2 keV to above 100 keV and monitor the flux of energetic electrons with pitch angles near 90 degrees. The primary objective of the payload is to provide the location of x-ray sources in the atmosphere and to measure the energy spectrum of x-rays emitted from these sources.

Special Sensor B/S (SSB/S) is an x-ray intensity detector which measures energies in levels of 25, 45, 75, and 115 keV. The difference between SSB/A and SSB/S and the Block 5D-1 sensor (SSB) is that the Block 5D-2 (SSB/A and SSB/S) detector fields-of-view are scanned rather than being fixed, as on the SSB.

Special Sensor M/T (SSM/T) is the passive microwave temperature sounder. It is a seven-channel scanning radiometer which measures radiation in the 5.0–6.0 μm wavelength region (50–60 GHz) to provide data for profiling on a global basis atmospheric temperatures from the Earth's surface to altitudes above 30 km. It has been designed to scan in synchronization with the infrared temperature and water vapor sounder (SSH) already developed.

Starting with S9, the 5D-2 series of satellites will have a microwave imaging sensor (SSM/I). The SSM/I is a passive microwave radiometer that detects thermal energy emitted and reflected by the Earth's atmosphere in the microwave portion of the electro-magnetic spectrum. This sensor's data will be used to measure ocean surface wind speed, ice coverage and age, areas and intensity of precipitation, cloud water content, and land surface moisture. The microwave sounder complements the infrared sounder by providing temperature soundings over previously inaccessible cloudy regions of the globe and at higher altitudes than are attainable with the infrared sensor. This data can be stored on recorders for delayed transmission or relayed directly to data acquisition centers via the spacecraft data transmitters. The SSM will occupy the SSB location on selected satellites.

Special Sensor IP (SSIP) is a high frequency (HF) receiver which passively monitors the ionospheric noise breakthrough frequency used in ionospheric forecasting. Noise from man-made and natural sources below the ionospheric F2 layer peak can be detected by an HF topside-receiver only at frequencies above the F2 critical frequency (foF2). By sweeping through the HF spectrum, the SSIP can monitor the frequency of the noise breakthrough. Electron density profiles are used to forecast ionospheric anomalies and tilts for systems propagating off the ionosphere. Electron density profiles are also used to determine total column electron content for systems propagating through the ionosphere.

An improved version of the Block 5D-1 spacecraft, called the Block 5D-2, is used on the F-6 and later flight vehicles. The Block 5D-2 spacecraft (1) carries the same OLS system as the Block 5D-1, (2) is larger in size and is able to carry a larger, non-OLS sensor payload, (3) has a greater redundancy of systems, (4) has a computer memory twice the size of that on the Block 5D-1, and (5) has a 36 month in orbit lifetime as opposed to the 18 month in orbit lifetime of Block 5D-1.

In addition to the Block 5D-2, plans for a Block 6 spacecraft (first launch 1984) are currently in the development stage. This series of spacecraft is being designed to satisfy both the military and civilian environmental data needs and to provide a growth capability so that several additional sensors can be incorporated.

For further information on DMSP contact:

Navy Space Systems Representative
SAMSO/YDN
P.O. Box 92960
Worldway Postal Center
Los Angeles, California 90009

Additional information on the Block 5C and Block 5D systems can be found in Volumes 1 and 3 of this series.

References

Dickinson, L.G., S.L. Boselly III, and W.S. Bergmann, 1974: Defense Meteorological Satellite Program (DMSP) User's Guide. AWS-TR-74-250, Air Weather Service, United States Air Force, Scott AFB, 109 pp.

Nichols, D.A., 1975: Block 5D Compendium. Headquarters, Space and Missile Systems Organization, Air Force System Command, United States Air Force, 106 pp.

Sample Imagery, DMSP

These simultaneous DMSP images show the cloud cover and thermal features over western Europe and northwestern Africa. In the visible picture (1A-12a), there is a small vortex over the western Mediterranean and an extensive area of cloudiness over France and Great Britain. The corresponding infrared picture (1A-13a) reveals that this cloudiness is low-level stratus or fog and also shows that there is considerable convective activity over the western Mediterranean ahead of the vortex.

SYSTEM ID SVROTA: FTV 1535: AM: ASCEND REV 6961: RT: DATE 78-015: TR 10:54:13: DATA TYPE LF 6 BIT: SCALE X1: MIDPNT 0000 NM
DATA MOD: L-LOW : TN 10:51:13: LN 350.09: ROLL +.000: ALT 459.7: SYS POS: LAT +36/LONG 006: +IMAGE: NE
15JAN78 35N-0.5EAST TAPE# 015-5

1A-12a. F-1. DMSP LF Low Enhancement. 1104 GMT 15 January 1978.

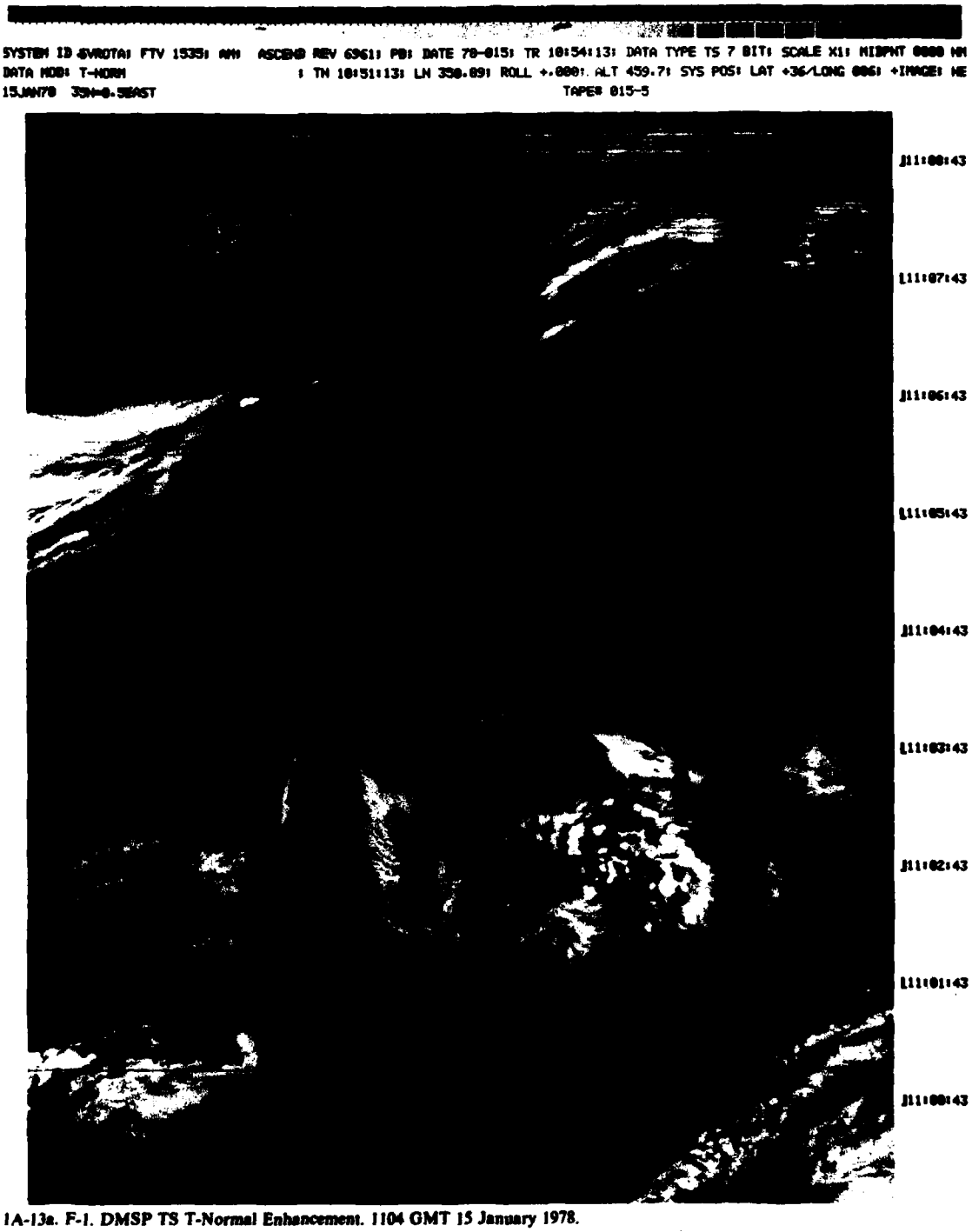

1A-13a. F-1. DMSP TS T-Normal Enhancement. 1104 GMT 15 January 1978.

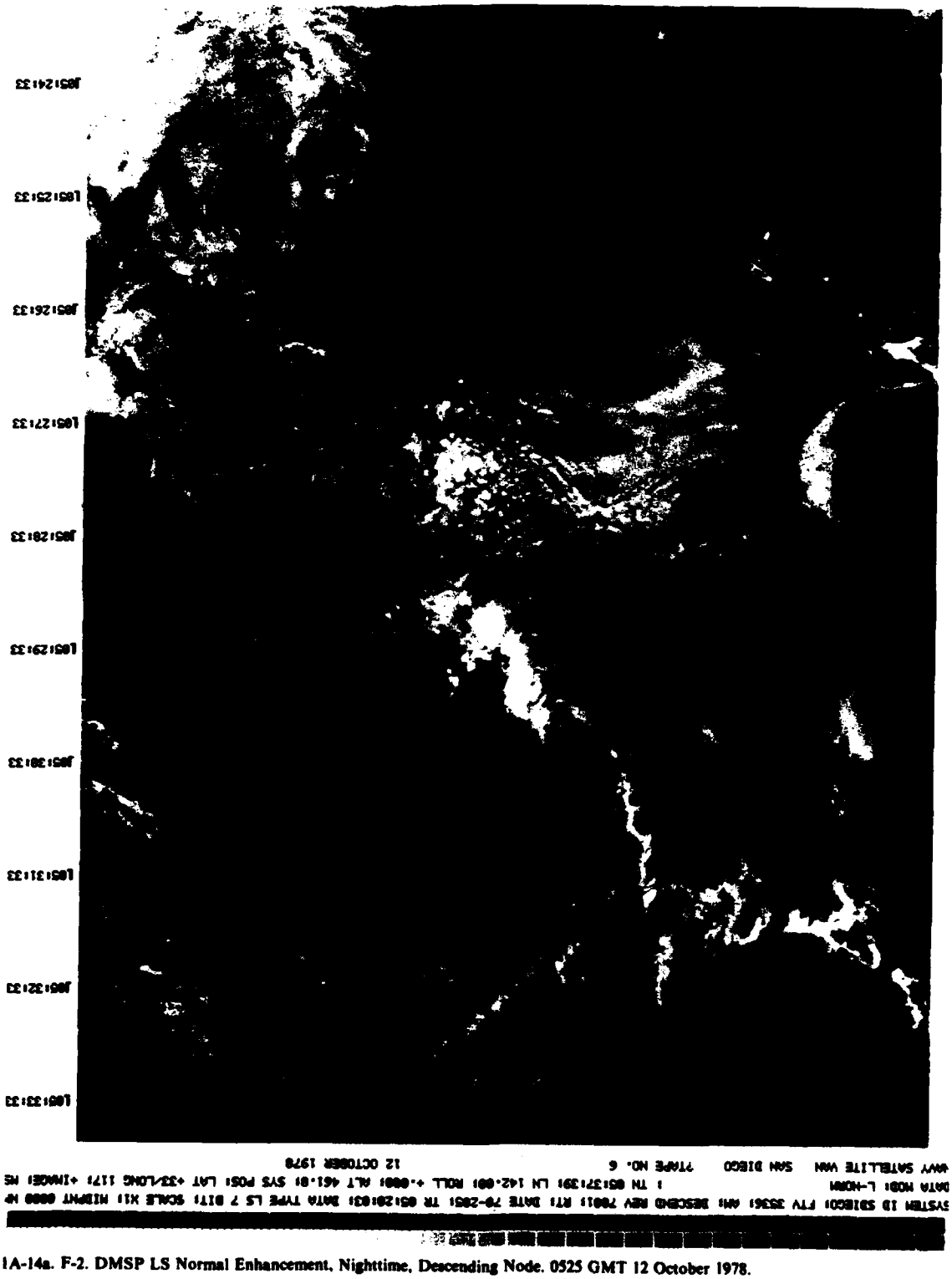

1A-14a. F-2. DMSP LS Normal Enhancement, Nighttime, Descending Node. 0525 GMT 12 October 1978.

Figures 1A-14a and 15a are simultaneous visible and infrared images showing the U.S. west coast. The nighttime visible picture reveals the lights of the major metropolitan areas as well as cloud patterns over the eastern North Pacific. Note the granular texture of the image at the right and left edges. This is caused by the reduction of the nighttime visible sensor's aperture which is necessary to keep the along-scan resolution nearly constant.

The infrared picture has been enhanced to display sea surface temperature gradients along the coast. This type of enhanced imagery is useful for oceanographic and air-sea interaction studies.

1A-15a. F-2. Enlarged View. DMSP TF (Special Table A), Descending Node. 0525 GMT 12 October 1978.

National Oceanic and Atmospheric Administration
Polar-orbiting Satellite Program
(TIROS-N/NOAA)

The NOAA polar-orbiting satellite program, TIROS-N/NOAA[1], provides (1) high resolution, day and night multispectral imagery of the Earth, its atmosphere, and clouds, (2) improved observations of vertical temperature and moisture profiles, and (3) a high capacity data collection and platform location system. Only the image products obtained from the satellite are described in this section.

The operational system includes at least two satellites; NOAA-6 in a morning pass (0730 LST descending node) and NOAA-7 in an afternoon pass (1500 LST ascending node). The original satellite in this series, TIROS-N, ceased collecting data in the fall of 1980. NOAA-6 and 7 are both in near-polar, sun-synchronous orbits. While TIROS-N orbited at an average altitude of 854 km, NOAA-6 and 7 and all future spacecraft in the series will orbit at an average altitude of 833 km. The orbital period is approximately 102 minutes which produces 14.2 revolutions per day.

NOAA-8 (replacement for NOAA-6) was launched on 28 March 1983, attaining an orbit with a morning-southbound equator crossing. In addition to environmental sensors, this spacecraft carries a search and rescue (SAR) instrument to detect and locate aircraft and ships in distress.

1. TIROS-N is the name of the first spacecraft in this program. Subsequent spacecraft are named NOAA-6 through NOAA-12.

1B-1a. The TIROS-N/NOAA satellite is a five-sided box-like structure which is approximately 13'9" long and 6'2" in diameter. Four of the five sides are equal in size and contain a total of twelve thermal cooling panels. The fifth side is wider than the other four and contains the communication antenna and the Earth-viewing sensors. At one end of the spacecraft is a large panel containing arrays of solar power cells. This panel is motor-driven to rotate once per orbit so that it continuously faces the sun during the daylight portions of the orbit.

Image Acquisition

Imagery from the Advanced Very High Resolution Radiometer (AVHRR) is available from each spacecraft in two operational modes to direct readout users. The first is direct readout of any two spectral channels to ground receiving stations of the Automatic Picture Transmission (APT) class at 2 n mi resolution. The second mode is direct readout of all four spectral channels to ground receiving stations of the High Resolution Picture Transmission (HRPT) class at 0.5 n mi resolution. The swath width of the AVHRR is approximately 1700 n mi. Presently, the AVHRR instrument on the NOAA-6 satellite is losing sync in an unpredictable manner; for this reason, the APT and the HRPT services are considered to be unreliable. All systems on the NOAA-7 satellite are fully operational, with no significant problems.

The APT systems receive an analog signal from the spacecraft on the standard APT frequencies. Visible Channel 2, 0.725–1.10 μm on both NOAA-6 and 7, is used to provide imagery during daytime; and infrared Channel 4, 10.5–11.5 μm on NOAA-6 and 7, is used to provide imagery day and night.

The APT data are output at a rate of 120 lines per minute and the along-scan samples are averaged so that the resolution is nearly constant. This greatly reduces panoramic distortion of the image at the edges. To produce this nearly constant resolution in the along-scan direction, each scan line is divided into five zones from the satellite subpoint (SSP) to the end of the scan line, with each zone using a different averaging algorithm. To obtain the 120 lines per minute rate, only every third line from the 360 lines per minute AVHRR HRPT output is transmitted. This reduces the resolution of the APT imagery to approximately 2 n mi (1B-2a). Simulations have shown that this algorithm retains all significant features near the SSP and near the ends of scan.

The HRPT system transmits all four AVHRR spectral channels at 0.5 n mi resolution. These data do not undergo any preprocessing on-board the spacecraft. Also, HRPT data are transmitted in digital form requiring software at user sites so that the data can be properly formatted for operational display.

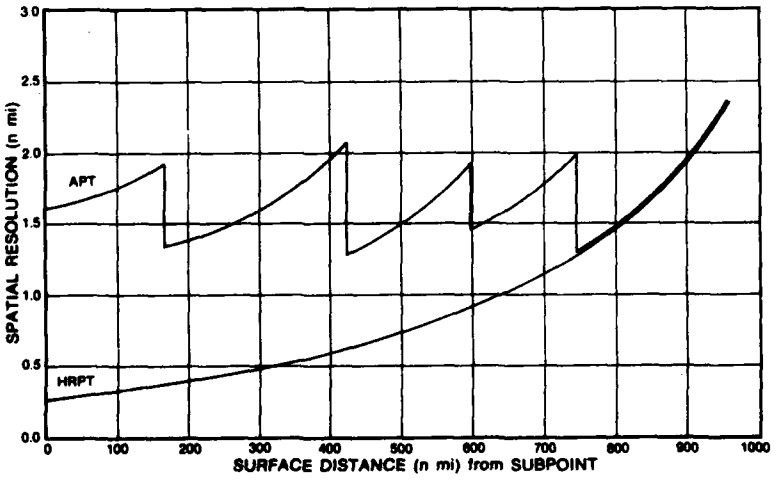

1B-2a. Surface resolution of the TIROS-N/NOAA APT and HRPT imagery.

Sensor System Description

The AVHRR sensors are mounted in a sensor package at one end of the spacecraft so that with nominal attitude control the sensors are always oriented toward the Earth. The basic operation of the AVHRR is similar

to its predecessor, the VHRR, which flew on the ITOS/NOAA series satellites. That is, it is a line scan device; global coverage is achieved from continuous horizon-to-horizon crosstrack scanning by a mirror combined with the forward motion of the spacecraft. The scanning mirror rotates at a constant rate of 360 revolutions per minute. Once during each revolution, a synchronization pulse is generated as the mirror reaches a precise pre-Earth position. Upon receipt of the synchronization pulse, a data sampling process begins which takes the appropriate number of samples at specified times during the scan line. The data from the AVHRR is then processed to provide separate outputs for APT and HRPT formats in real-time.

Radiation from the Earth scene is gathered by an optical system which consists of a Cassegrain telescope combined with secondary optics. The secondary optics separate the radiant energy into discrete spectral bands which are focused onto their respective focal planes. The instantaneous field-of-view (IFOV) for all channels is specified to be 1.3±0.1 milliradians which gives a spatial resolution of 0.5 n mi at the SSP. The IFOV was chosen so that the satellite motion along its orbital path would cause successive scan lines to be contiguous at the SSP. The instrument has been designed so that the IFOV of the four channels can be made coincident within ±0.1 milliradians (±8%).

The visible and near infrared channels of the AVHRR use silicon detectors to measure incident radiation. The infrared channels use metal-segment detectors cooled to 105° K. A bimetal (InSb) has been chosen for the 3.55–3.93 μm channel, while the 10.5–11.5 μm channel uses a tri-metal (HgCdTe) detector. In all channels, the zero point for detected energy is restored to a zero level once each scan while viewing space. The output of the radiometer during the remainder of the scan is equal to the difference in detected energy between space and the radiated energy from the detection scene. The system has been designed so that instrument output is linear with input energy.

Variations in the electronic signal used to gather and transmit the infrared data produce random or coherent noise patterns on the signal radiated from the Earth. When the noise patterns are of comparable magnitude to the temperature gradient under scrutiny, it becomes difficult to distinguish one from the other. A measure of the total noise produced by an infrared sensing system is the net equivalent temperature difference (NETD). The NETD of the TIROS-N/NOAA infrared channels is better than 0.12° K (for a 300° K scene). The temperature sensitivity of these channels is approximately 0.5° K at the same temperature. Since the NETD is less than the temperature sensitivity, accurate identification of thermal gradients is made feasible.

During every scan line, the AVHRR views cold space (zero radiance) and its housing (approximately 290° K). The housing portion of the instrument has been designed to be a blackbody target to be used in orbit for instrument calibration. Four thermometers whose output values are included in the data stream are embedded in the housing and monitor the temperature of the target. By determining the instrument output while viewing cold space and the known warm target, it is possible to ascertain the instrument response curve. This permits on-board calibration of the infrared channels.

Channel Characteristics

The AVHRR channel characteristics are summarized in Table 1. After the fourth spacecraft in the series (NOAA-8), the AVHRR will be expanded to include a fifth channel, and the system will be renamed AVHRR/2.

TABLE 1
TIROS-N/NOAA
AVHRR Spectral Channel Characteristics

Channel 1 wavelength will be 0.58–0.68 μm for all instruments after the TIROS-N flight model. Channel 4 wavelength will be 10.3–11.3 μm for all AVHRR/2 instruments. Channel 5 has been added to the AVHRR/2 instrument to further enhance sea surface temperature measurements in the tropics.

Channel	Resolution at Subpoint	Wavelength (μm)
1	0.5 n mi	0.55–0.90
2	0.5 n mi	0.725–1.10
3	0.5 n mi	3.55–3.93
4	0.5 n mi	10.5–11.5
5	0.5 n mi	11.5–12.5

The normalized sensor response curve of TIROS-N/NOAA Channel 1 (0.55–0.90 μm) is shown in 1B-4a. As can be seen, this channel has a broad peak response in the interval of 0.7–0.9 μm, in the near infrared, and there is little or no response in the blue portion of the visible spectrum (<0.5 μm). This channel is used for daytime mapping of clouds and Earth surface features. On NOAA-6 and all future spacecraft in the series, the response of this channel has been narrowed to 0.58–0.68 μm so that the sensor responds only in the visible light portion of the spectrum and does not overlap with the response of Channel 2.

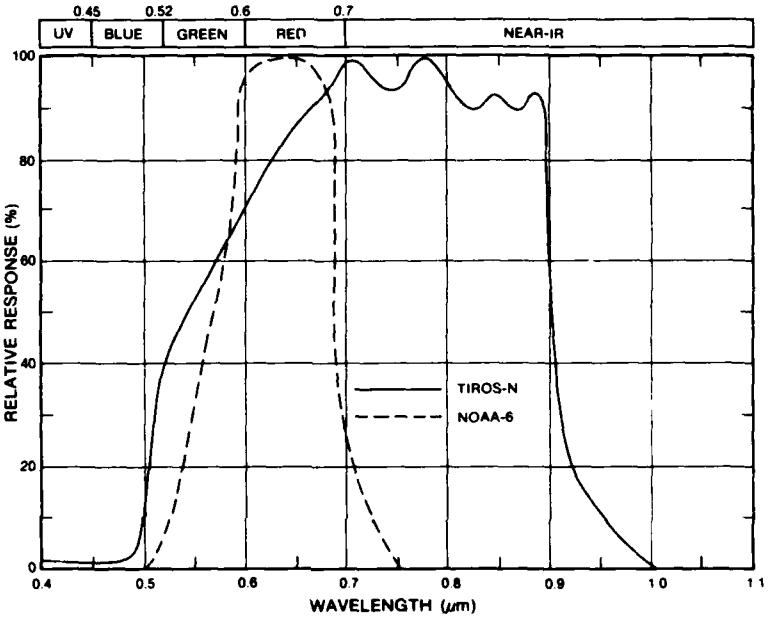

1B-4a. TIROS-N/NOAA channel 1 normalized sensor response curves.

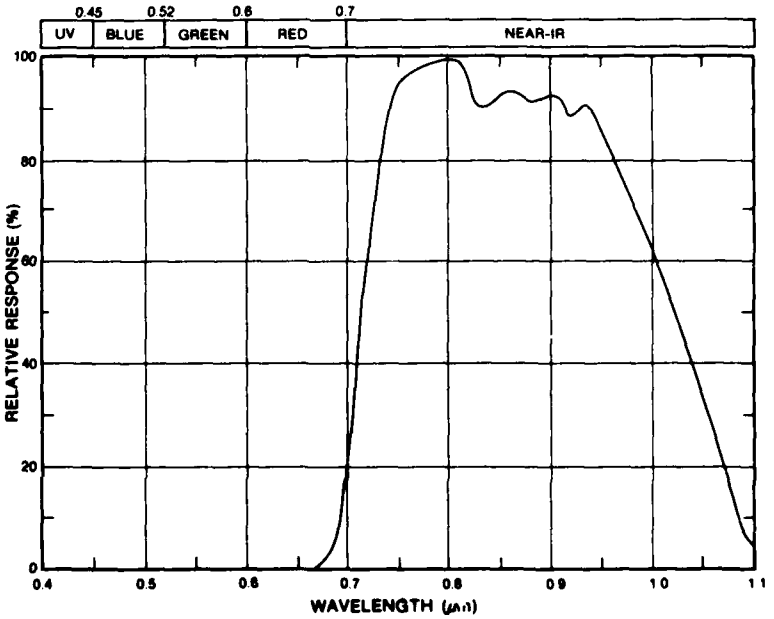

1B-4b. TIROS-N/NOAA channel 2 normalized sensor response curve.

The normalized response curve of Channel 2 (0.725–1.10 μm, 1B-4b) is limited to the near infrared with a peak response near 0.8 μm. Since liquid water absorbs near infrared radiation more strongly than visible radiation, this channel is used primarily for daytime delineation of surface water and land/water boundaries. Additionally, a comparison of data from Channels 1 and 2 makes it possible to locate areas of ice-snow melt.

The normalized sensor response curves of the two infrared channels are shown in 1B-5a and 5b. These channels are used for determining the temperature of the radiating surface (land, sea, or atmosphere). Channel 3 (3.55–3.93 μm) is normally used at night, since the response of this channel is contaminated by reflected solar radiation during the day.

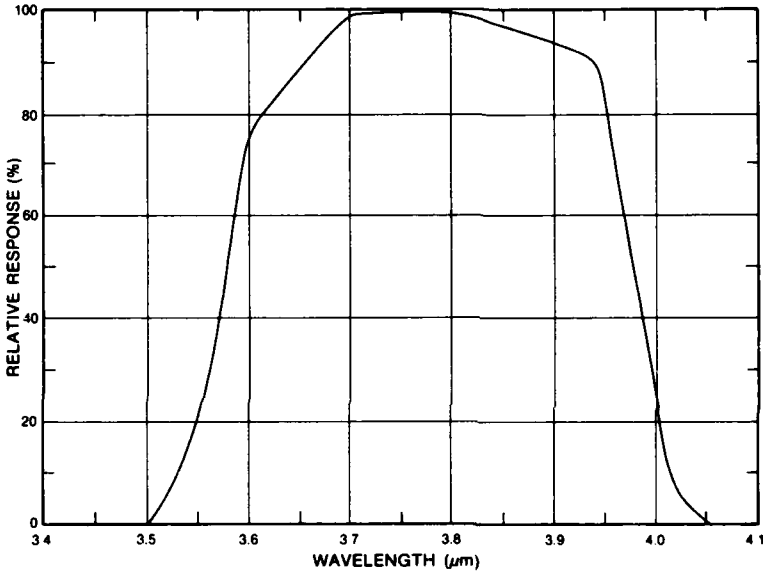

1B-5a. TIROS-N/NOAA channel 3 normalized sensor response curve.

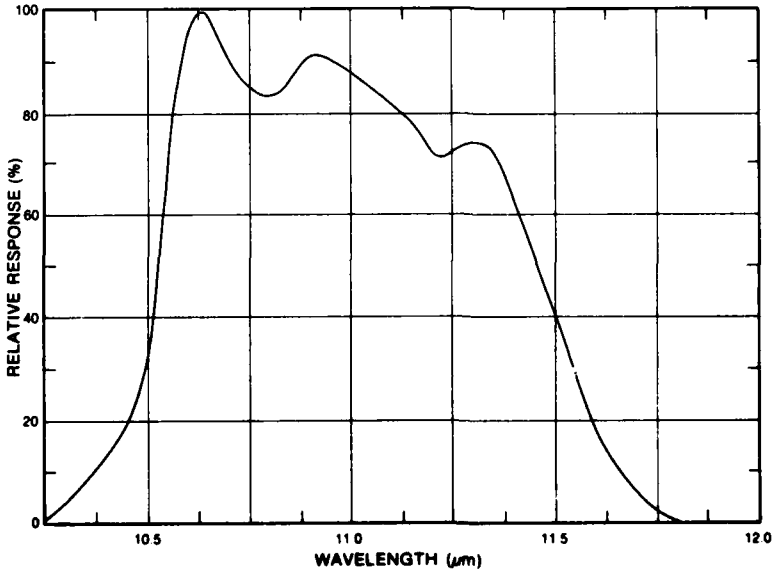

1B-5b. TIROS-N/NOAA channel 4 normalized sensor response curve.

In this spectral range, there is almost no absorption by water vapor. As a result, surface radiation can penetrate heavy water vapor concentrations and some thin clouds with little loss of energy. This channel is especially useful in the tropics for delineating sea surface temperatures because of these characteristics.

Channel 4 (10.5–11.5 μm) is used continuously day and night since it responds to the peak radiations emitted by the Earth and its atmosphere and is not affected by reflected solar radiation. Although attenuation by water vapor is minimized in this region, variations in water vapor concentrations, both horizontally and vertically, still cause significant attenuation when viewing Earth surface temperatures. A fifth channel, Channel 5, sensitive in the 11.5–12.5 μm region, will be added later to the AVHRR making it possible to account for some effects of water vapor attenuation in the determination of surface temperatures.

For additional information on the TIROS-N/NOAA system, contact:

National Climatic Data Center
Satellite Data Services Center
NOAA/National Environmental Satellite,
Data, and Information Services
Washington, D.C. 20233

References

Hussey, W.J., 1979: The TIROS-N/NOAA Operational Satellite System. National Environmental Satellite Service, NOAA, Washington, D.C., 35 pp.

Kidwell, K.B., 1979: NOAA Polar Orbiter Data (TIROS-N) Users Guide Preliminary Version. National Climatic Center, Satellite Data Services Division, Washington, D.C., 172 pp.

Schwalb, A., 1982: The TIROS-N/NOAA A-G Satellite Series. NOAA Tech. Memo. NESS 95, National Environmental Satellite Service, NOAA, Washington, D.C., 75 pp.

Schwalb, A. 1982: Modified Version of the TIROS-N/NOAA A-G Satellite Series (NOAA E-J)—Advanced TIROS-N (ATN). NOAA Tech. Memo. NESS 116, National Earth Satellite Service, NOAA, Washington, D.C., 23 pp.

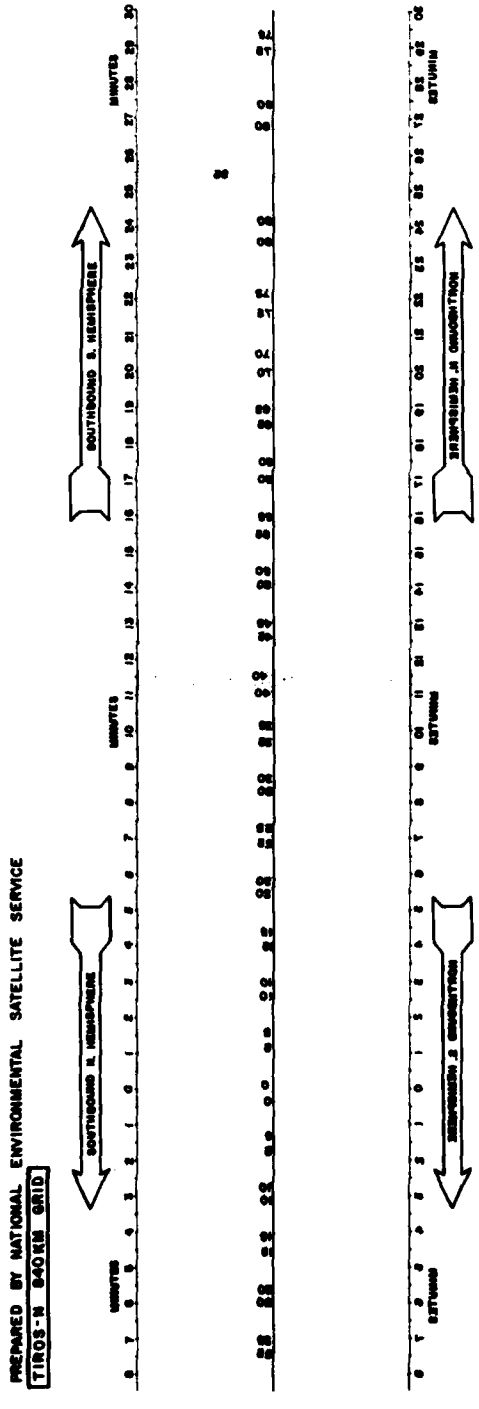

Operational User Aid

This TIROS-N APT grid shows the orbital subtrack and areal coverage for any satellite pass. To use the grid:

1. Make an acetate copy of the grid to the same scale as the satellite image so that the border of the image and grid coincide.

2. Determine whether the satellite pass is northbound (ascending) or southbound (descending) and rotate or flip the grid appropriately.

3. Use standard APT techniques for grid registration to the picture.

Due to recorder characteristics, this grid may not fit your display device. Individual sites should check the accuracy of this grid and, if necessary, hand-construct a grid that fits your display. *For additional information on gridding, individual* sites may contact NEPRF.

Sample Imagery TIROS-N/NOAA

These images (1B-8a and 9a) were acquired operationally on-board R/V Knorr on a research cruise out of Woods Hole, Mass., to the Grand Banks area of Newfoundland.

In the visible picture, sunglint is apparent along the right edge of the image, while a large area of cellular cloudiness occurs to the northwest behind a frontal cloud band. The infrared picture shows a Gulf Stream meander south of Nova Scotia.

1B-8a. NOAA-6 APT. Visible Picture (Channel 1). 2 n mi Resolution. 1137 GMT 15 October 1979.

Sample Imagery TIROS-N/NOAA

These images (1B-8a and 9a) were acquired operationally on-board R/V Knorr on a research cruise out of Woods Hole, Mass., to the Grand Banks area of Newfoundland.

In the visible picture, sunglint is apparent along the right edge of the image, while a large area of cellular cloudiness occurs to the northwest behind a frontal cloud band. The infrared picture shows a Gulf Stream meander south of Nova Scotia.

1B-8a. NOAA-6 APT. Visible Picture (Channel 1), 2 n mi Resolution. 1137 GMT 15 October 1979.

1B-9a. NOAA-6 APT. Enhanced Infrared Picture (Channel 4), 2 n mi Resolution. 1152 GMT 19 October 1979.

In 1B-10a, sunglint appears along the western portion of the image in this afternoon, descending pass. The long, narrow, north-south oriented line east of the sunglint may be related to a surface slick formation. Such slicks have been frequently noted in association with seaweed and organic material which stretches for great distances over the Sargasso Sea and Gulf Stream region. In the corresponding infrared picture (1B-11a), note that some apparent sea surface temperature features are actually clouds in the visible picture, while the sunglint apparent in the visible picture is not detected by the infrared channel. These pictures reveal the importance of having both visible and infrared imagery simultaneously for accurate interpretation of phenomena and effects.

1B-10a. TIROS-N HRPT. Visible Picture (Channel 1), 0.5 n mi Resolution, Descending Node. 1915 GMT 15 June 1979. (Photo Courtesy of NOAA/EDIS.)

1B-11a. TIROS-N HRPT. Infrared Picture (Channel 4), 0.5 n mi Resolution, Descending Node. 1915 GMT 15 June 1979. (Photo Courtesy of NOAA/EDIS.)

This example of NOAA-6 Channel 1 (0.58–0.68 μm) data at 1847 GMT (0847 LST, 1B-12a) shows sunglint on the east side of the image. The islands of Oahu and Hawaii are faintly discernable. A large cloud plume extends downwind from the island of Hawaii. A dark gray shade is apparent extending southwestward from Oahu. This indicates a calm sea state region in the lee of the island. A simultaneous comparison of Channel 3 data is shown in 1B-13a.

Channel 3 (3.55–3.93 μm) data are strongly contaminated by sunglint during daylight hours. Note that the sunglint region over-powers the infrared signal due to strong reflection from the sea except over cloudy areas, and in the calm sea region in the lee of Oahu.

1B-12a. NOAA-6 APT. Visible Picture (Channel 1), 2 n mi Resolution. 1847 GMT 19 June 1980.

In the calm sea region, reflection to the satellite is reduced as indicated by the Channel 3 data and by the Channel 1 data (1B-12a). Such reduction of sunglint is normal in calm sea areas at the outer edge of a sunglint pattern. This application indicates the usefulness of Channel 3 data during daylight hours in locating such features.

Thin low clouds in Channel 3 daytime data appear black, implying a strong total energy response, because reflectance is much larger than that of the open ocean and temperatures are almost as warm. Higher cloud tops may have the same reflectance but the temperature is much colder, so the total energy transmittal to the satellite is reduced.

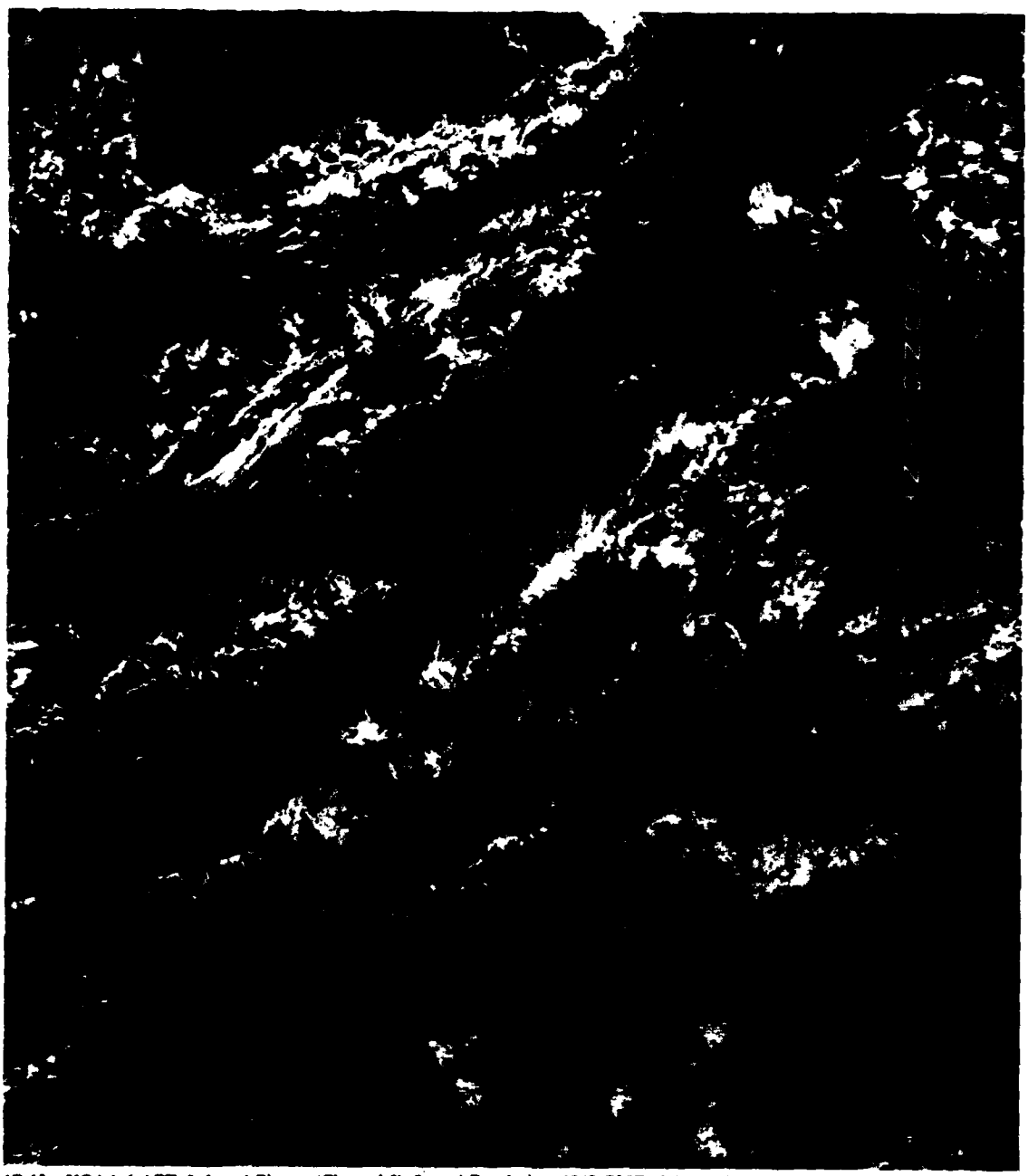

1B-13a. NOAA-6 APT. Infrared Picture (Channel 3), 2 n mi Resolution. 1847 GMT 19 June 1980.

Meteor

Since 1969, the U.S.S.R. has been operating a polar orbiting satellite system, Meteor. Meteor 1 is the experimental phase of the system. A few of these satellites are still active near the Soviet Union, but they are not in regular service. The Meteor 2 type spacecraft are providing fairly regular service to ground receiving stations of the Automatic Picture Transmission (APT) class since 1976, with three spacecraft being active—Meteor 2-7 in an evening pass (2109 GMT descending node), Meteor 2-8 in an evening pass (1905 GMT ascending node), and Meteor 2-9 in an afternoon pass (1214 GMT ascending node). The satellites are in near-polar orbits at an altitude of 900 km with an inclination of 81°. The orbital period of revolution for Meteor 2 is approximately 102 minutes, which produces 14.1 revolutions per day.

The APT video product obtained from the Meteor 2 spacecraft is similar to that of the TIROS N series of U.S. spacecraft, in that the APT data are output at a rate of 120 lines per minute. Over the U.S.S.R., data is transmitted directly to only three ground receiving centers: Moscow, Novosibirsk, and Khabarovsk. When out of communication range, data is recorded and stored on-board until the satellite passes over one of the receiving centers, where it is processed, reduced, and sent to the hydrometeorological center in Moscow for analysis and distribution to forecast centers (Stoldt, 1973).

The following is a brief summary of current Soviet metsat activity, provided in a recent memo by Dr. Grant A. Zehr, as monitored by reports and observations by amateurs in North America and Europe:

References

Stoldt, Norman W., and Peter J. Havanac, 1973: Compendium of meteorological satellites and instrumentation, NASA, Greenbelt, Md. pp. 301-359.

Zehr, Grant A., personal communication, 6 May 1983.

Current Soviet Metsat Activity—30 April 1983

Meteor 2 series

Spacecraft in the Meteor 2 series have provided APT service over the United States on a fairly regular basis recently. It appears that Meteor 2-7, 2-8, and 2-9 are the currently active spacecraft in this series. Amateurs have received imagery from these spacecraft since about 1976.

The orbit of these spacecraft is antegrade (angle of inclination is 81.2°) and not sun-synchronous. The orbital period is about 102.3 minutes. Amateur measurements of the orbital period suggest that it is a bit longer, perhaps 102.5 minutes.

Meteor 2 satellites are now using the frequencies of 137.3 and 137.85 MHz. In the past, 137.4 MHz has also been used. At the present time there are two satellites transmitting on 137.3 MHz (Meteor 2-7 and 2-9). Meteor 2-8 is currently active on 137.85 MHz. The satellites now transmitting on 137.3 MHz have similar orbits and follow each other by about 12 hours.

The video product is similar to that of the TIROS N series of U.S. spacecraft. The scan rate is 120 lines per minute which is compatible with the TIROS N product. The video signal is carried as an amplitude modulation of the audio subcarrier (similar to TIROS N APT). The frequency of this subcarrier is near 2400 Hz, but has been measured and is clearly not exactly 2400 Hz. At times, the frequency of this subcarrier has seemed to drift. The subcarrier does seem to fit within the simple bandpass filters centered on 2400 Hz which are used by many amateurs. An important difference lies in the fact that the subcarrier seems to disappear during the transmission of the synchronizing pulses. This means that systems which depend on locking on the 2400 Hz subcarrier will require modification to provide an alternate 2400 Hz signal. Phase lock detection systems may not work properly, either.

In contrast to the TIROS N series, there is only one product of the image received. This appears to be in the visible light spectrum, but at times some of the characteristics suggest an infrared image. The published spectrum of the visible image is 0.5 to 0.7 μm. This spectral range is similar to Channel 1 of the TIROS N series (0.55 to 0.90 μm). Amateurs have observed that the image from the Meteor 2 spacecraft tends to show a poor delineation of the land-water boundaries. This was also true of NOAA 7 when it was transmitting Channel 1 video for the visible portion of the APT signal. At this time, the NOAA 7 spacecraft has been switched to Channel 2 (0.725 to 1.1 μm) and this spectral range does provide much improved land-water contrast. Probably the published spectral range is correct for the Meteor 2 spacecraft now in service.

The Meteor 2 image does provide some advantages compared to the TIROS N image. There is excellent resolution of snow cover during the winter. Snow cover analysis is somewhat easier with the Meteor image. In addition, the resolution of the Meteor 2 image is somewhat greater (1 km) than the TIROS N APT signal (4 km).

Some amateurs have reported a very slow line rate infrared image being transmitted from these satellites during nighttime passes. I have heard this signal on several occasions, but it does not seem to be regularly available over the U.S.

Like the TIROS N APT, the Meteor image does not provide any gridding to orient the user. This fact, combined with the rather poor demarcation of the land-water boundaries, means that in some cases the

Meteor 2 image may be difficult to orient with respect to land masses or other geographical features (compared to the TIROS N image).

It must be remembered that the Meteor 2 satellites are at times switched off and may be unavailable even though the orbital predictions have been correctly prepared. In addition, the satellites appear to turn off their APT signal when the satellite passes into darkness. This may account for some unexpected results during the winter months as the satellites suddenly begin transmitting with a loud signal (being at closer range than predicted). The signal will also disappear abruptly as the spacecraft passes from light into darkness. This spacecraft characteristic complicates the gathering of data for orbital prediction.

As previously noted, these spacecraft have provided fairly regular service during the past six years. Having demonstrated the ability to be switched on and off, it is assumed that this service could be interrupted at any time.

Meteor 1 series

Spacecraft in the Meteor 1 series have been monitored by amateurs in North America on an irregular basis during the past five years. These spacecraft appear to serve a sort of experimental or testing function. They are not in regular service on a predictible basis.

These spacecraft are in a low, sun-synchronous orbit with an orbital period of about 97.5 minutes. This is a retrograde orbit with an angle of inclination of about 97°. It is believed that these spacecraft are the ones which have been heard on 137.15 MHz. Early in 1982 amateurs in the U.S. monitored similar spacecraft on 137.13 MHz. During the latter part of 1982 and early in 1983, transmissions from a Meteor 1 type spacecraft were monitored by Italian amateur radio operators. The frequency of these transmissions was 137.12 MHz. The orbital characteristics of the spacecraft on these frequencies coincide with those of the Meteor 1 series. A review of the NASA Satellite Situation Report does not suggest any other candidate which might be responsible for these transmissions. The spacecraft monitored most recently in Italy on 137.12 MHz has been identified as Meteor 1-30 using orbital data generated on an Apple II microcomputer.

The image from this series of spacecraft is also transmitted as an APT signal. The video is carried as an amplitude modulated audio subcarrier, similar to the TIROS N APT signal. The line rate for this image is 240 lines per minute. The synchronization segment of the scan line contains a four digit number and a gray scale. The significance of these numbers has not been learned.

The image from the Meteor 1 spacecraft shows panoramic distortion near the edge of the image. This contrasts with the TIROS N image which has a corrected image to eliminate panoramic distortion. The Meteor 2 image has little or no panoramic distortion.

The Meteor 1 spacecraft provide the best resolution of any APT signal yet available. Because of this, the satellites have been favorites among the amateur community.

Unfortunately, this satellite does not transmit regularly over North America. Signals were received in February and March of 1982 by at least six amateurs in the U.S. and Canada. The frequency was 137.13 MHz although some amateurs felt the correct frequency was 137.14 MHz. The satellite was observed in a north to south sun-synchronous orbit passing over North America with an overhead pass at about 10:30 a.m. local time. It was frequently transmitting an APT signal on Saturday mornings (local time).

Like the Meteor 2 series, no grid lines are available to orient the user with respect to land masses. This is not a serious handicap in the case of Meteor 1, however, since the imagery provides superior resolution of land-water boundaries. It is usually easy to orient the image with respect to land masses.

Section 2

Geostationary Satellites

Geostationary Satellite System

Five meteorological satellites in geostationary orbit (altitude 35,800 km) are to be maintained continuously on station above the equator, at intervals of about 70° longitude around the globe. Figure 2-1a shows the satellite subpoint (SSP) position and areal coverage of each satellite. As can be seen, this system will give continuous coverage of the Earth except for the polar regions.

The geostationary satellite system provides (1) data in the visible, water vapor (GOES and METEOSAT only), and infrared modes, (2) real-time transmission of these data (reformatted) to users, (3) relay of conventional meteorological data from remote data collection platforms to users, and (4) transmission of conventional meteorological charts via the satellite to users.

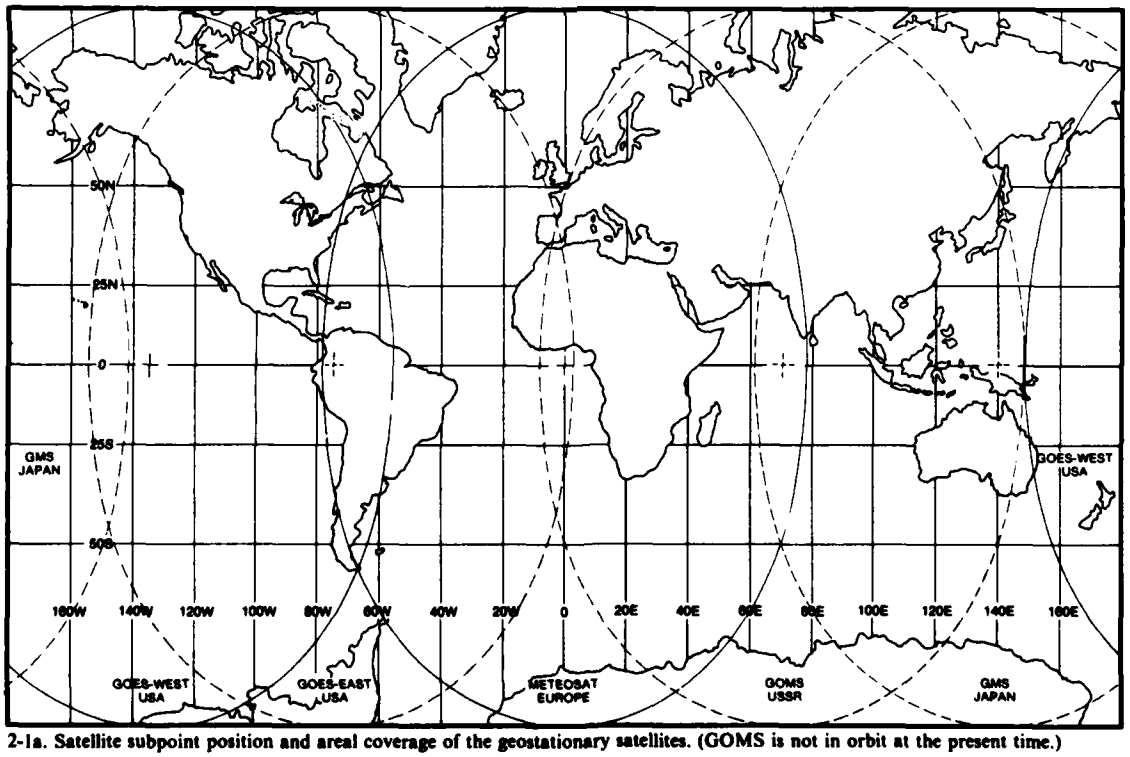

2-1a. Satellite subpoint position and areal coverage of the geostationary satellites. (GOMS is not in orbit at the present time.)

Earth Scanning Technique

The GOES, GMS, and METEOSAT spacecraft utilize a scanning radiometer telescope for obtaining visible, infrared, and water vapor data. The same principle for Earth scanning is used on each spacecraft; that is, horizontal lines of data are generated by a telescope imaging device looking out of the side of the spacecraft as it spins on an axis oriented parallel to the spin axis of the Earth. Successive contiguous lines are obtained by stepping the telescope in discrete increments (north-south) on successive rotations of the spacecraft. One rotation of the spacecraft generates one line of infrared data (plus one line of water vapor absorption band data in the case of GOES and METEOSAT) and either 2, 4, or 8 lines of visible data. A scan of the full Earth disc is accomplished in either 18 minutes (GOES) or 25 minutes (GMS and METEOSAT). Since it takes several minutes for the telescope to retrace to the starting position, a new full disc image can only be generated every thirty minutes. In addition to the normal scan mode, the telescope can be placed into a limited scan mode. In this mode, the north-south motion of the telescope is limited to a fewer number of line scans. This reduces the area of coverage, but increases the frequency of imaging.

The major characteristics of the geostationary imaging radiometers are listed in Table 1. Note that GOES and METEOSAT are the only spacecraft that have a water vapor channel and the scan mode for METEOSAT is east-west and south-north, which is opposite to the scan mode used on the GOES and GMS.

TABLE 1
GEOSTATIONARY SATELLITE RADIOMETER SUMMARY

		GOES	GMS	METEOSAT
Spin Rate (RPM)		100		
Line scan direction		W-E		E-W
Telescope step direction		N-S		S-N
Number of scan lines for full disc IR		1821	2500	
Number of VIS detectors		8	4	2
Resolution at SSP	VIS	0.5 n mi	0.7 n mi	1.4 n mi
	IR	5 n mi	2.8 n mi	2.8 n mi
	WV	5 n mi	—	2.8 n mi
Full disc scan time, minutes		18.21	25	
Sensor type	VIS	Photomultipliers		Si Photo Diode
	IR	Hg Cd Te		Hg Cd Te & WV
Spectral Response (μm)	VIS	0.55-0.75		0.4-1.1
	IR	10.5-12.5		10.5-12.5
	WV	6.7 (peak)		5.7-7.1

Determination of Ground Spatial Resolution

The ground spatial resolution of a geostationary satellite image degrades with distance away from the SSP due to the curvature of the Earth's surface when viewed from geostationary altitude (Glover, 1974). Figure 2-3a gives small circle arcs of normalized resolution degradation as a function of the resolution at the SSP (R_{SSP}). The figure shows that from the SSP to about 42° of arc away from the SSP the resolution degrades to 1.5 R_{SSP}. Beyond 42° of arc from the SSP the resolution degrades rather rapidly.

To determine the ground resolution of the imagery from a particular satellite at a given location, plot the location relative to the latitude/longitude of the SSP and then multiply the SSP resolution by the appropriate factor. For example, Monterey (x in 2-3a) is at 37° N, 122° W relative to GOES-West SSP at 0° N, 135° W. This gives a factor of approximately 1.4 R_{SSP}. Since GOES-West resolution at the SSP is 0.5 n mi for visible imagery, 5 n mi for infrared imagery, and 5 n mi for water vapor imagery, the resolution at Monterey is 0.7 n mi for visible imagery, 7 n mi for infrared imagery, and 7 n mi for water vapor imagery.

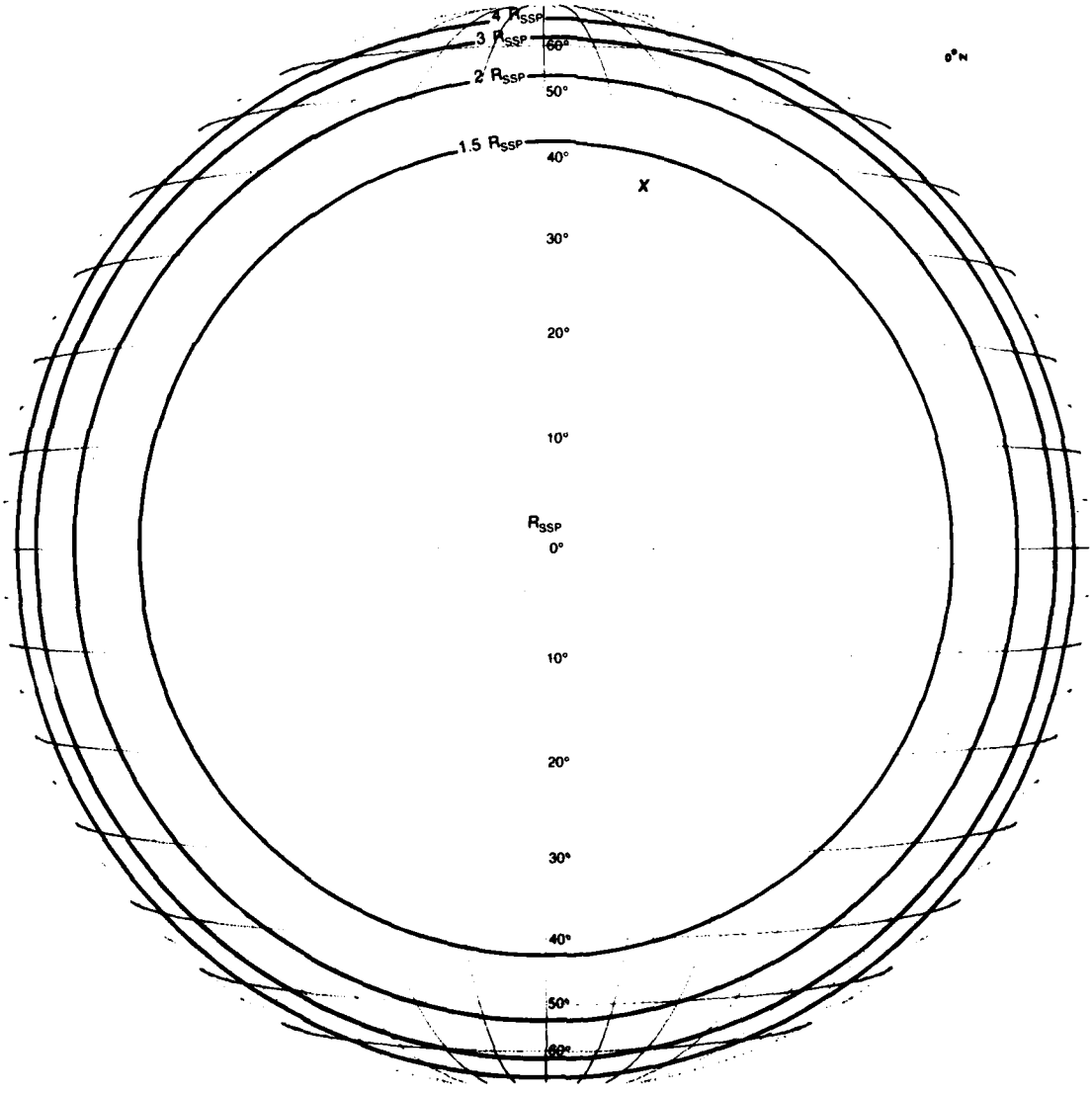

2-3a. Determination of ground spatial resolution.

Reference

Glover, J.C., 1974: Degradation of resolution in GOES imagery with distance away from the satellite subpoint. Unpublished Manuscript, NOAA/NESS, 4 pp.

Cloud Top Location Corrections

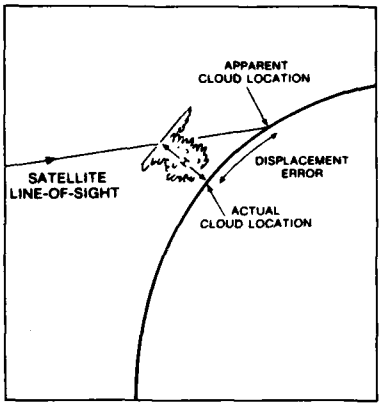

2-4a. Schematic illustrating an actual verses apparent cloud location.

Because the Earth's surface curves rapidly away from the geostationary satellite line-of-sight (2-4a), a cloud top at height **H** appears to be displaced from its actual position (NWS, 1977 and Weiss, 1978). For a cloud located precisely over the SSP, the apparent and actual cloud positions coincide, but the distance between the apparent and actual cloud positions (displacement error) increases in a direction away from the SSP as the cloud's distance from the SSP increases. The amount of the correction is also a function of cloud top height.

Figure 2-4b shows the calculated lines of equal displacement error for a 40,000 ft cloud top. An adjustment for cloud tops at other heights can be made as the error is essentially a linear function of height and would be 50% greater for a 60,000 ft top and 50% less for a 20,000 ft top. To correct for the displacement error and obtain the actual cloud top location, move the cloud top the amount of the error in a radial direction towards the SSP.

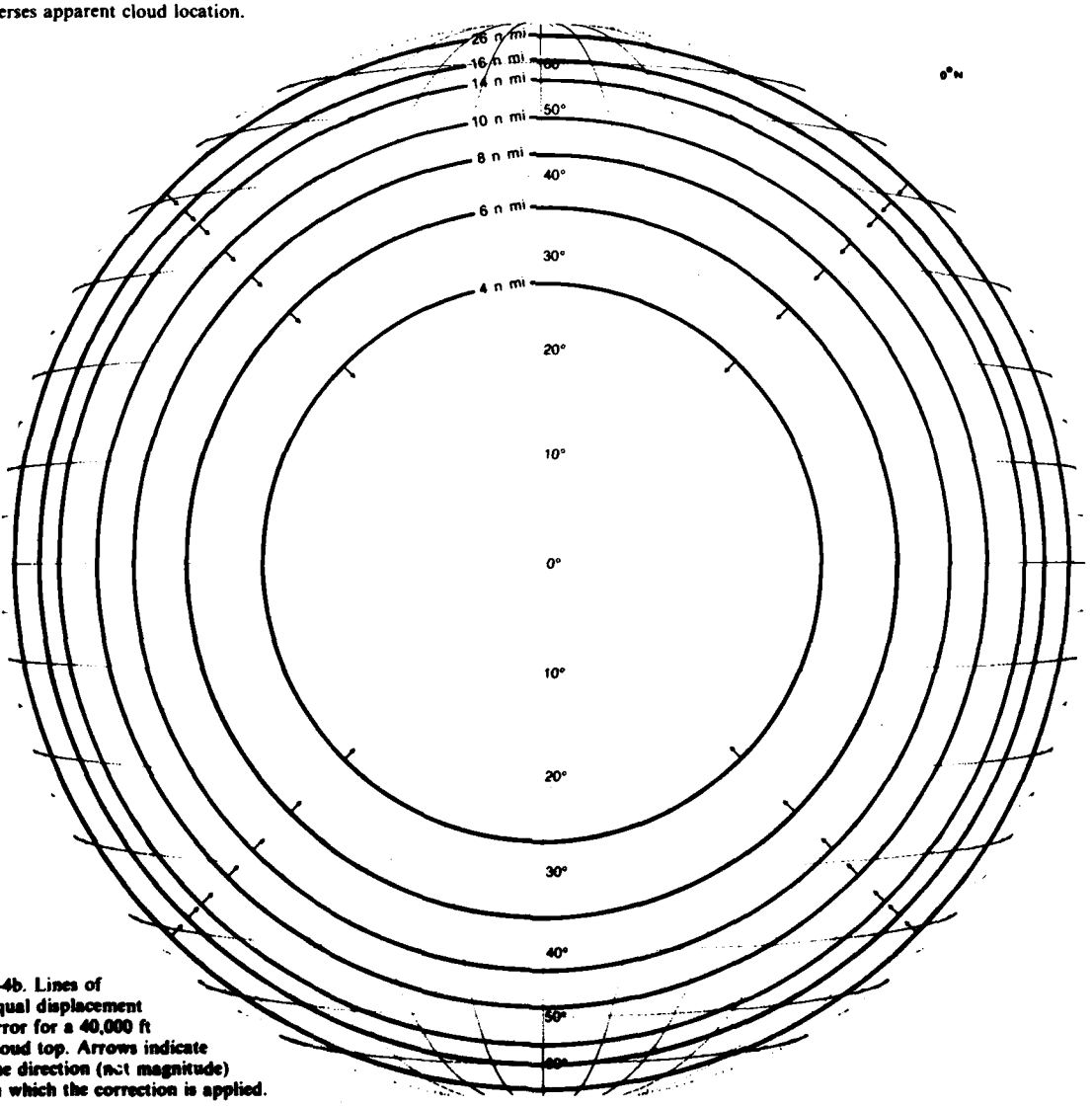

2-4b. Lines of equal displacement error for a 40,000 ft cloud top. Arrows indicate the direction (not magnitude) in which the correction is applied.

Universal Latitude/Longitude Grid

This universal grid can be used with any geostationary satellite imagery. Make an acetate copy to the desired size and label the latitudes and longitudes (dark lines appear every 10°) from the SSP.

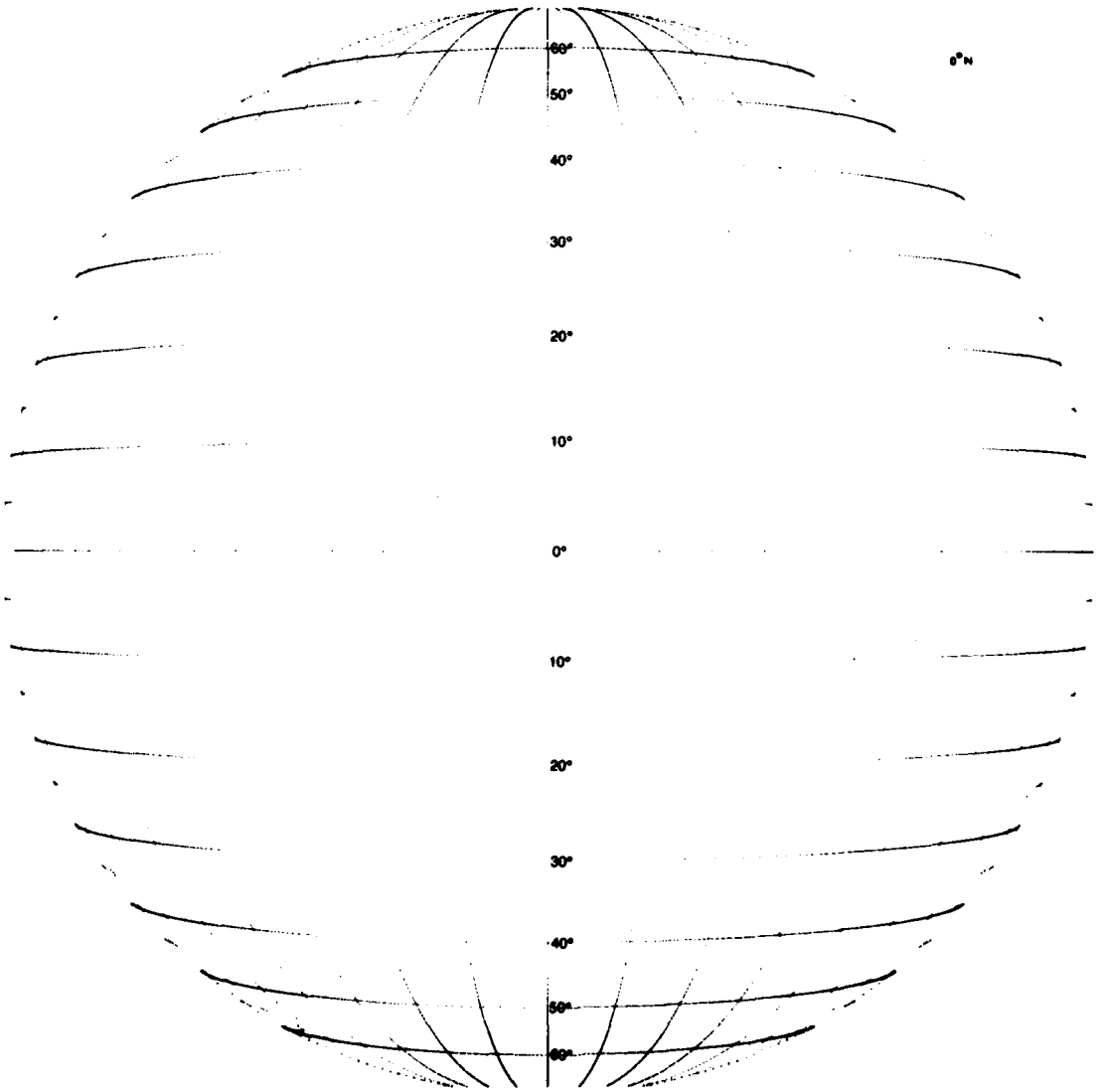

Image Distribution

The Panel on Meteorological Satellites (WMO, 1975) has worked with the multi-national sponsoring agencies developing geostationary satellite systems so that the modes of satellite data transmission to users are functionally similar. Thus, all spacecraft types (United States-GOES, Japan-GMS, Europe-METEOSAT, Soviet Union-not yet in orbit) make weather facsimile (WEFAX) transmissions on a common frequency.

In addition to WEFAX transmissions, each spacecraft type has another image distribution system. In the United States, a system called GOES-TAP uses surface, high-quality telephone lines to provide visible and infrared imagery for a wide variety of users. The European system has two fully independent spacecraft data transmission channels so that raw image data, high resolution facsimile data, and WEFAX data can be transmitted simultaneously. In contrast, these three data transmission functions must be time-shared in the Japanese system.

For naval operations, U.S. Department of Defense communication centers around the world provide radio facsimile transmissions of geostationary satellite imagery. The radio facsimile products are similar to the WEFAX products and ships can receive radio facsimile transmissions up to several hundred miles out to sea.

Data Display

In the field, geostationary satellite imagery transmitted on WEFAX or radio facsimile is usually displayed as hardcopy (film print or transparency). Current hardcopy display equipment converts analog data transmissions into discrete gray shades to provide a visual product. These image display devices are readily available, permitting wide distribution of the image products to operational users.

2-6a. Digital data display systems, such as the Naval Environmental Prediction Research Facility's Satellite Processing and Display System (SPADS), are currently under development. These systems will enable the user to obtain real-time winds from cloud motions, derived fields of motion, and false color enhancement of the imagery for highlighting selected phenomena. The user will also be able to superimpose conventional meteorological data and analysis on the satellite imagery and make time-lapse loops of a series of geostationary satellite pictures. These systems permit great flexibility in monitoring atmospheric and oceanographic phenomena in a quantitative manner.

References

NWS Central Regional Technical Attachment No. 77-G4, April 1977, Displacement error of satellite and tops. 4 pp.

Weiss, C.E., 1978: Cloud-location corrections near the horizon of an SMS image. Satellite Application Information Note 78/8, NWS/NESS, U.S. Dept. of Commerce, Washington, D.C. 8 pp.

World Meteorological Organization, 1975: World Weather Watch Global Observing System—Satellite Sub-System—Information on Meteorological Satellite Programmes Operated by Members and Organizations. UNIPUB, New York, N.Y., 74 pp.

Geostationary Operational Environmental Satellite
(GOES)

The United States currently operates two geostationary satellites, GOES-East with a satellite subpoint (SSP) at 75°W, 0°N and GOES-West with a SSP at 135°W, 0°N. Both satellites orbit at an altitude of 22,300 miles above the equator. GOES-East gives an areal coverage from Antarctica to Greenland and from Africa into the the eastern Pacific, while GOES-West areal coverage extends from Antarctica to Alaska and from the western Americas to the western Pacific.

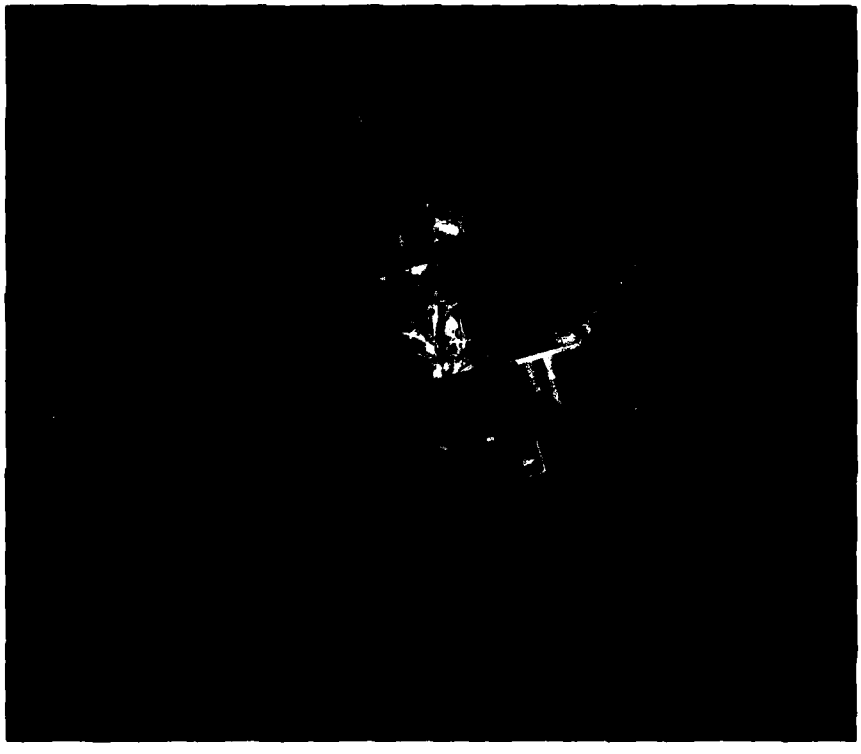

2A-1a. The main body of the GOES spacecraft is cylindrical, about 11'6" high and 7'1" in diameter, with an aperture in the side through which the radiometer telescope views the Earth. The outside of the spacecraft is covered with solar cells which supply power. Attached to the main body is a smaller cylinder supporting multiple elements of combined S-band and UHF antenna.

Image Acquisition and Distribution

The National Environmental Satellite, Data, and Information Service (NESDIS) of NOAA has implemented a central data distribution system to receive, process and distribute GOES visible and infrared spin-scan radiometer (VISSR) data to users in near real-time. The VISSR data-flow diagram (2A-2a) shows the system for communicating the image data to various users at numerous locations.

The GOES image distribution system begins with the acquisition of raw VISSR image data from the spacecraft by the Command and Data Acquisition (CDA) station at Wallops Island, Virginia. These data are received during the time that the radiometer views the Earth (approximately 20° of one full rotation). In the CDA, the raw VISSR data are processed in a synchronizer/data buffer (line stretcher) which reduces the bandwidth required for retransmitting the data. These stretched data are then retransmitted through the spacecraft and on to users during the remaining 340° of spacecraft rotation. Although the stretched data are transmitted at a slower rate than the raw data, quite sophisticated reception equipment is still required to receive it.

In addition, the lower data rate infrared imagery is formatted in the CDA for direct analog transmission via high quality telephone lines to Satellite Field Services Stations (SFSS), and for digital transmission via a special landline to the NESDIS Central Data Distribution Facility (CDDF) at Camp Springs, Maryland.

The NESDIS central facility, located at Suitland, Maryland, receives the stretched VISSR data from the satellite for in-house use and also relays the data via dedicated microwave link to the CDDF. The NESDIS-Suitland facility also receives infrared imagery via special landline for use by the NOAA/NESDIS large-scale data processing facility.

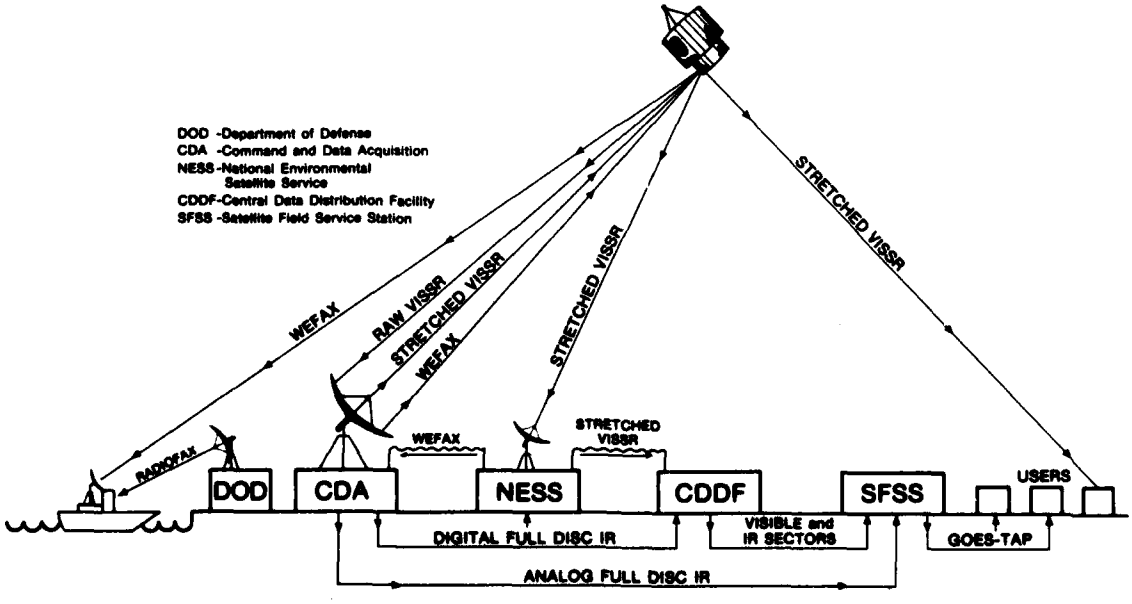

2A-2a. GOES Data Distribution.

At the CDDF, a series of sectorized units select and convert geographical areas of the full disc visible image into analog form, and subsequently make an analog transmission of the sectorized data to SFSS's. This data distribution system is called GOES-TAP. The sectors consist of specified geographical areas and have resolutions of 0.5, 1, or 2 n mi. The sectorizer operates in a serial fashion (i.e., it does not have the capability of receiving and transmitting data simultaneously) which causes the transmission of the sectors from the CDDF to be on a near real-time rather than real-time basis. The average data user in the United States requires data only in the Northern Hemisphere. Because of this, the sectorizer utilizes only 9 minutes of the 18 minute full disc imaging interval to receive the data. Approximately 17 more minutes are required for handling and transmission of the sectors, making it possible to complete the processing and transmission of the sectors well within the 30-minute interval between successive full disc VISSR readouts. Numerous sectors cover the contiguous 48 states, Alaska, and the North Pacific west to about 170°E. All standard sectors have automatically implanted geographical grids.

Infrared data are also sectorized at the CDDF to provide equivalent infrared sectors with the same geographical coverage as the 1 n mi resolution visible sectors. This facilitates the comparison of visible and infrared imagery. The CDDF also has the capability of temperature (infrared) enhancement to highlight selected features in the imagery (e.g., sea surface temperatures, severe storm cloud top temperatures, etc.).

The SFSS's receive sectorized data from the CDDF and the full disc infrared data from the CDA over high quality telephone lines. Since only one sector at a time can be transmitted over a single line, several lines to each SFSS are needed for simultaneous transmission of several sectors. A user in line with a SFSS may receive any one of the standard sectors available to the SFSS every 30 minutes. The user may vary his choice of sectors so long as he remains within the data set available to the SFSS to which he is connected.

Ships or remote land stations within a 60° small circle arc of the SSP may receive imagery on the WEFAX channel. The WEFAX data are centrally produced by the NOAA computers in Suitland, Maryland, and then transmitted through the spacecraft and on to users from the CDA. Since WEFAX broadcasts are on the same frequency as the stretched VISSR data, WEFAX broadcasts are scheduled only in the 12-minute interval between successive VISSR readouts.

The WEFAX product line consists of both visible and infrared full disc imagery transmitted in sections or chips. Each chip requires slightly more than four minutes for transmission. Complete full disc coverage in both the visible and infrared channels (at 4 n mi resolution at SSP) requires the transmission of four chips. Each chip covers an area from the equator to 60°N (or S), and 60°E (or W), from the central longitude. Requests for information on ground equipment requirements, data reception, and WEFAX products and schedules may be addressed to:

National Climatic Center
Satellite Data Services Center
NOAA/National Environmental Satellite,
Data, and Information Services
Washington, D.C. 20233

Sensor System Description

At the spacecraft (2A-4a), radiation from the Earth image scene enters an aperture and is reflected 45° by an object-space scan mirror. This mirror is an elliptically-shaped plane mirror that is tilted about its axis to obtain the north-south scan steps. Radiation reflected from the scan mirror enters a Cassegrain telescope (primary and secondary mirrors) which focuses the radiant energy onto the detector array.

At the detector array, visible spectrum energy is collected by eight fiber optics and passed on to eight separate photomultiplier tubes (PMT's) *which respond in the 0.55–0.75 μm range.* Each PMT has an instantaneous field-of-view (IFOV) of 0.021 by 0.025 milliradians which gives a spatial resolution at the SSP of approximately 0.5 n mi. On-board the spacecraft, the voltage output from each PMT is converted to one of 64 digital count values proportional to the amount of reflected solar radiation received. A conversion in the digital count is made so that there is more contrast between dark objects in the imagery (terrain features) than in light objects in the imagery (highly reflective clouds).

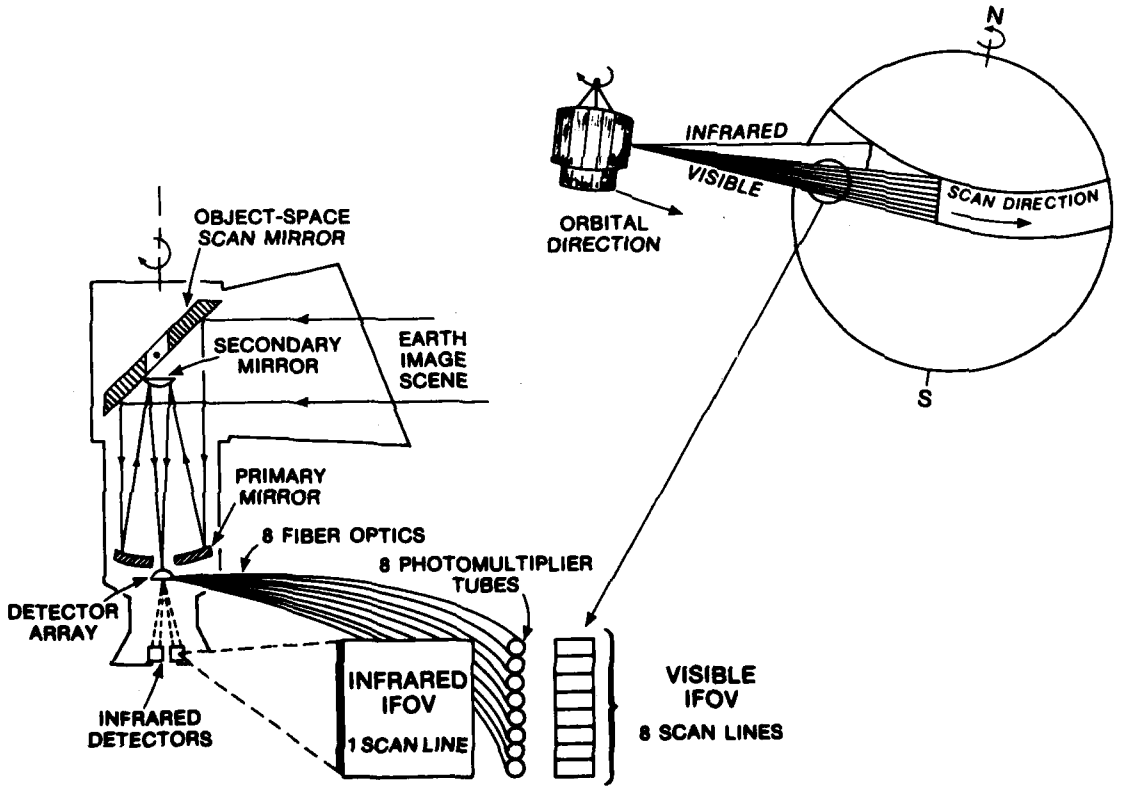

2A-4a. Schematic of the GOES VISSR optics.

Infrared imagery is also relayed and filtered from the detector array to two identical (one primary, one redundant) infrared detectors. The detectors are mounted on a plate that is passively cooled by a radiation device to a controlled temperature of 95° K so as not to interfere with detected Earth scene radiation. Optical filters pass only radiation in the 10.5–12.5 μm region. Each infrared detector has an IFOV of 0.192 by 0.192 milliradians which gives a spatial resolution of 5 n mi at the SSP. In order to better define sharp temperature gradients, the infrared detector is oversampled in the along-scan direction resulting in a 50% overlap in the IFOV of adjacent samples. Although these data are displayed as 5 by 2.5 n mi rectangles, the instantaneous resolution remains 5 by 5 n mi.

The infrared detector output is normalized in terms of the equivalent blackbody temperature of the radiating object so that the detector output is a simple, nearly-linear function of scene temperature. The infrared temperature sensitivity is a 0.5° K change in the range of 330°–242° K, and 1.0° K change from 242° to 163° K. The net equivalent temperature difference (NETD) of the GOES is a 0.3° K change across the entire temperature range sensed.

Since 1974, operational geostationary satellites have provided users with only visible (VIS) imagery, and infrared (IR) imagery in the 11.5 μm window. In November 1980, GOES-4 was launched with a new version of the VISSR, called the VISSR Atmospheric Sounder (VAS), that will be carried on all future GOES satellites. It has a radiometer possessing the standard visible channel detector array, plus six thermal detectors that sense IR radiation in 12 spectral bands. One of these spectral bands is the 6.7 μm moisture channel which was chosen for initial operational evaluation, since it directly augments the standard 11.5 μm window channel IR by providing the operational meteorologist with additional information for diagnosing and monitoring upper-tropospheric flow.

Moisture channel imagery helps to define the large-scale upper-level flow better than IR in areas devoid of wind reports and cirrus cloud motion vectors. It also helps to more precisely locate and diagnose upper-level circulation features such as wind maxima, circulation centers, and deformation zones. It is possible to infer a great deal about the upper-level flow patterns from the motions of cirrus and the evolution of large-scale cloud formations as they appear in the IR window channel. The IR moisture channel makes this process easier since it shows the spatial continuity of upper-level moisture and cloud fields which are related to circulation features. Moisture patterns are present even when clouds are absent, thus providing clues to the upper-level flow.

In October 1981, NESS began providing users of GOES-West imagery with two pictures per day from the 6.7 μm IR moisture channel, one at 0015 GMT and one at 1215 GMT. In February 1982, the number was increased to once every six hours. The 6.7 μm data currently being sent to users from GOES-West is 8.7 n mi (14 km) resolution; the standard 11.5 μm IR from this satellite is 4.3 n mi (7 km) resolution.

Spectral Characteristics

The GOES spacecraft carries a VISSR which measures reflected solar radiation in the 0.55–0.75 μm region during the daylight, emitted Earth, atmosphere, and cloud radiation in the 10.5–12.5 μm region, and moisture in the 6.7 μm region day and night. The normalized sensor response curve of the GOES visible channel is shown in 2A-6a. Comparison of this sensor's response curve with the color spectrum of visible light reveals that the sensor has no response in the blue light region (<5 μm). This eliminates the effects of blue light backscattering of the atmosphere. The peak response of the sensor is in the green and red

portions of the visible spectrum with the response decreasing, but extending slightly into the near infrared. Imagery obtained from this sensor is used for daytime mapping of the Earth's surface and cloud cover.

Imagery obtained from the VISSR infrared sensor is used for determining the temperature of the radiating surface and for continuous cloud cover mapping day and night. The normalized response curve of the GOES infrared sensor is shown in 2A-6b. The 10.5–12.5 μm range is used because it contains the peak radiations emitted by the Earth and its atmosphere and also because it is within an atmospheric window more

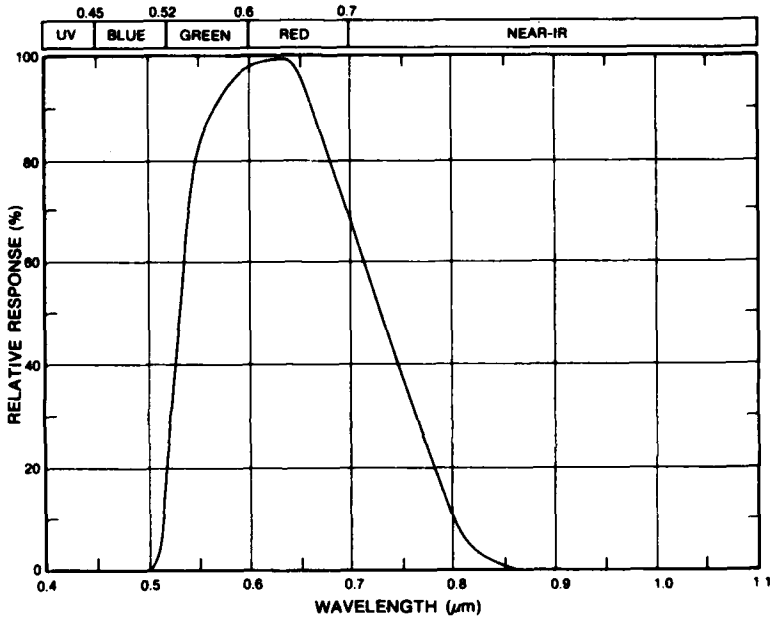

2A-6a. GOES visible channel normalized sensor response curve.

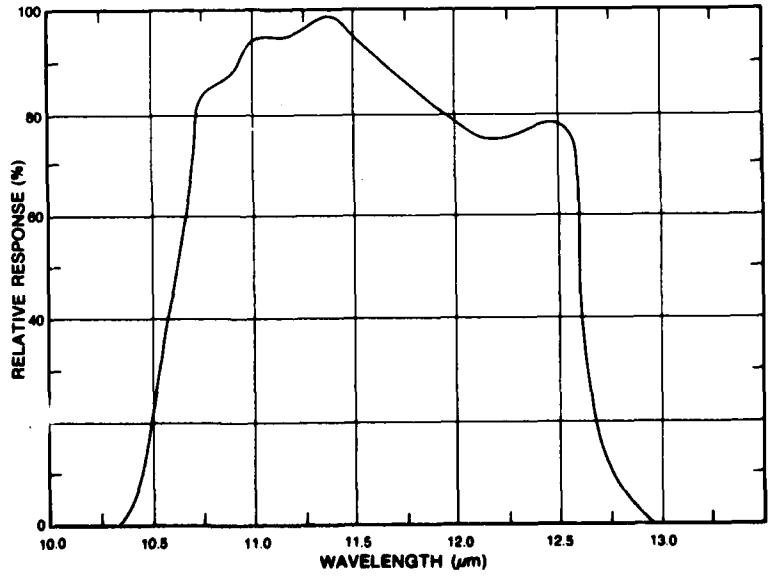

2A-6b. GOES infrared channel normalized sensor response curve.

transparent than other adjacent wavelengths to outgoing radiation. When examining infrared imagery qualitatively and quantitatively, it is important to note that infrared radiation in this range is attenuated by water vapor, aerosols, carbon dioxide and ozone. Depending on atmospheric conditions then, the Earth's surface temperature can appear to be 1.0°-10.0° K lower at the satellite sensor. The temperature corrections are estimated to range from 1.0° to 10.0° K for water vapor, 0.1° to 1.0° K for aerosols, and 0.1° K for carbon dioxide and ozone. Although there is no absolute calibration of the infrared sensors on GOES, data corrected for atmospheric attenuation have verified well with ground truth and appear consistent.

For additional information on the GOES spacecraft, contact:

National Climatic Center
Satellite Data Services Center
NOAA/National Environmental Satellite,
Data, and Information Services
Washington, D.C. 20233

References

Anderson, R.K., J.J. Gurka, and S.J. Steinmetz, 1982: Application of VAS multispectral imagery to aviation forecasting. Preprints, Ninth Conference on Weather Forecasting and Analysis, Seattle, Am. Met. Soc., p. 227-234.

Bristor, C.L., 1975: Central processing and analysis of geostationary satellite data. NOAA Tech. Memo. NESS 64, U.S. Dept. of Commer., Washington, D.C., 155 pp.

Corbell, R.P., C.J. Callahan, and W.J. Kotsch, 1976: The GOES/SMS Users Guide. Management and Technical Services Company, Rep. No. NAS 5-20694, 118 pp.

Sample Imagery, GOES

Figures 2A-8a and 9a are examples of corresponding visible and infrared pictures from the GOES-4 spacecraft. Figure 2A-9b is a picture from the latest GOES sensor—a moisture channel to directly augment the standard IR channel by providing the operational meteorologist with additional information for diagnosing and monitoring upper-tropospheric flow. As in the infrared imagery, the whitest portions of the picture in a water vapor display are always the highest cloud tops.

2A-8a. GOES-W. Visible Picture. 2345 GMT 4 September 1981.

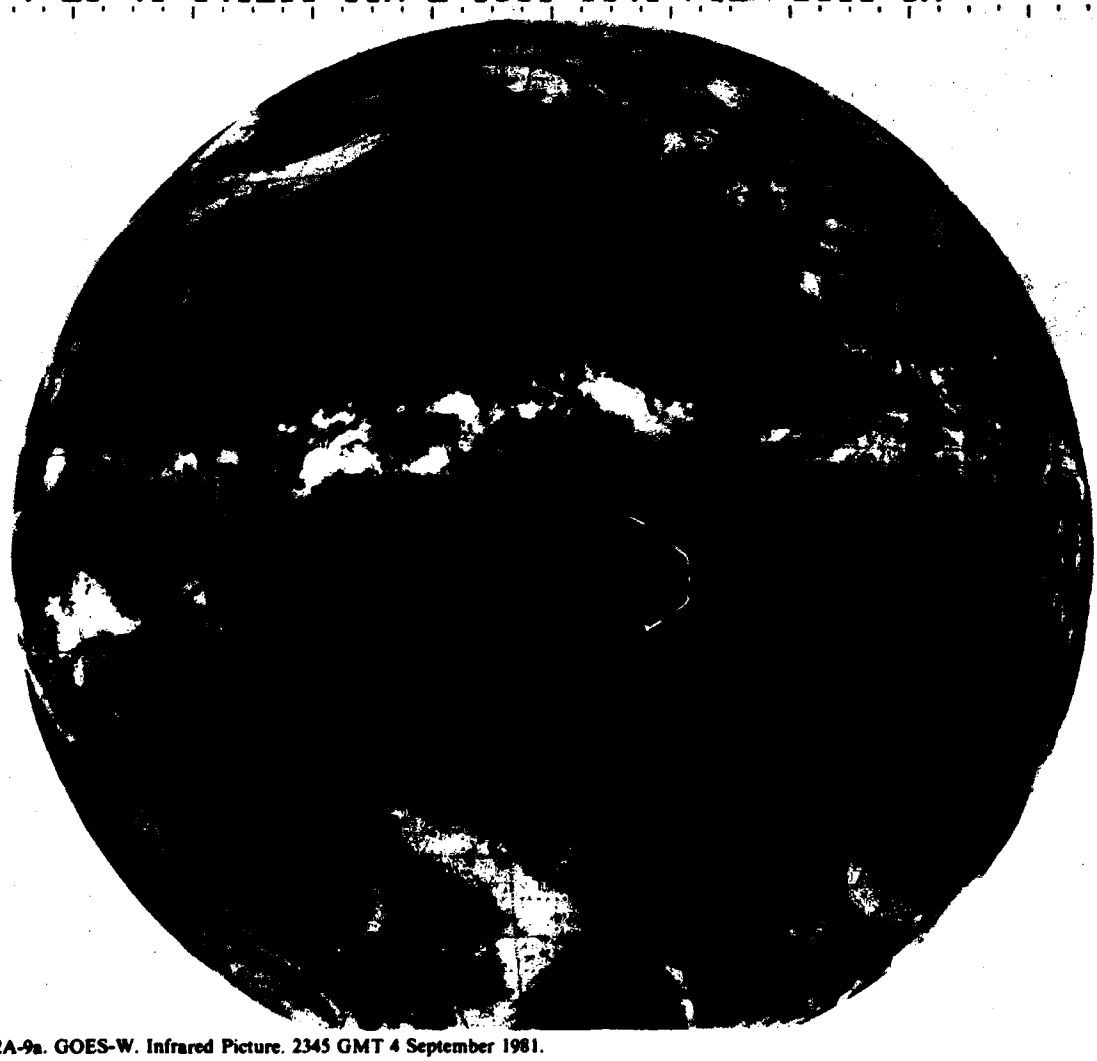

2A-9a. GOES-W. Infrared Picture. 2345 GMT 4 September 1981.

2A-9b. GOES-W. Water Vapor Picture. 0015 GMT 5 September 1981.

Figures 2A-10a and 11a are examples of simultaneous visible and infrared pictures from the GOES-East spacecraft during the northern hemisphere winter. The visible picture shows sunglint off the northwest coast of South America, considerable cloudiness over much of the Atlantic and Pacific Oceans, and a large clear area behind a cold frontal cloud band off the U.S. east coast. The infrared picture reveals the strong thermal boundaries of the Gulf Stream, upwelling of cold water in the Gulf of Tehuantepec, and the relative heights (temperatures) of the clouds. The brightest clouds are the highest and coldest, while the medium gray clouds are lower and warmer. The land masses are the darkest and warmest.

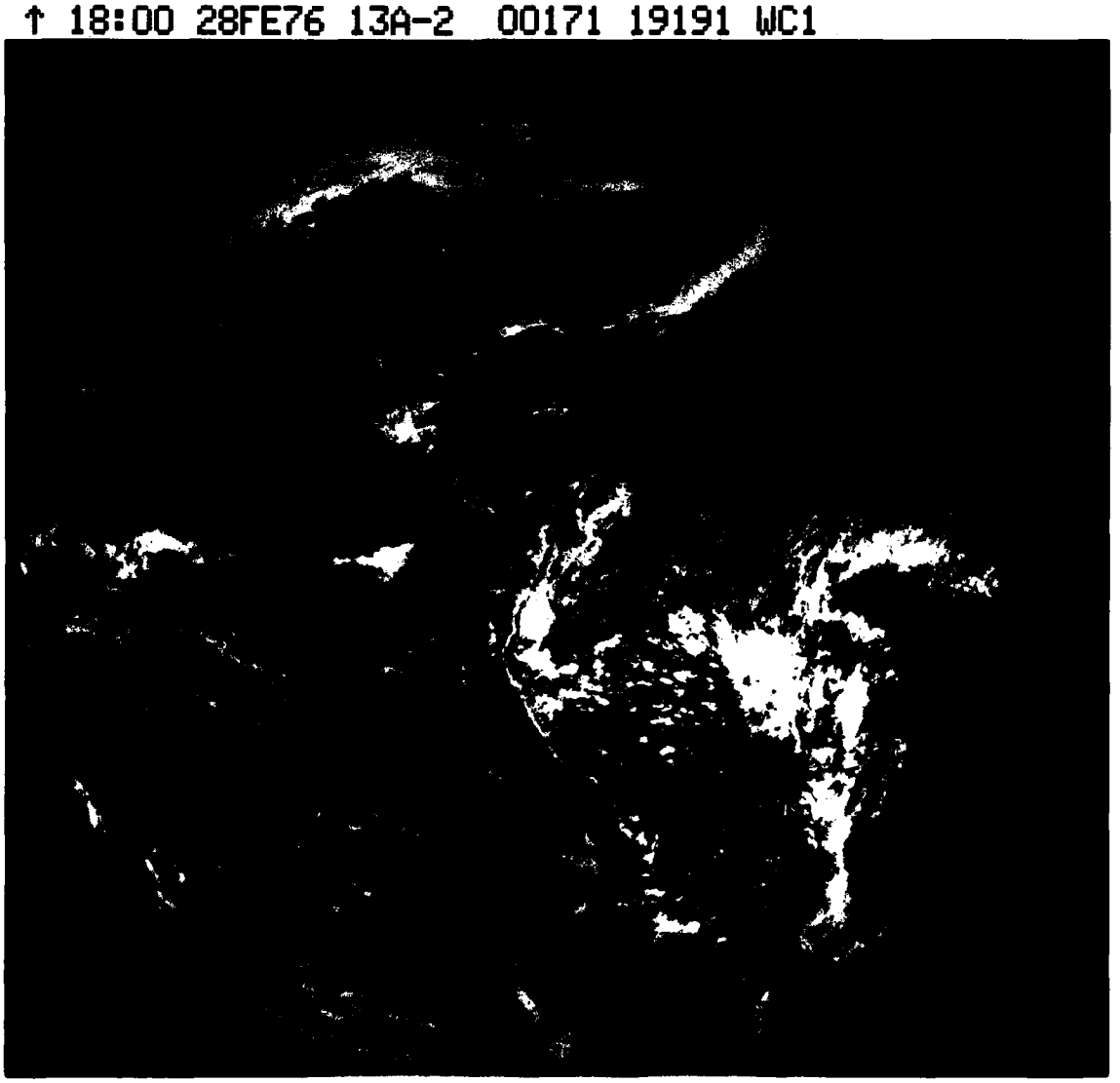

2A-10a. GOES-E. Visible Picture, 2 n mi Resolution. 1800 GMT 28 February 1976.

18:00 28FE76 13A-Z 0006-1640 FULL DISC IR

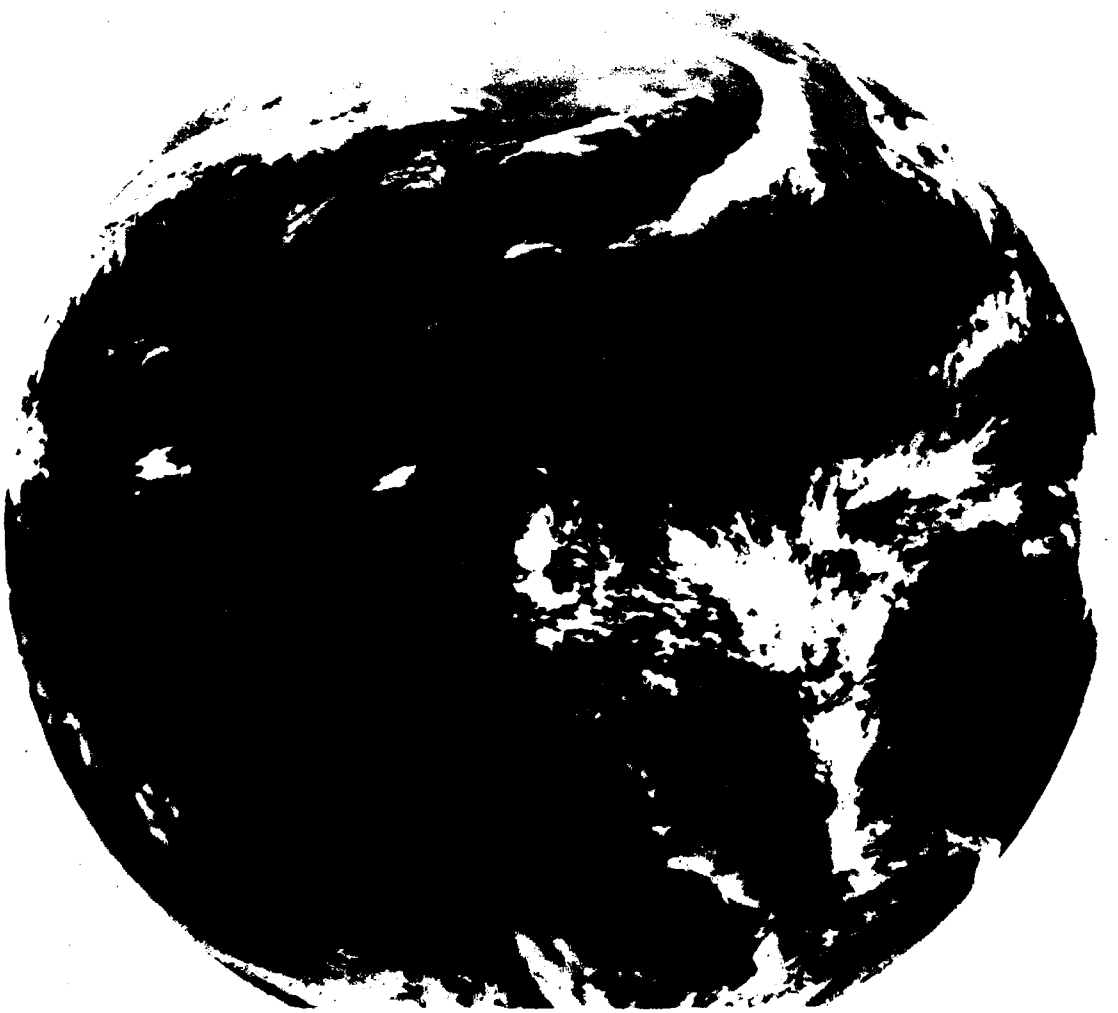

2A-11a. GOES-E. Infrared Picture, 5 n mi Resolution. 1800 GMT 28 February 1976.

Figures 2A-12a and 13a are simultaneous views of the Earth from GOES-West. The western portion of North America appears in the upper right corner, while the wide expanse of the Pacific Ocean is visible beneath the cloud free skies in the remainder of the picture. Cirrus cloudiness associated with the subtropical jet stream stands out well in the infrared picture, but is difficult to distinguish in the visible. The large area of cellular cloudiness west of Baja California occurs in the northerly flow around the high pressure area over the eastern North Pacific.

2A-12a. GOES-W. Visible Picture, 2 n mi Resolution. 2045 GMT 31 May 1979.

↑ 20:45 31MY79 35A-Z 0006-1640 FULL DISC IR

2A-13a. GOES-W. Infrared Picture, 5 n mi Resolution. 2045 GMT 31 May 1979.

GOES IMAGERY CODED IDENTIFICATION HEADER

GOES HEADER	1230	27JN79	12A-2		01044	18162	DB5 (sector identification see below)				
Coding Elements	a	b	c	d	e	f	g	h	i	j	k

Coding Elements

a Greenwich time in hours and minutes indicating time of actual picture start.

b Calender day, month, and year.

c Line stretcher/data buffer identification:

Identifier	Satellite
1	GOES-East
2 or 3	GOES-West

d Satellite Identification:

Identifier	Satellite
1	SMS-1
2	SMS-2
3	SMS-3
4	GOES-2
5	GOES-3

e Image type:

Identifier	Image type
A,B,C,D	Visible sectors
E	Equivalent IR sector
A-Z	Full-disc IR

f Image resolution:

Identifier	Resolution
1	0.9 km x 0.9 km (0.5 n mi x 0.5 n mi)
2	1.8 km x 1.8 km (1 n mi x 1 n mi)
4	3.7 km x 3.7 km (2 n mi x 2 n mi)
E*	9 km x 9 km (4.85 n mi x 4.85 n mi)

*Equivalent IR sector, same geographical area as corresponding visible sector.

g Enhancement curve identifier for IR data only. A single letter, Z, identifies the enhancement curve used on full-disc IR data. On all other IR data, the enhancement curve displayed is identified by two letters (AA-ZZ). Absence of letters indicates no enhancement of data.

h Starting scan line number for the image (Y-axis). Range: 0000-1821.

i Vernier correction factor for starting scan line number.

j The X-axis element number of the midpoint of each horizontal line contained in the sector. Range: 0000-3822.

k Vernier correction factor for sector center location.

Sector Identification

	Standard Sector	Floating Sector	Rapid Scan Sector
GOES HEADER	DB5	DA37N82W-1	PQ35N95W-1
Coding Elements	a b c	a b d e f	g h i j k

Coding Elements

a Major NESS hub (SFSS or regional area requirement) for which the sector is generated.

Identifier	Station	Identifier	Region
A	Anchorage	W	Washington complex production only (not transmitted over GOES network).
D	Washington, D.C.		
H	Honolulu	WB	4 km (2 n mi) geographical sector with 2 km (1 n mi) resolution.
K	Kansas City		
M	Miami	WC	9 km (4.85 n mi) full-disc with 4 km (2 n mi) resolution.
S	San Francieco		
U	Universal		

b Sector resolution. (See f above.)

c Identifier number for the specific standard sector (1-9).

d Latitude of image center point.

e Longitude of image center point.

f Identifier number for the selected floater (1 or 2).

g Identifier for type of scan:

Identifier	Scan
P	Partial disc
L	Limited scan

h Identifier for cycle time of the rapid scan data.

Identifier	Scan Cycle
(1-9)	Number indicates approximate minutes of scan cycle.
Q	15 min. (standard scan cycle).

i Latitude of image center point.

j Longitude of image center point.

k Identifier number for the selected floater (1 or 2).

This information was taken from the following publication:
Corbell, R.P., et al., 1976: The GOES/SMS User's Guide. National Environmental Satellite Service, NOAA, Washington, D.C.

Figures 2A-14a and 15a are examples of visible and enhanced infrared imagery transmitted on the GOES-TAP distribution system over the eastern U.S. The infrared image has been enhanced according to the MB curve. This curve is designed to highlight thunderstorm cloud top temperatures and thus helps isolate the areas of most intense convective activity.

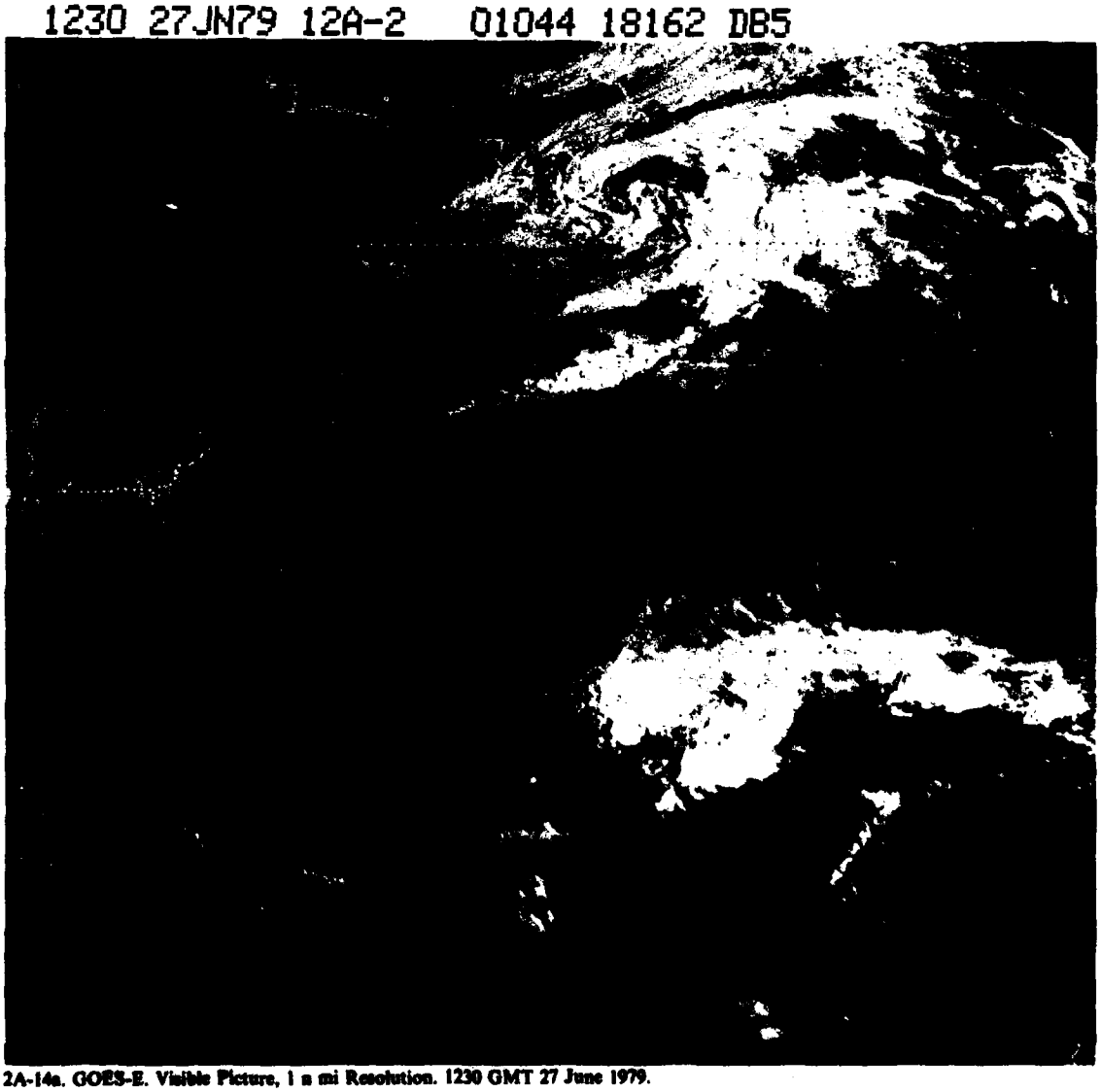

2A-14a. GOES-E. Visible Picture, 1 n mi Resolution. 1230 GMT 27 June 1979.

Infrared Temperature Gray Scale

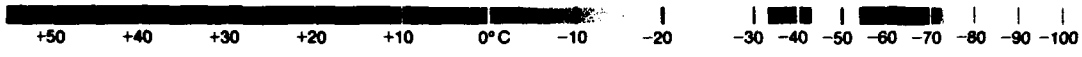

Temperature values are marked at ten degree intervals, from +50° C to −100° C, along the bottom of the gray scale. The gray shades are a photographic display of the enhancement curve used for the picture. Uniform changes in the gray shades from black to white in the lower end of the scale, in this example, correspond to linear temperature changes. Abrupt changes in the gray shades at the upper end of the scale, in this example, designate temperature steps in the enhancement curve to obtain "contouring" of the temperature features in the picture, as shown in the figure below.

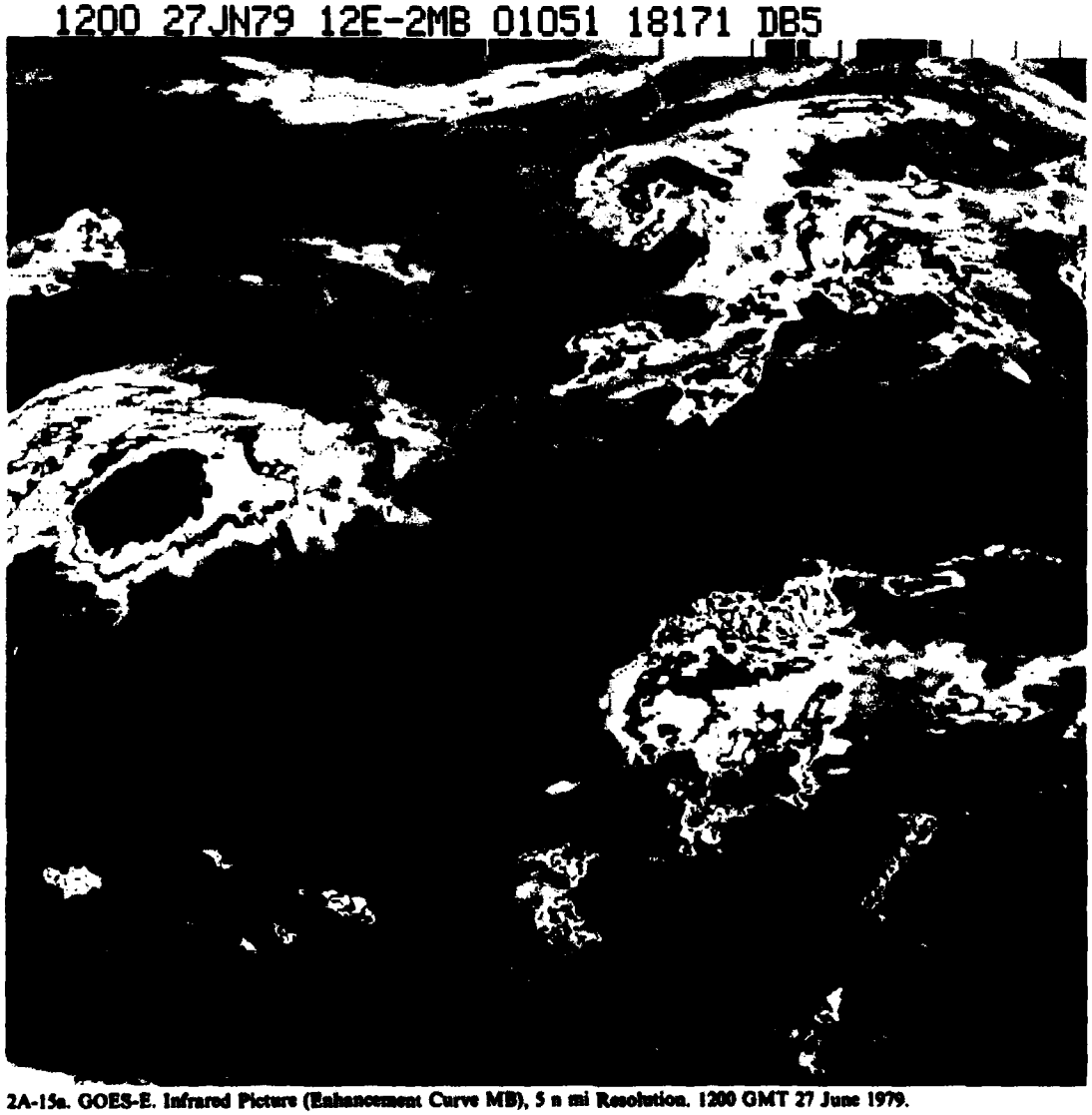

2A-15a. GOES-E. Infrared Picture (Enhancement Curve MB), 5 n mi Resolution. 1200 GMT 27 June 1979.

European Geostationary Meteorological Satellite
(METEOSAT)

The European Space Agency (member-states Belgium, Denmark, France, Italy, Sweden, Switzerland, the United Kingdom, and West Germany) currently operates one geostationary satellite, METEOSAT-2, which has a satellite subpoint (SSP) at 0°E, 0°N. This position gives METEOSAT an areal coverage from Antarctica to Greenland and from Saudi Arabia to Brazil.

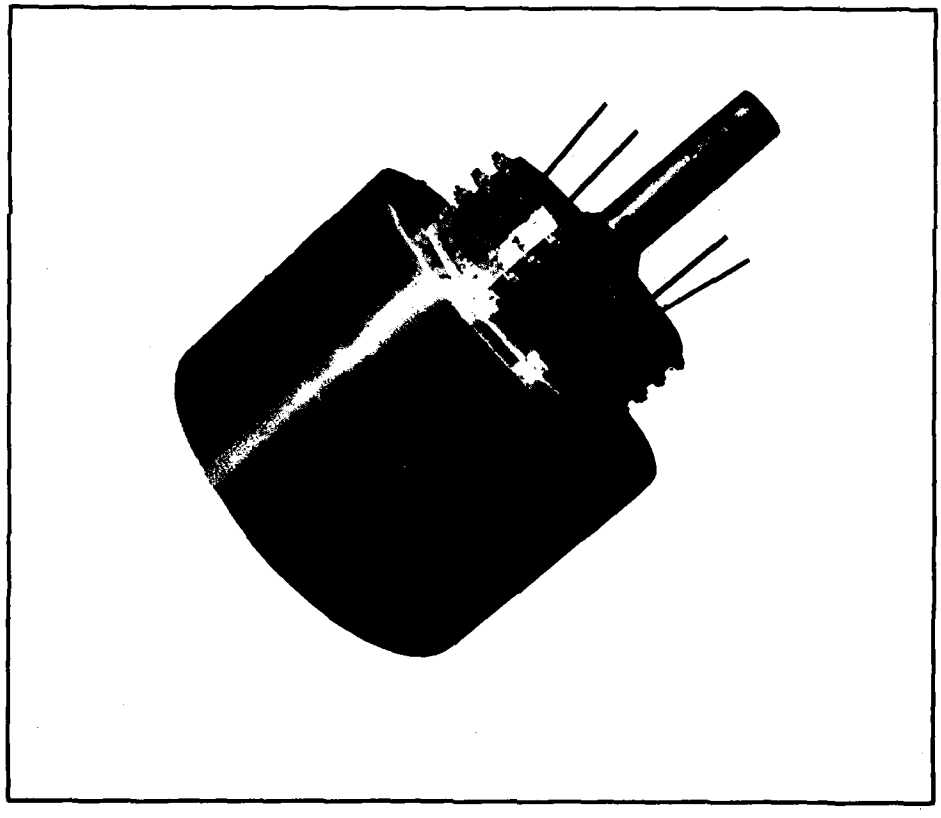

2B-1a. METEOSAT is composed of a main cylindrical body, 82 inches in diameter, on top of which a drum-shaped section and two cylinders are stacked concentrically. The main cylinder contains the radiometer aperture and arrays of solar power cells, while the drum-shaped section contains elements of the combined S-band and UHF antennas. The thin concentric cylinders on top are additional antennas for S-band and low UHF.

Image Acquisition and Distribution

The METEOSAT image distribution system (2B-2a) begins with the acquisition of stretched VISSR image data (visible, infrared, and water vapor) from the spacecraft by the Data Acquisition, Telemetry, and Tracking Station (DATTS) which is situated in open country some 30 mi southeast of Darmstadt, West Germany. Stretching of the raw radiometer data is done by an on-board computer unit, although should the unit fail, raw radiometer data can be broadcast directly to the ground. At DATTS, the stretched data are preprocessed and timing data are entered. The data are then relayed by landline to the European Space Operations Center (ESOC) located in Darmstadt.

At ESOC, the stretched image data are processed to remove calibration errors, variations in satellite spin speed, etc., and to mutually register the three channels of data. Because the detectors for the three channels of data are at physically different locations on the focal plane of the telescope, the data values for the same locations in the data chain do not correspond to the same Earth location. The process used to mutually register the three channels of data is called image conditioning. After image conditioning, special computers format the data for digital transmission (HR-FAX) to Primary Data User Stations (PDUS) and analog transmission (WEFAX) to Secondary Data User Stations (SDUS). For broadcast, the facsimile data are relayed back to DATTS and transmitted through the spacecraft on to users.

Both types of facsimile imagery have latitude/longitude grids and coastlines added before transmission. In the case of WEFAX images this information is superimposed on the actual picture, but with HR-FAX images it is added to the transmission as coded data to be used at the discretion of the individual user.

Images from all three spectral channels (visible, infrared, and water vapor) are included in the distribution schedule, which is designed to cover the entire METEOSAT field-of-view once every three hours and the European region every half hour. In addition, imagery from the GOES-East satellite is relayed through a station at Lannion, France, and rebroadcast through METEOSAT to users at selected times.

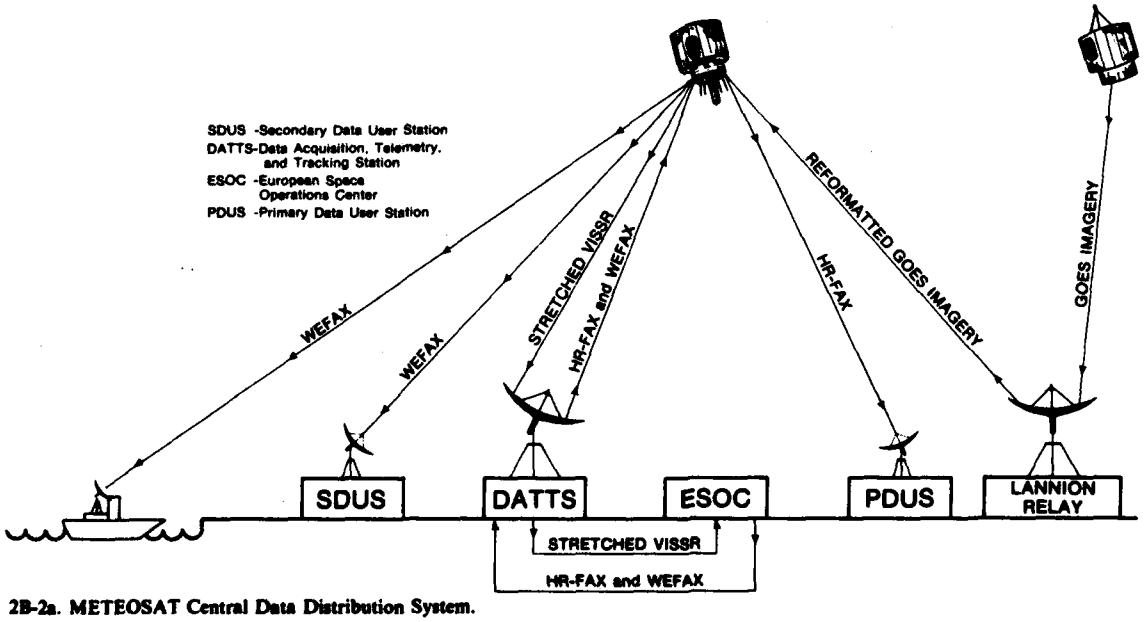

2B-2a. METEOSAT Central Data Distribution System.

Formats used for HR-FAX digital transmissions include format A (2B-3a) which covers the full Earth disc and is transmitted once every three hours, and format B which is a sector covering the European region and is transmitted every half hour. A and B formats include data from all three spectral channels multiplexed on a line by line basis. This allows the user to select the channels as needed or to combine the channels in real-time by employing line buffers in the receiving equipment.

Figures 2B-3a and 3b show the areal coverage of formats used for the transmission of WEFAX sectors. The C formats are used for transmission of high resolution visible data. A total of 24 sectors covers most of the full Earth disc. Of the C formats, the European formats C2 and C3 are transmitted at half hourly intervals and the remaining sectors are transmitted at intervals of between one and three hours during daylight.

The D and E formats are used to transmit the infrared and water vapor band imagery. The European infrared sector D2 is transmitted every half hour with full disc coverage in all infrared D sectors at least once every three hours. The nine E sectors used for water vapor band data are transmitted at least twice each day.

Sensor System Description

At the METEOSAT spacecraft, radiation from the Earth scene enters a telescope aperture, is focused by the primary telescope, and is reflected along the spin axis of the spacecraft to two different focal planes. One focal plane contains two visible sensors while the second focal plane contains three infrared sensors.

In the focal plane of the visible sensors, two silicon diode detectors collect reflected Earth, atmosphere, and cloud radiation in the 0.4–1.1 μm range. Each visible detector has an IFOV of 0.065 by 0.065 milliradians which gives a spatial resolution of 1.6 n mi at the SSP. When the water vapor channel is in operation, only one visible detector can be sampled. This reduces the spatial resolution of the visible data to 3.2 n mi in the north-south direction. The resolution in the east-west direction remains 1.6 n mi.

2B-3a. HR-FAX digital transmission formats (A and B) and WEFAX visible imagery formats (C).

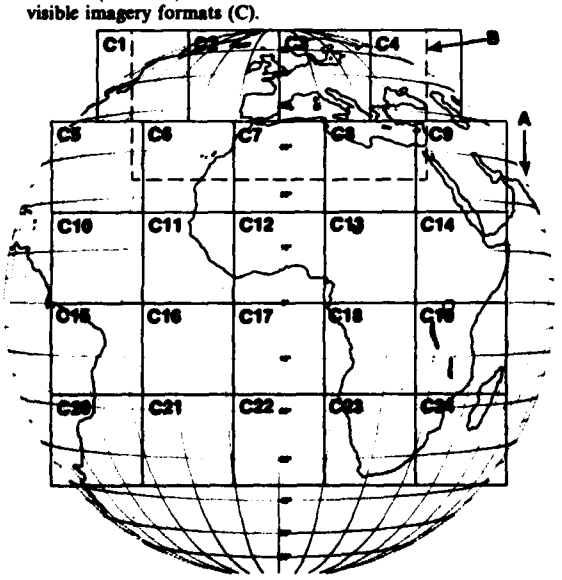

2B-3b. WEFAX infrared formats (D) and water vapor formats (E).

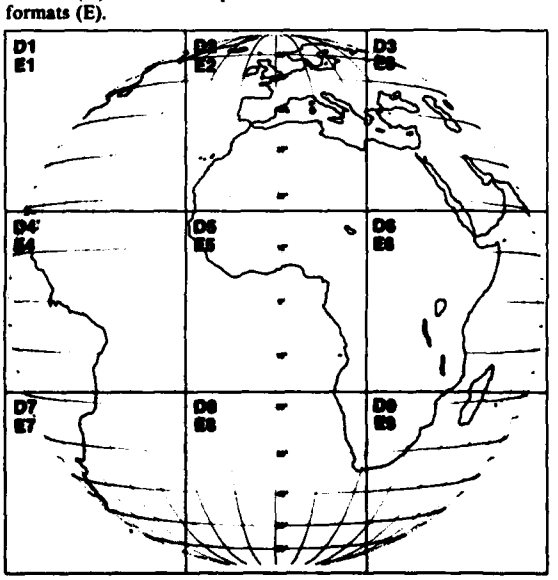

Radiation is also reflected to the infrared sensors which are mounted on a passive cooling plate and cooled to an ambient temperature of 95° K. The infrared detectors include a redundant pair for sensing infrared radiation (10.5–12.6 μm) and a single detector for sensing in the atmospheric water vapor band (5.7–7.1 μm). Each detector has an IFOV of 0.14 by 0.14 milliradians and gives a spatial resolution of 3.2 n mi at the SSP.

The infrared sensor output is normalized in terms of the equivalent blackbody temperature of the radiating object so that the sensor output is a simple, nearly-linear function of scene temperature. The infrared temperature sensitivity is a 0.5° K change when viewing a 300° K scene degrading to a 1.5° K change when viewing a 200° K scene. The net equivalent temperature difference (NETD) is less than a 0.2° K change across the entire temperature range sensed.

The water vapor detector uses the sampling electronics of one of the two visible channels and, consequently, it is sampled 5000 times per line although the ground resolution is only 3.2 n mi. This means that the water vapor detector is oversampled so there is a 50% overlap in the IFOV between adjacent samples in the east-west direction. To display this imagery, the data from the overlapping samples in each direction are averaged with the center sample.

Spectral Characteristics

The METEOSAT spacecraft carries a spin-scan radiometer that senses radiation in the visible, water vapor, and infrared. The visible sensor's normalized response curve is shown in 2B-5a. There is little response in the blue end of the visible spectrum in order to minimize the effects of blue light backscattering of the atmosphere. Since a silicon diode is used as the detector, the peak response is in the near infrared region. The response also extends further into the near infrared than the visible sensors of the other geostationary satellites. This extension into the near infrared makes the sensor more responsive to haze detection and also provides better land/water contrast.

Infrared radiation is collected in the 10.5–12.6 μm atmospheric window region (2B-5b). Either one of the two redundant infrared detectors is used for imaging. The IR-1 detector curve has a bell-shaped response throughout this spectral interval, while the IR-2 curve has a somewhat broader response through this interval. The data obtained from both detectors are essentially the same.

METEOSAT-1, launched in 1979, was the first geostationary satellite with a channel in the 6.3 μm water vapor band. This satellite failed in November 1979 and was replaced by METEOSAT-2 in June 1980. In order to associate the radiance measured in the water vapor channel with an atmospheric layer, forward calculations (Fischer *et al*, 1981) with the radiative transfer equation are needed within the spectral response region (2B-5c) of the instrument. Transmittance functions are used, based on line-by-line calculations for specified spectral intervals (25 cm^{-1}) covering the whole 6.3 μm water vapor band, to determine weighting functions. The weighting function curve (2B-5d), based on the Standard Atmosphere and an integrated moisture column, shows that the major contributing layer of the water vapor channel is from about 250 mb to 500 mb (half-width center), with a peak contribution near 350 mb (upper troposphere).

Fischer *loc cit*, however, shows that when the transmittance functions include the temperature dependent Planck function and are based on the water vapor profile, and not on the total water vapor content in the vertical column, a contribution function is obtained which appears

to be more appropriate for specifying the major contributing layers. The contribution function (2B-5d), based on the Standard Atmosphere, shows the major contributing layer between 330 mb and 720 mb (half-width center), with a maximum at 480 mb. This means that the phenomena to be seen in water vapor images are associated with the middle troposphere rather than with the upper troposphere, as indicated by the weighting function alone. The effect of stratospheric water vapor is negligible, and clouds below 800 mb are a minor influence on the measured radiance in the water vapor channel.

References

Fischer, H., N. Eigenwillig, and H. Muller, 1981: Information content of METEOSAT and Nimbus/THIR water vapor channel data: altitude association of observed phenomena. *J. Appl. Meteor.*, **20**, pp. 1344–1352.

Houghton, D.D., and V.E. Suomi, 1978: Information content of satellite images. *Bull. Amer. Meteor. Soc.*, **59**, 1614–1617.

Morel, P., M. Desbois, and G. Szejuach, 1978: A new insight into the troposphere with the water vapor channel of METEOSAT. *Bull. Amer. Meteor. Soc.*, **59**, 711–714.

Morgan, J., 1978: Introduction to the METEOSAT system. ESTEC Reproduction Services, Darmstadt, 54 pp.

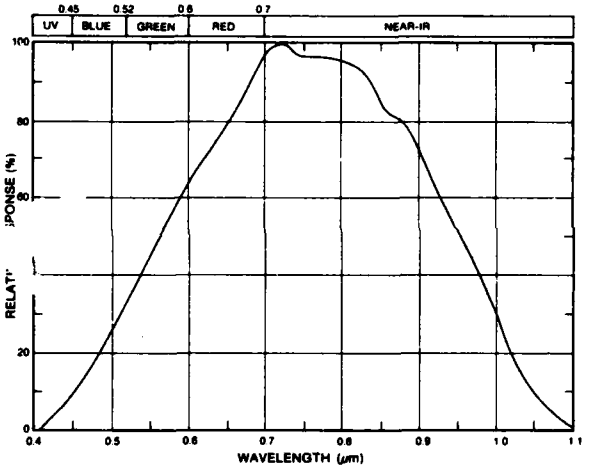

2B-5a. METEOSAT visible channel normalized sensor response curve.

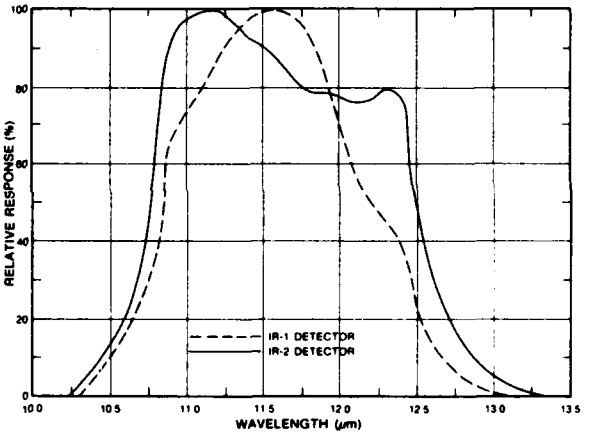

2B-5b. METEOSAT infrared channel normalized sensor response curve.

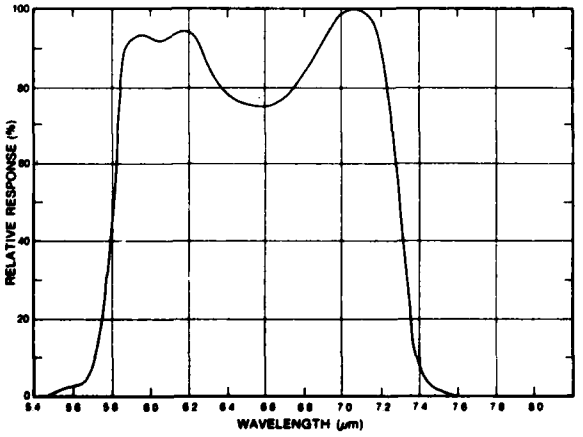

2B-5c. METEOSAT water vapor channel normalized sensor response curve.

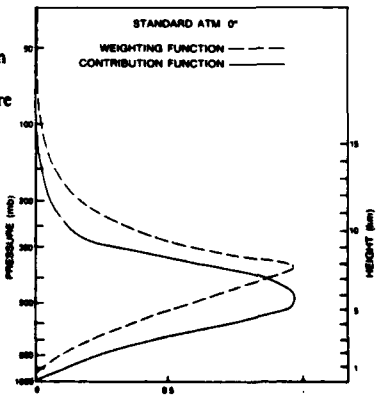

2B-5d. Normalized weighting and contribution function curves, based on Standard Atmosphere assumptions, of the METEOSAT water vapor channel.

Sample Imagery, METEOSAT

Imagery from the METEOSAT spacecraft is available in three spectral intervals; visible (2B-6a), infrared (2B-7a), and water vapor absorption band (2B-7b). The visible and infrared imagery can be interpreted using established analysis techniques. Guidelines for the interpretation of water vapor imagery are in the process of development. It is apparent from 2B-7b that features appear in the water vapor imagery that cannot be discerned in either the visible or infrared imagery. At the same time some features, such as low-level cloudiness, are not detected at all in the water vapor channel.

In general, the data obtained from the water vapor channel are representative of the humidity content of the middle troposphere (600–300 mb). Brighter regions correspond to lower radiative temperatures where radiation comes from higher altitudes, while darker regions correspond to higher temperatures where the radiation comes from lower altitudes.

2B-6a. METEOSAT. Visible Picture, 1.6 n mi Resolution. 1155 GMT 17 February 1983. (©European Space Agency, 1983)

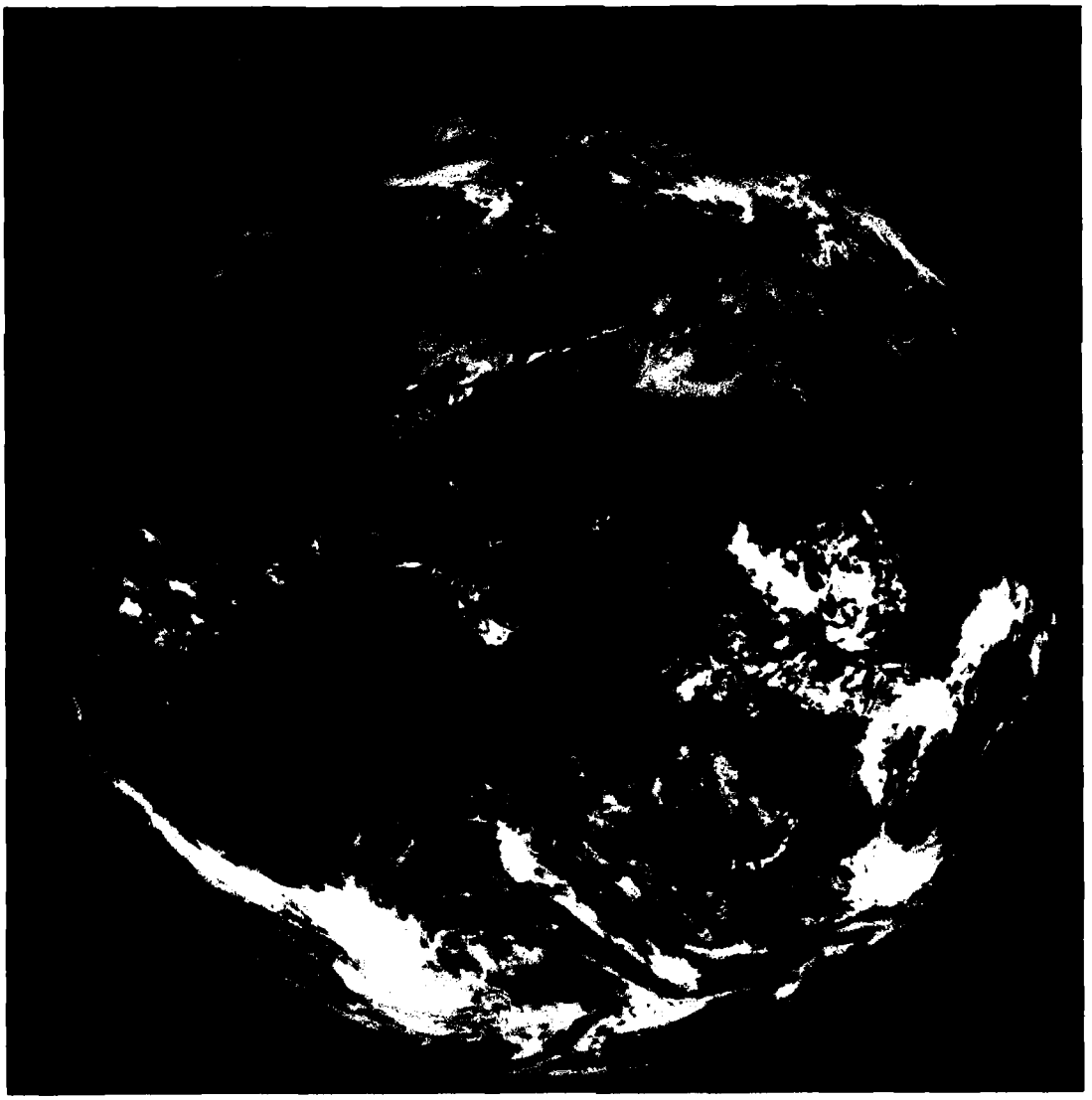

2B-7a. METEOSAT. Infrared Picture, 3.2 n mi Resolution. 1155 GMT 17 February 1983. (©European Space Agency, 1983)

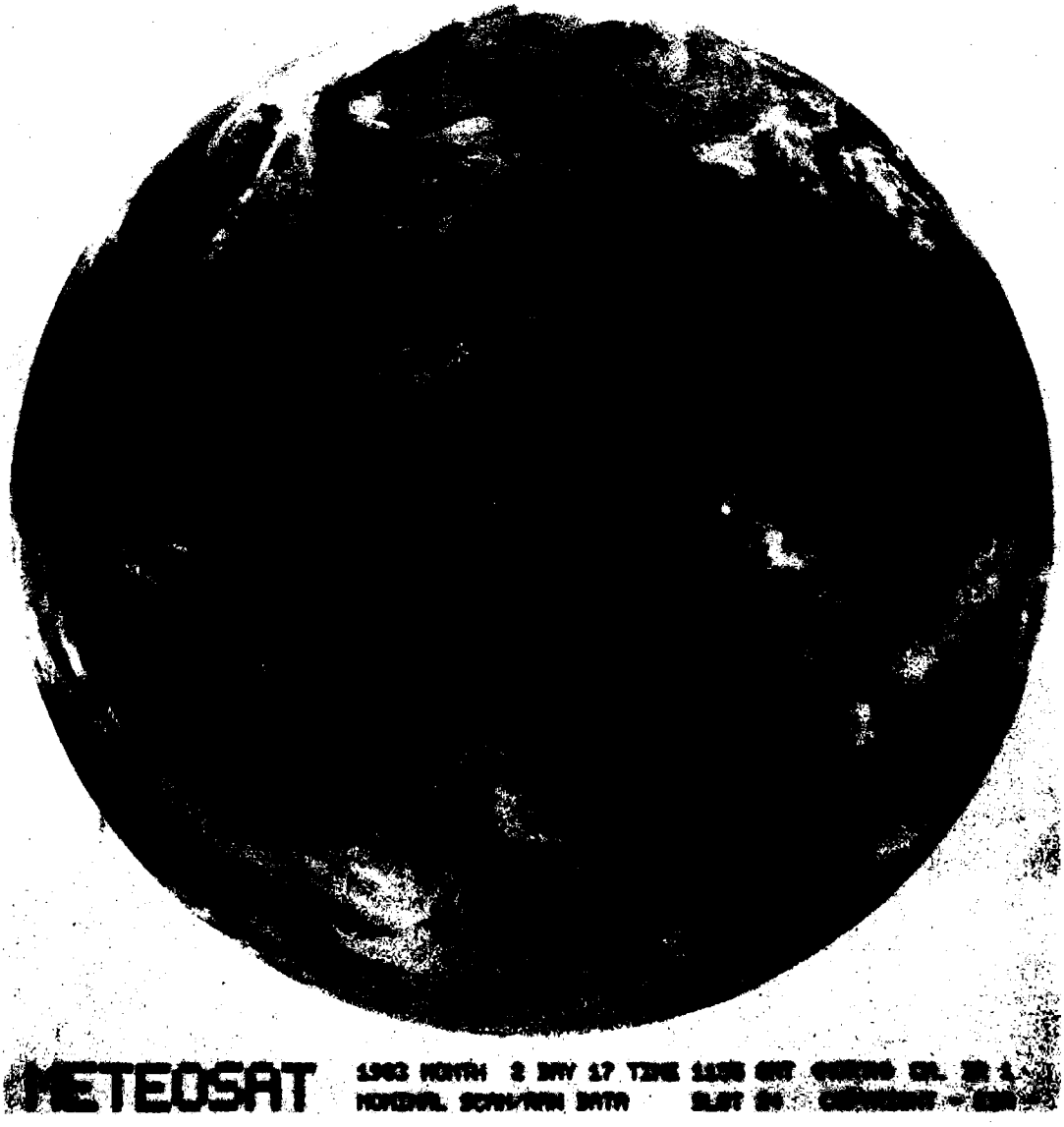

2B-7b. METEOSAT. Water Vapor Picture, 3.2 n mi Resolution. 1155 GMT 17 February 1983. (©European Space Agency, 1983)

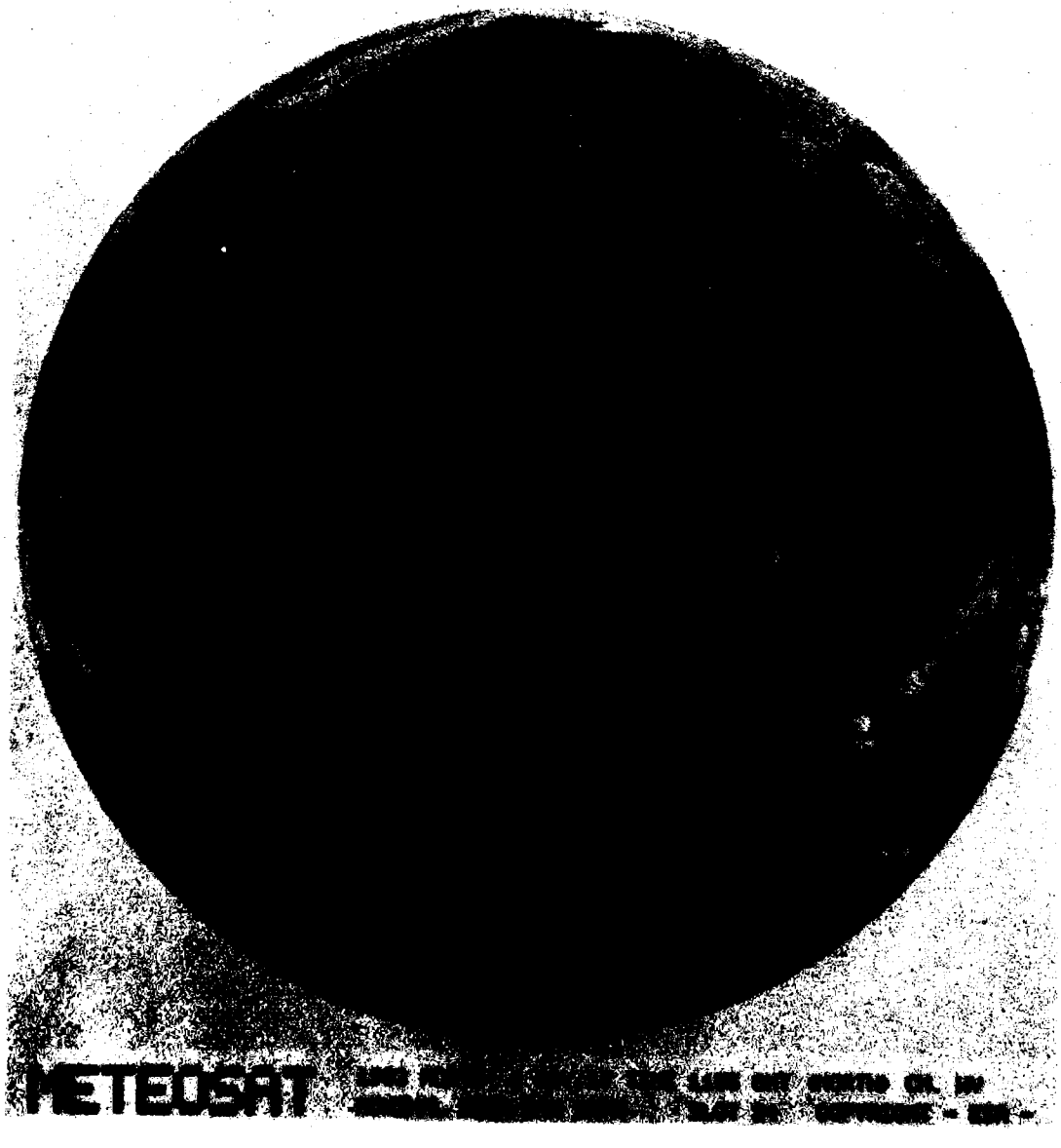

Geostationary Meteorological Satellite

(GMS)

Japan currently operates one geostationary satellite, GMS-2, located at 140° E, 0° N, which gives an areal coverage from Antarctica to Siberia, and from Hawaii to India. The original GMS, in operation from 1977 to 1981, was transferred to a geostationary orbit at 160° E to be utilized as back-up satellite for GMS-2, when necessary.

2C-1a. On the GMS-2 spacecraft, the S-band and UHF antennas and the radiometer aperture protrude from the main cylindrical body. As with the GOES spacecraft, the outside of GMS-2 is covered with solar power cells.

Image Acquisition and Distribution

The frequency of picture taking by the GMS-2 satellite and the method of picture distribution to the user are different from those of the GOES satellite due to differences in satellite design, the ground processing system, and other factors. Since distribution of satellite image data (visible and infrared) by landline facsimile is very difficult in the western Pacific and eastern Asia, image data are distributed through the GMS-2 spacecraft on a time-delayed basis (i.e., facsimile pictures are not transmitted until after the complete full disc image of the western Pacific area is acquired, which is every 30 minutes).

The GMS-2 image distribution system (2C-2a) begins with the acquisition of raw Visible and Infrared Spin-Scan Radiometer (VISSR) data from the spacecraft by the Command and Data Acquisition Station (CDAS) located at Hatoyama (about 34 mi northwest of Tokyo). In the CDAS, the raw VISSR data are processed by a synchronizer/data buffer which stretches the data rate to the length of one spin period of the spacecraft. Picture parameter data and a gray scale are added to the stretched data, and the data are sent to the Data Processing Center (DPC) at Kiyose (about 15 mi northwest of Tokyo) by microwave.

At the DPC, the stretched VISSR data are processed to produce a full disc, high resolution analog facsimile (HR-FAX) picture. The HR-FAX visible picture has a resolution of 0.7 n mi (1.25 km) at the SSP, while the infrared picture has a 2.7 n mi (5 km) resolution. The picture also includes grid lines, gray scale wedge, and annotations (specifying observation time, sensor type, etc.). The HR-FAX picture data are transmitted to the CDAS, via microwave link, and then transmitted to the GMS-2 spacecraft and retransmitted to Medium-scale Data Utilization Stations (MDUS). Transmission of one HR-FAX picture takes approximately 14 minutes and transmissions are scheduled for eight 28-minute time slots per day. Since raw VISSR data transmission and facsimile transmissions operate on the same frequency, they are time-shared in the routine operation of GMS-2. In addition to the full disc picture, a Mercator projection picture covering an area from 36°N to 36°S (schematically shown in 2C-3a) is also produced and transmitted on HR-FAX four times a day.

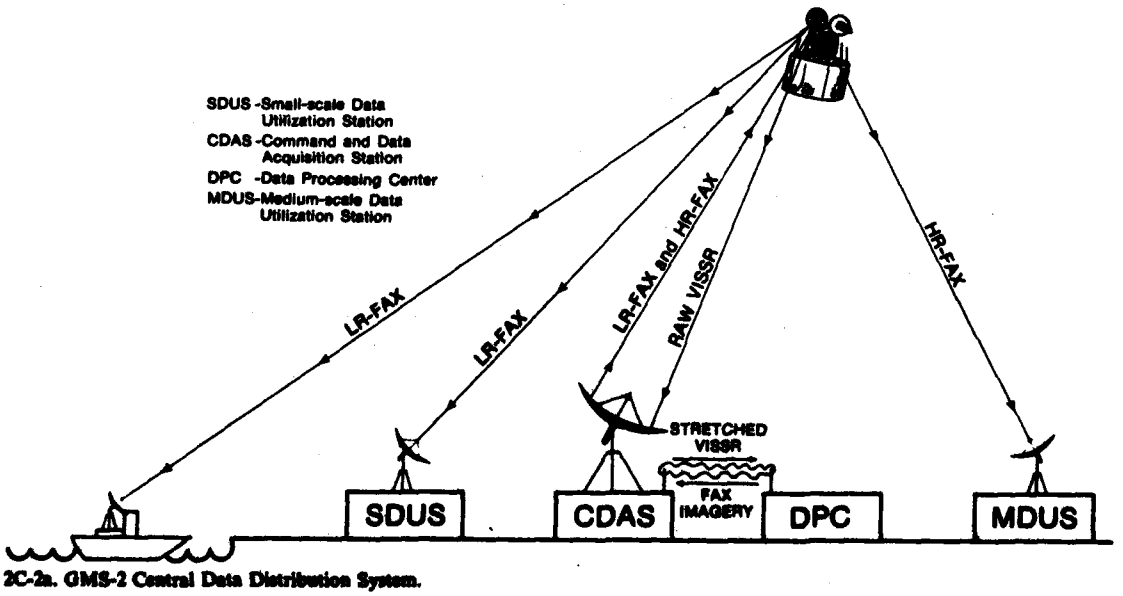

2C-2a. GMS-2 Central Data Distribution System.

Next, the low resolution facsimile (LR-FAX) pictures are prepared at the DPC for transmission to Small-scale Data Utilization Stations (SDUS). This time the full disc picture of the Earth is sectorized into seven portions (as shown in 2C-3b), and each portion is stored on a separate magnetic disc. Each disc contains all necessary information to construct one LR-FAX image and takes approximately four minutes to transmit. All seven sectors are transmitted through GMS-2 to the SDUS in a 28-minute time slot eight times per day. The resolution of the LR-FAX images at the SSP is 4 n mi for the visible and infrared imagery.

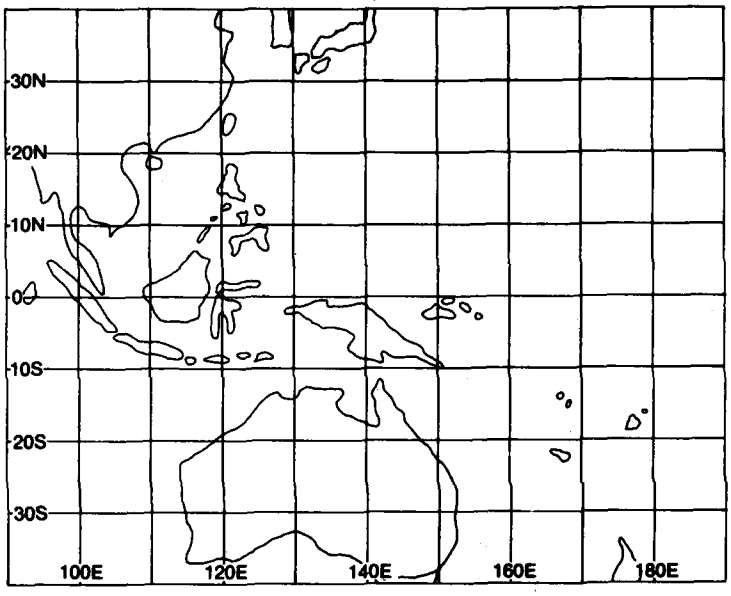

2C-3a. GMS-2 Mercator Projection Picture.

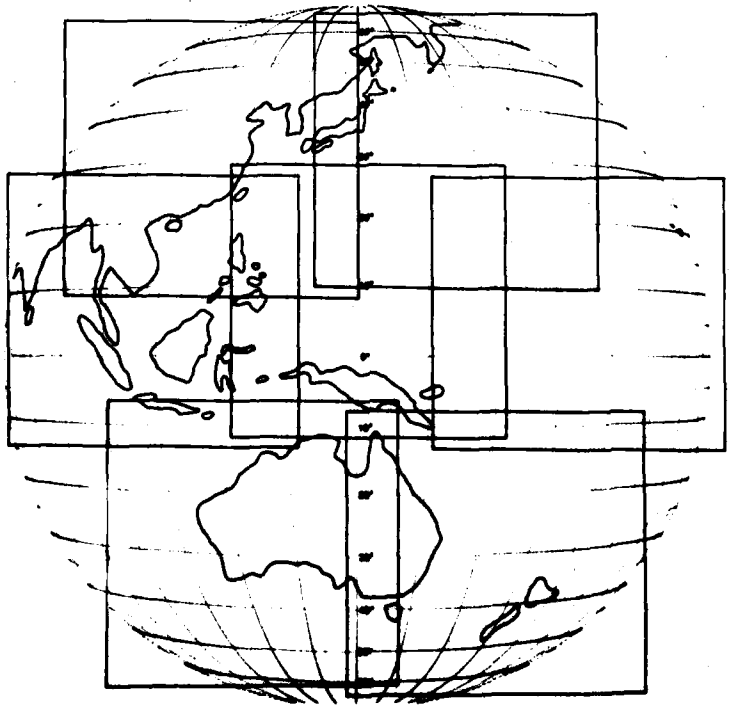

2C-3b. GMS-2 LR-FAX Sectors.

Because the Japanese government has not granted blanket approval for reception of direct broadcast HR-FAX and LR-FAX signals from GMS-2, approval is granted on a case-by-case basis by the Planning Director, Japan Meteorological Agency.

Sensor System Description

At the GMS-2 spacecraft, radiation from the Earth scene enters a telescope aperture and is reflected 45° by an object-space scan mirror. Radiation reflected from the scan mirror enters a Cassegrain telescope (primary and secondary mirrors) which focuses the radiant energy onto the detector array.

Energy in the visible spectrum is detected during daylight hours by eight fiber optics located at the focal plane. The other ends of the fibers are incident upon eight photomultiplier tube (PMT) detectors (four primary, four redundant) responding in the 0.55–0.75 μm range, converting visible light into four visible analog signals. Each PMT has an instantaneous field-of-view (IFOV) of 0.031 by 0.035 milliradians which gives a spatial resolution of approximately 0.7 n mi (1.25 km) at the satellite subpoint (SSP). As with GOES, the output voltage from each PMT is converted to one of 64 digital counts for transmission to the ground.

Infrared spectrum energy (10.5–12.5 μm) is also relayed day and night by fiber optics from the trimetal (HgCdTe) detector array to two infrared detectors (one primary, one redundant) cooled to a controlled temperature of 93.5° K. Each infrared sensor has an IFOV of 0.14 by 0.14 milliradians which gives a spatial resolution of 2.7 n mi (5 km) at the SSP.

The infrared sensor output is normalized in terms of the equivalent blackbody temperature of the radiating object so that the sensor output is a simple, nearly-linear function of scene temperature. The infrared temperature sensitivity is a 0.5° K change when viewing a 300° K object, degrading to a 1.5° K change when viewing a 200° K object.

Spectral Characteristics

The spectral response characteristics of the GMS-2 visible and infrared sensors are identical to those of GOES. See the discussion on GOES Spectral Characteristics (2A-5) for a discussion of the corresponding response curves.

For additional information on the GMS-2 system write to:

Japan Meteorological Agency
Ote-machi
Chiyoda-ku
Tokyo, Japan

References

Hirai, M., 1978: Current status of Japanese meteorological satellites GMS and GMS-2. WMO/UN Regional Training Seminar on the Interpretation, Analysis, and Use of Meteorological Satellite Data, Tokyo, Japan, SAT/L2A 1-14.

Kodaira, N., 1978: Outline of the GMS system. WMO/UN Regional Training Seminar on the Interpretation, Analysis, and Use of Meteorological Satellite Data, Tokyo, Japan, SAT/L1C 1-13.

Sample Imagery, GMS

These simultaneous visible and infrared pictures show cloud patterns and thermal features over the western Pacific, eastern Asia, and Australia. Geographical boundaries and a latitude/longitude grid have been added to both pictures. Additionally, registration marks (+) are implanted on the pictures to facilitate alignment of a series of images.

2C-6a. GMS. Visible Picture, 0.7 n mi Resolution. 0300 GMT 15 February 1979. (Photo Courtesy of Japan Weather Association.)

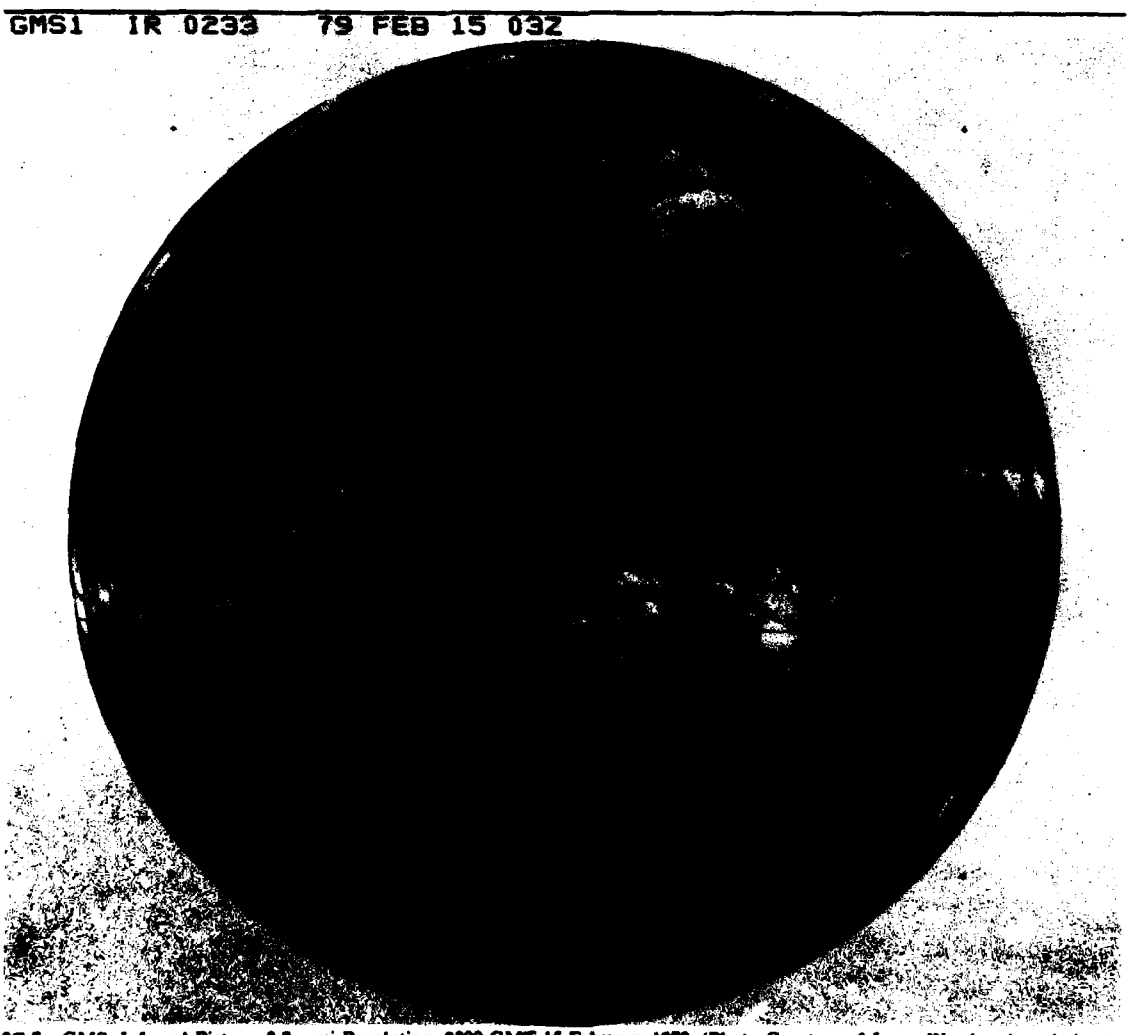

2C-7a. GMS. Infrared Picture, 2.7 n mi Resolution. 0300 GMT 15 February 1979. (Photo Courtesy of Japan Weather Association.)

Indian National Satellite
(INSAT)

INSAT (Indian National Satellite) is India's first operational domestic satellite and is a joint venture of the Space Department, Posts and Telegraph Department of the Ministry of Communications, Indian Meteorological Department of the Ministry of Tourism and Civil Aviation, and Doordarshan, the television arm of the Ministry of Information and Broadcasting. The Meteorological Department is responsible for the meteorological ground segment and its utilization.

INSAT is designed to be a multi-purpose satellite system for telecommunications, broadcasting, and meteorology. The multi-purpose design, besides providing improved telephone and television service throughout India, includes (1) a meteorological payload which will obtain visible and infrared images of weather systems, and (2) a meteorological communication subsystem for real-time relay of data from unattended land- and sea-based meteorological, hydrological, and oceanographic platforms.

INSAT-1A was launched in 1981, and it was operational for only five months due to excess fuel usage. Good images were received during this period. INSAT-1B was launched on 31 August 1983 by the U.S. Space Transportation System (Space Shuttle). A payload assist module was used to raise the satellite from low earth orbit to a geostationary orbit (35,800 km), at 74° E.

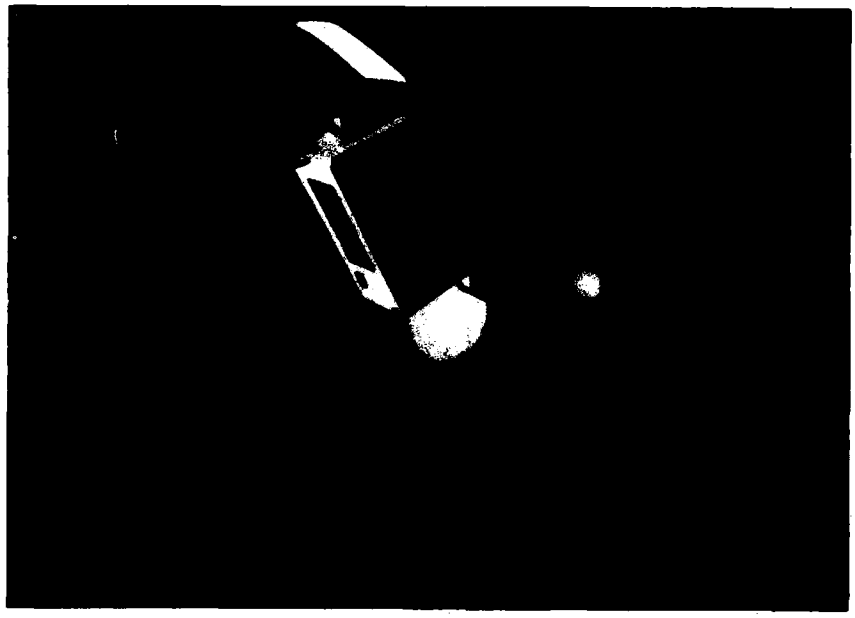

2D-1a. The INSAT-1 spacecraft differs from the GOES spacecraft in that it is momentum wheel stabilized, not spin stabilized. A planar solar array, as shown in the above illustration, is used for the power source. INSAT-1 utilizes two systems to maintain earth-oriented stability: (1) a precision momentum bias attitude control system which maintains stabilization on three axes, and (2) a conical-shaped solar sail which compensates for solar pressure on the planar solar array. The overall dimensions of the spacecraft when all hardware is deployed is 5.8 by 17.9 by 1.4 meters (19 by 59 by 4.5 feet).

Data Acquisition and Distribution

INSAT carries a 2-channel (visible and infrared) Very High Resolution Radiometer (VHRR) that collects images of the earth. These images are transmitted to India's Meteorological Data Utilization Center (MDUC) in New Delhi through the Delhi Telecommunications earth station. Additionally, the satellite is capable of relaying meteorological data from unattended remote Data Collection Platforms (DCPs) to the MDUC, which can be merged with data derived from the imagery received at the MDUC, such as cloud motion derived winds, snow fields, and cloud top and large water body temperatures. The New Delhi MDUC facility disseminates remote platform and derived satellite imagery data over telecommunications lines (including INSAT links) to forecasting offices of the Indian Meteorology Department.

Sensor System Description/Spectral Characteristics

Much of the INSAT technology is based on the U.S. Geostationary Operational Environmental Satellite (GOES) series. INSAT carries a VHRR that will furnish visible (0.55–0.75 μm) and infrared (10.5–12.5 μm) images (see 2A-6a and 6b for response curves) of the earth with surface resolutions of 2.5 km (1.6 n mi) and 11 km (6.8 n mi), respectively. Full disc visible and infrared imagery is transmitted at 30-minute intervals or partial frame imagery is transmitted at six-minute intervals, in support of both synoptic and mesosynoptic observations of weather systems.

For further information on INSAT contact:

Government of India
Meteorological Department
Lodi Road
New Delhi 110003
INDIA

attn: D.K. Mishra
Director - Satellite Applications

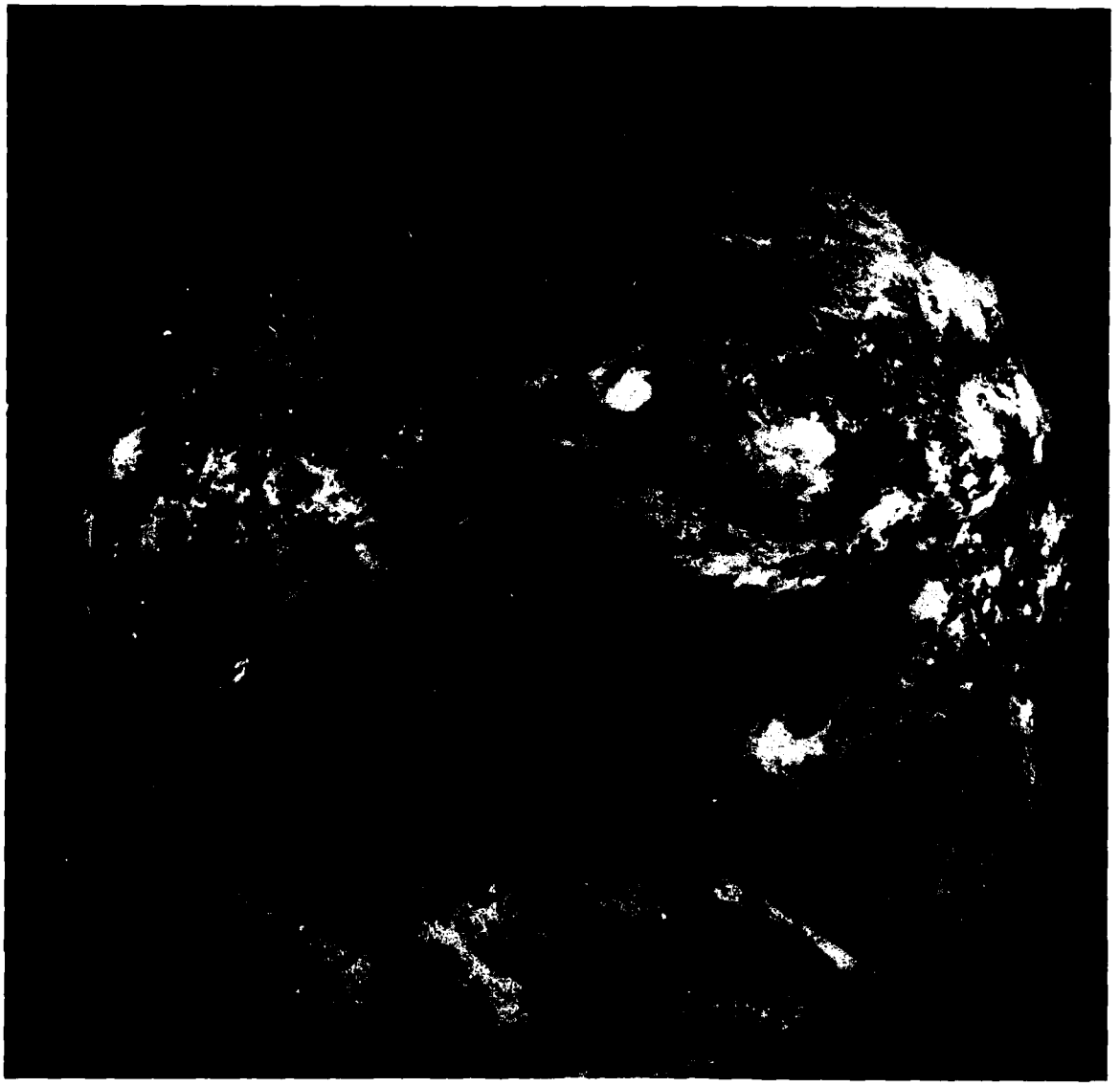

2D-3a. GOES-I. Visible picture. 0730 GMT 15 April 1979. (Acquired at Meteorologie Nationale, Lannion, France, in support of the WMO-MONEX project). This picture shows the approximate earth coverage provided by INSAT.

Geostationary Operational Meteorological Satellite
(GOMS)

GOMS (Geostationary Operational Meteorological Satellite) is the U.S.S.R. equivalent of the U.S. GOES spacecraft. A tentative 1983 launch date is reported in the literature (Miller, 1982). When launched, the satellite is to be placed in a geostationary orbit at 76°E. Its mission objectives are the same as other geostationary meteorological spacecraft: high resolution imaging of the earth's surface and of it cloud cover in both the visible and infrared spectral ranges, dissemination of cloud cover images to remote Data User Stations (DUS), and collection of environmental data from remote fixed or mobile Data Collection Platforms (DCP). Coverage of the data relay capability extends outward in a 75° great circle arc around the satellite subpoint (SSP).

Reference
Miller, Donald B., and Joseph R. Silverman, 1982: Meteorological satellites—past, present, and future. NASA Conference Publications, 2227, pp. 54.

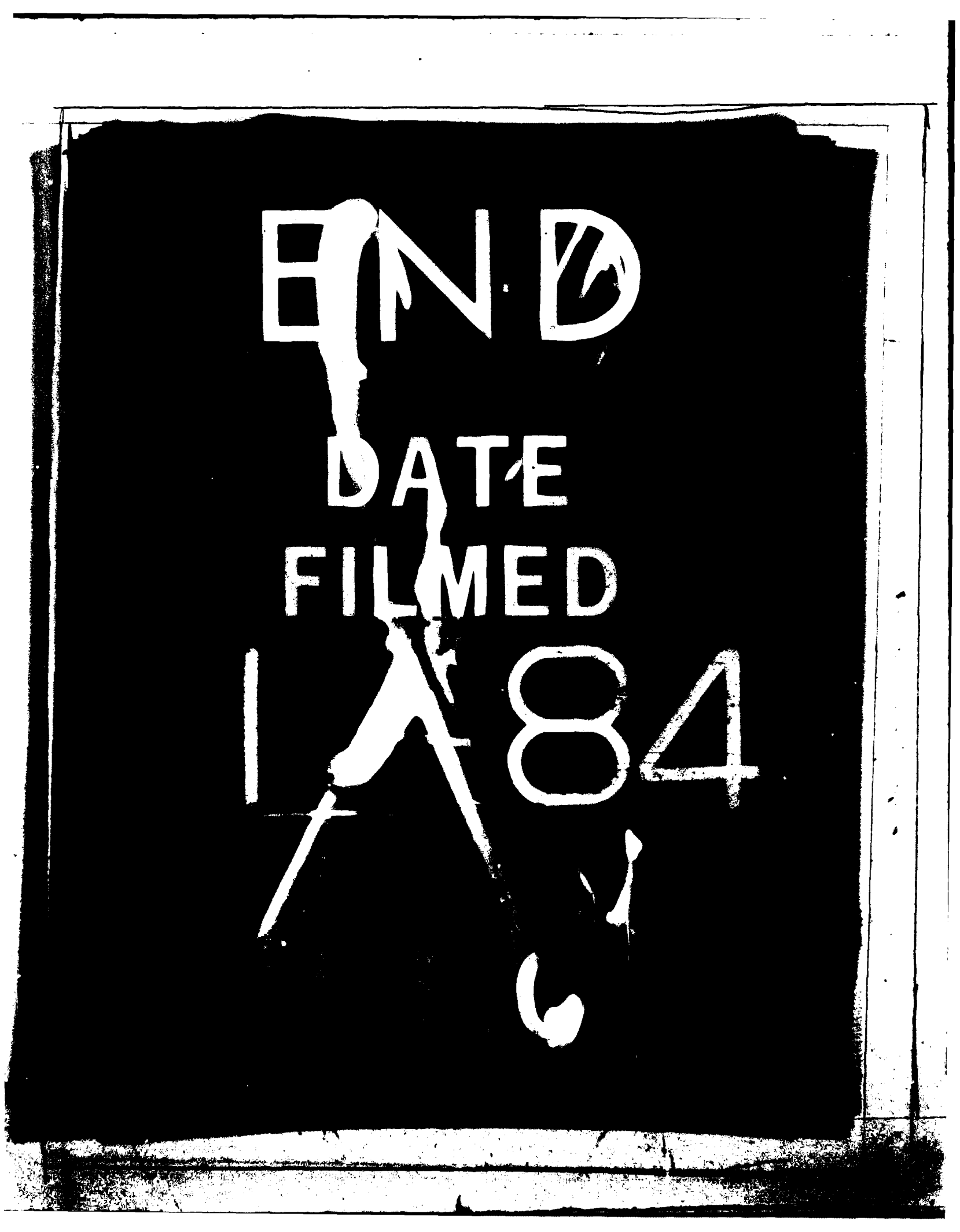
END
DATE
FILMED
1-84

AD-A135 466 NAVY TACTICAL APPLICATIONS GUIDE VOLUME 3 SECTION 1 OPERATIONAL ENVIRONME..(U) BOHAN (WALTER A) CO PARK RIDGE IL R W FETT ET AL. JUN 83 NEPRF-TR-83-02 2/2

UNCLASSIFIED N00228-82-C-6222 F/G 4/2 NL

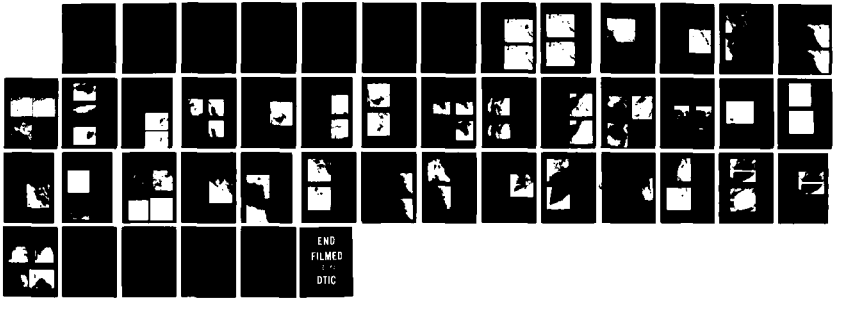

IMAGE EVALUATION
TEST TARGET (MT-3)

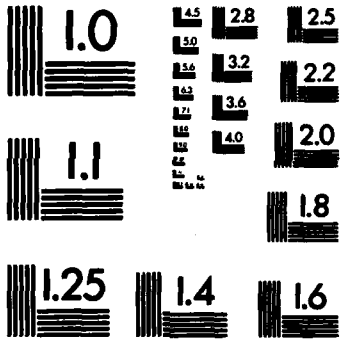

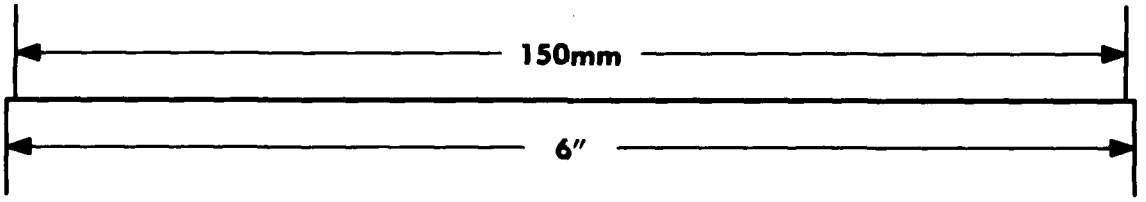

PHOTOGRAPHIC SCIENCES CORPORATION
770 BASKET ROAD
P.O. BOX 338
WEBSTER, NEW YORK 14580
(716) 265-1600

Errata AD-A135466

NEPRF Technical Report 83-02
Revision 1

UPDATE BULLETIN

Navy Tactical Applications Guide
Operational Environmental Satellites
Polar-Orbiting Satellites
Geostationary Satellites

Revised pages dated January 1992 and an additional section are enclosed. This is the first mailing since the initial distribution of this volume.

Replacement pages:
- DD Form 298 (formerly DD 1473)
- Contents (page v)
- Divider Page (Section 1D)
- Section 1D Meteor (This was formerly Section 1C; no textual changes have been made.)

Additional Section:
- Divider Page (Section 1C)
- Section 1C Processing and Display of NOAA Direct Readout Environmental Imagery (This section replaces Section 1C Meteor, which was deleted [illegible])

REPORT DOCUMENTATION PAGE

Form Approved
OMB No. 0704–0188

1. Agency Use Only *(Leave blank).*	2. Report Date.	3. Report Type and Dates Covered.
	June 1983	Final

4. Title and Subtitle.

Navy Tactical Applications Guide
Operational Environmental Satellites

5. Funding Numbers.

Program Element No. 62759N
Project No. WF 59–553
Task No. NEPRF WU: 6.3–18
Accession No.

6. Author(s).

Robert W. Fett, Walter A. Bohan, John J. Bates,
Sherree L. Tipton, Thomas F. Lee, and Philip A. Durkee

7. Performing Organization Name(s) and Address(es).

The Walter A. Bohan Company
2026 Oakton Street
Park Ridge, IL 60068

8. Performing Organization Report Number.

9. Sponsoring/Monitoring Agency Name(s) and Address(es).

Naval Environmental Prediction Research Facility
Monterey, California 93940

10. Sponsoring/Monitoring Agency Report Number.

NAVENVPREDRSCHFAC
Technical Report
83–02

11. Supplementary Notes.

12a. Distribution/Availability Statement.

Approved for public release; distribution is unlimited.

12b. Distribution Code.

13. Abstract *(Maximum 200 words).*

This volume contains user-oriented sections on current operational satellite systems that describe imagery acquisition and distribution, sensor systems, and spectral characteristics. In addition, sample imagery is included for each of the meteorological satellite systems.

14. Subject Terms.

Meteorological Satellite Systems, Defense Meteorological Satellite Program (DMSP), National Oceanic and Atmospheric Administration (NOAA) satellites, geostationary satellites, polar-orbiting satellites, METEOSAT, GOES, GMS, INSAT, and Meteor, and GOMS satellites

15. Number of Pages. 70

16. Price Code.

17. Security Classification of Report.	18. Security Classification of This Page.	19. Security Classification of Abstract.	20. Limitation of Abstract.
UNCLASSIFIED	UNCLASSIFIED	UNCLASSIFIED	Same as report

Contents

PROCESSING AND DISPLAY OF NOAA DIGITAL MULTISPECTRAL IMAGERY

The capability to process satellite digital data on a graphics display workstation offers an unprecedented opportunity to produce useful images. The digital data from the Advanced Very High Resolution Radiometer (AVHRR) are divided into five separate bands. The five bands enable "multispectral processing," allowing enhancements and applications not possible with other satellites (e.g., GOES, METEOSAT, and DMSP).

The AVHRR has a 10-bit radiometric resolution allowing 1,024 levels of discrimination in measured response. In practice, computer monitors degrade the display of the AVHRR data to no more than 256 (8-bit resolution) of the 1,024 gray shades. Still, the 10-bit resolution is very useful in the calculation of multispectral image products, as will be discussed in the following examples.

Comparison of Five AVHRR Channels

The following summaries describe the characteristics and applications of the different channels. To extract the maximum amount of information, the user should compare and contrast the different channels rather than focus on individual images.

Channel 1 (0.63 μm) lies in the visible portion of the spectrum. Calibrated values range from 0 to 100% albedo. Common applications include cloud detection, ice detection, smoke detection, water turbidity, identification of shallow water regions, aerosol optical depth, identification of terrain features, dust over water, and sunglint effects.

Channel 2 (0.86 μm) lies in the near infrared portion of the spectrum. Calibrated values range from 0 to 100% albedo. Channel 2 images represent reflected solar radiation and often resemble Channel 1 images. There are important differences, however.

First, Channel 2 is almost totally unreflective over water, which appears black in comparison to vegetated land areas. Thus, melting snow areas and flooded land areas can easily be detected in Channel 2 images but not in Channel 1 images. Second, vegetated land regions appear much brighter in Channel 2 images than in Channel 1 images. Applications of Channel 2 include cloud detection, ice detection, smoke detection, identification of terrain features, land–water distinction, dust over water, sunglint effects, and cloud screening for sea surface temperature algorithms. Combinations of Channels 1 and 2 can yield snow and ice categorization, cloud properties, aerosol size index, surface typing, and vegetative index.

Channel 3 (3.7 μm) lies in the near infrared portion of the spectrum. Brightness temperatures range from a minimum of −83 °C to a maximum of 47 °C. At night, Channel 3 measures thermal energy from the Earth's surface and from clouds. Atmospheric water vapor is only weakly absorptive at 3.7 μm. Thus, even vapor-laden atmospheres do not greatly attenuate the Channel 3 radiance as it passes from the Earth's surface to the satellite. Nighttime Channel 3 images (no reflected solar radiation) resemble thermal infrared images. During the daytime, on the other hand, solar reflection from clouds and surface features is not negligible at 3.7 μm. Therefore, daytime Channel 3 images represent a combination of thermal emission and reflected solar radiation. For this reason daytime Channel 3 images can be very difficult to interpret. Over deserts, for example, daytime Channel 3 images often become "saturated," meaning that brightness temperatures are everywhere equal to the maximum measurable brightness temperature.

General (day and night) applications of Channel 3 include low cloud detection, anomalous cloud-line detection, and fire detection. Daytime-only applications include low cloud over ice and snow, inferences of cloud phase, smoke detection, aerosol detection, dust detection, and sunglint effects. Nighttime-only applications include land temperature, sea surface temperature, and cloud screening for sea surface temperature algorithms.

Channel 4 (10.8 μm) senses thermal radiation from a minimum brightness temperature of −83 °C to a maximum of 47 °C. Although 10.8 μm is in a water vapor window, surface emission in Channel 4 is still significantly attenuated by water vapor. Applications include cloud detection, smoke detection, cloud temperature, cloud height, dust detection over land, land temperature, and sea surface temperature.

Channel 5 (11.8 μm), like Channel 4, senses thermal radiation. It measures brightness temperatures from −83 °C to 53 °C. To even a greater degree than in Channel 4, surface emission is attenuated by atmospheric water vapor. Applications include cloud detection, smoke detection, cloud temperature, cloud height, dust detection over land, land temperature, and sea surface temperature.

Combinations of Channels 3 and 4 can provide improved fire detection and low cloud detection. Combinations of Channels 4 and 5 provide the basis for sea surface temperature estimates. Also, Channels 4 and 5 can be processed together to identify thin cirrus, including contrails.

As an alternative to comparing images from the five AVHRR channels, the user can increase the usefulness of the information by producing computer composites of two or more channels. The simplest manipulation is the subtraction of two images to produce a new "difference" image. The most useful difference images are derived from Channels 4, 5, and nighttime Channel 3. Common applications include the subtraction of Channels 4 and 5 (4 minus 5) or Channels 3 and 4 (3 minus 4). Another simple manipulation is the computation of ratio images, commonly using Channels 1 and 2 for input (1 divided by 2).

Workstation Display Options

Computer workstations offer a number of capabilities to make the display and interpretation of satellite data easier. A summary of some of the more common options follows.

Zoom: A portion of an image is greatly expanded through a software or hardware operation. Often a zoomed image will show features that an analyst will fail to notice on the original image, such as contrails, shiptracks, fires, sunglint effects, etc.

Coastline Overlay: This optional feature adds greatly to images with poor water–land contrast, e.g., infrared images at night or visible images of polar scenes. Software is available on most systems to correct small errors in the position of the coastline overlay with respect to the coastline on the image. Such an adjustment improves image display and satellite navigation. Other overlay capabilities that are often available include bathymetric contours, terrain height contours, latitude and longitude grids, and contours of supplementary environmental fields (e.g., 500-mb height contours).

Negative Images: Computer workstations usually offer the capability to reverse the tonality on black and white images. Thus, the user can display an image either as "positive" or "negative." On longwave infrared images the positive convention is to display warm scenes in dark gray shades and cold scenes in bright gray shades. On visible images the positive convention is to display poorly reflective features as dark gray shades and reflective features as bright gray shades. A negative image reverses these schemes and is used when an original image does not match the expectations of the user. For example, on daytime Channel 3 (3.7 μm) images, a positive infrared display will cause low water clouds to appear black against a bright background. So as not to confuse the analyst, these images are often made negative, making low clouds appear white against a dark background.

Examples of the Display and Processing of AVHRR Imagery

The five imaging channels aboard the NOAA AVHRR can produce a greater variety of images than traditional weather satellites, which only give infrared and visible images. Unfortunately, the larger number of channels can be very confusing for the inexperienced analyst. Therefore, in the following examples the appearances of the five channels have been carefully compared, illustrating how the analyst would interpret each and illustrating arithmetic operations such as difference and ratio images.

1. Comparison of All Five AVHRR Channels

Figure 1C-4a (Channel 1) shows the Italian Peninsula poorly against the surrounding seas. Figure 1C-4b (Channel 2) shows the peninsula far more distinctly against the ocean background. This figure also shows outlines of lakes that tend to be invisible in the Channel 1 image. The enhanced reflectivity of most land surfaces in the Channel 2 image compared to the Channel 1 image makes the former more useful in the detection of familiar landmarks.

1C-4a. NOAA-9 Channel 1 (0.63 μm), 1323 GMT, 23 June 1986.

1C-4b. NOAA-9 Channel 2 (0.86 μm), 1323 GMT, 23 June 1986.

The images of Channels 4 and 5 appear nearly identical (Figs. 1C-5b and 5c, respectively). This similarity in appearance masks important differences in the two channels. See Figs. 1C-28a, 1C-29a-29b, 1C-30a-30c, and 1C-31a-31d for specific applications highlighting these differences.

1C-5b. NOAA-9 Channel 4 (10.8 μm), 1323 GMT, 23 June 1986.

1C-5c. NOAA-9 Channel 5 (11.8 μm), 1323 GMT, 23 June 1986.

In daytime scenes Channel 3 responds to a mixture of reflected solar radiation and longwave thermal emission by clouds and surface features. In Fig. 1C-5a, the Channel 3 image shows high clouds (relatively poor reflectors of solar radiation and emitting at low temperature) as black. Land surfaces (highly reflective of solar radiation and emitting at a high temperature) appear in bright gray shades. The Channel 3 image (Fig. 1C-5a) also reveals sunglint (in the southwestern portion of the image) more distinctly than Channel 1 and 2 images (Figs. 1C-4a and 4b).

1C-5a. NOAA-9 Channel 3 (3.7 μm), 1323 GMT, 23 June 1986.

2. Contrast with Ocean, Clouds, and Smoke

Figures 1C-6a, 1C-7a, and 1C-7b show a daytime scene of California. It is difficult to see the coastline in the Channel 1 image (Fig. 1C-6a) because the reflectivity of land is only slightly greater than that of the ocean. Land areas in the Channel 2 image (Fig. 1C-7a) are much brighter, revealing the coastline distinctly. A number of features however, can be distinguished more easily in the Channel 1 image (Fig. 1C-6a) than in the Channel 2 image (Fig. 1C-7a). For example, a cirrus cloud shows up distinctly against a dark background in the Channel 1 image (Fig. 1C-6a) but tends to blend in with the bright background in the Channel 2 image (Fig. 1C-7a). For the same reason, a smoke plume from a wildfire stands out from the background better in Channel 1 than in Channel 2. In a Channel 3 negative image (Fig. 1C-7b) low stratus, being relatively warm and very reflective, appears white. High cirrus, being relatively cold and poorly reflective, appears black. A very bright spot marks the fire that produced the smoke plume in Channel 1. The ability to detect very hot but tiny features is limited to Channel 3. For more cases using Channel 3 in fire detection, see examples 14–17.

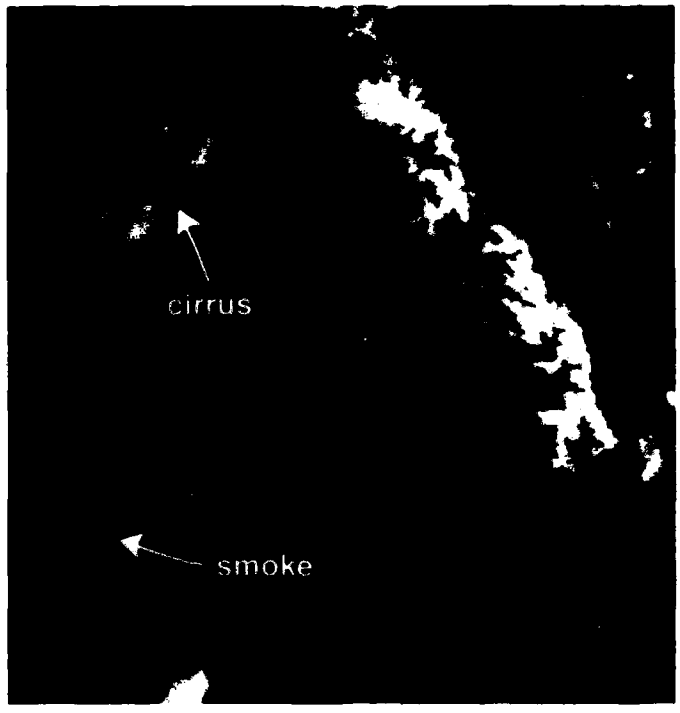

1C-6a. NOAA-9 Channel 1 (0.63 μm), 2223 GMT, 1 May 1985.

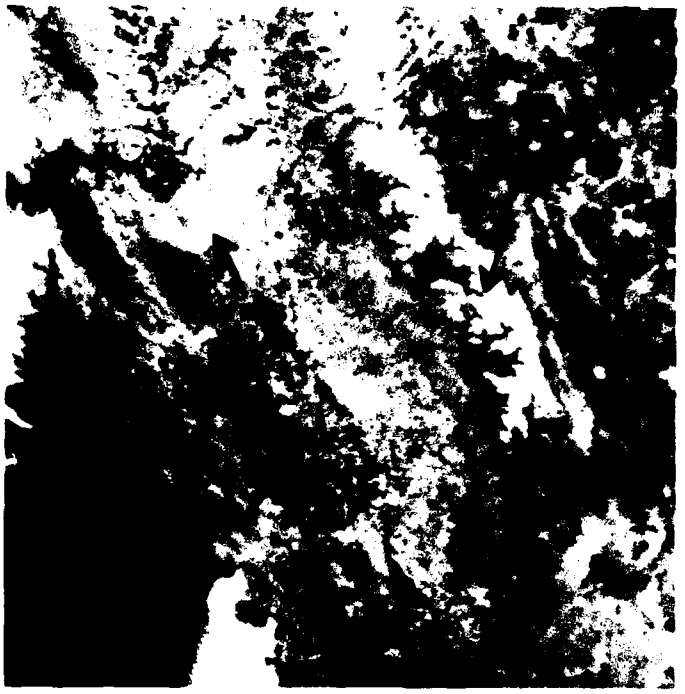

1C-7a. NOAA-9 Channel 2 (0.86 μm), 2223 GMT, 1 May 1985.

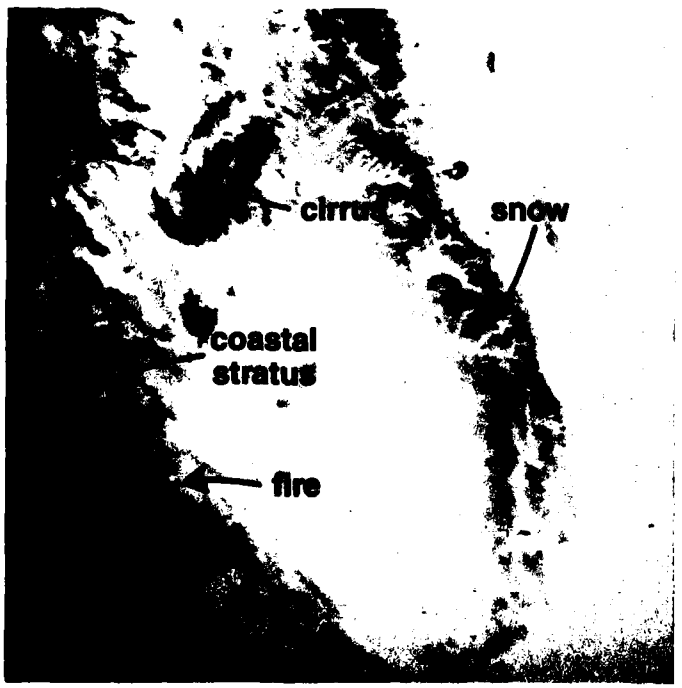

1C-7b. NOAA-9 Channel 3 (3.7 μm), 2223 GMT, 1 May 1985.

3. Sediment Detection

Channels 1 and 2 can be used to detect shallow areas and coastal sediments. Figures 1C-8a and 8b show the Persian Gulf region. Sediment, washed down through the Tigris-Euphrates River system, appears in the Channel 1 image (Fig. 1C-8a). In Channel 2 images (Fig. 1C-8b), however, the sediment is not nearly as distinct. The difference in the appearance of the two channels arises because water is far more absorptive of incoming solar radiation in Channel 2 wavelengths than in Channel 1 wavelengths. Thus, reflection from sediment is favored in Channel 1. It is important to note, however, that the sea floor under clear, shallow water may also be reflective in Channel 1. These shallow areas may be mistaken for sediment in Channel 1 images (see Figs. 1C-9a–9c).

1C-8a. NOAA-9 Channel 1 (0.63 μm), 1131 GMT, 10 November 1987.

1C-8b. NOAA-9 Channel 2 (0.86 μm), 1131 GMT, 10 November 1987

4. Identification of Shallow Regions

Figure 1C-9a is a Channel 2 image of the Bahamas Island chain. Figure 1C-9b is the corresponding Channel 1 image of the same region. A ratio image (Fig. 1C-9c) shows shallow water regions in dark gray shades. The dark areas south of Florida, off the north coast of Cuba and adjacent to the Bahamas, show the exact location of shallow regions that agree with bathymetric maps of the region (see NTAG, Vol. 2, Sec. 2E, Case 6). This effect occurs because solar radiation at Channel 1 wavelengths penetrates to the shallow bottom and back to the satellite more effectively than at Channel 2 wavelengths. The ratio of the two channels helps highlight this difference, indicating shallow water regions.

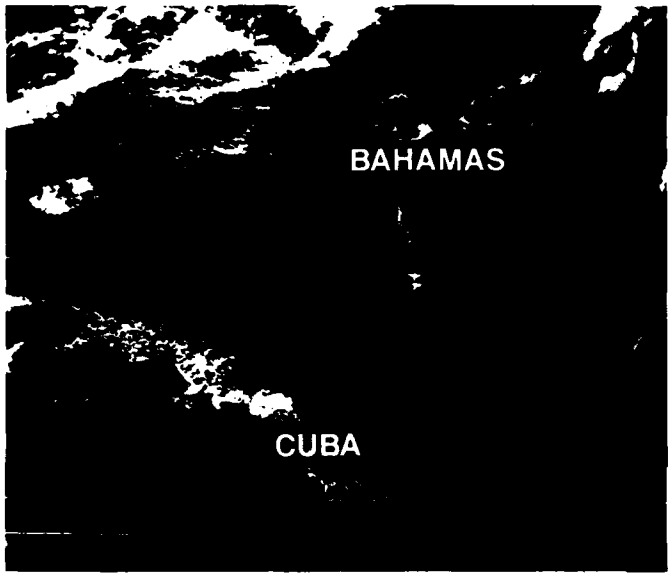

1C-9a. NOAA-9 Channel 2 (0.86 μm), 1942 GMT, 23 February 1986.

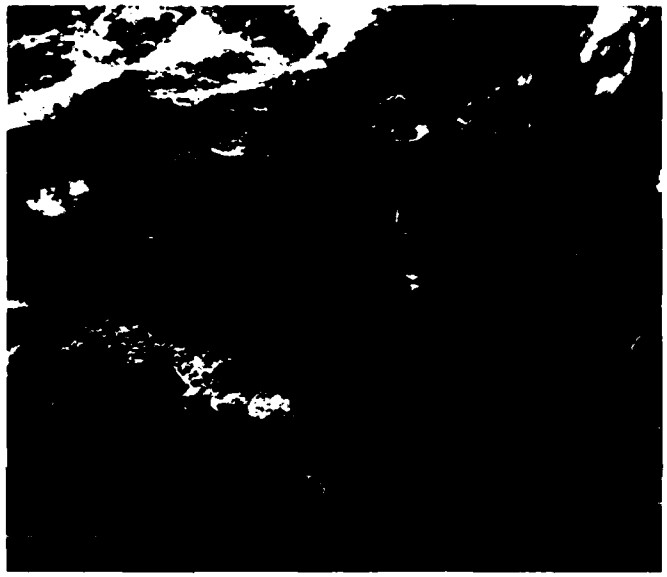

1C-9b. NOAA-9 Channel 1 (0.63 μm), 1942 GMT, 23 February 1986.

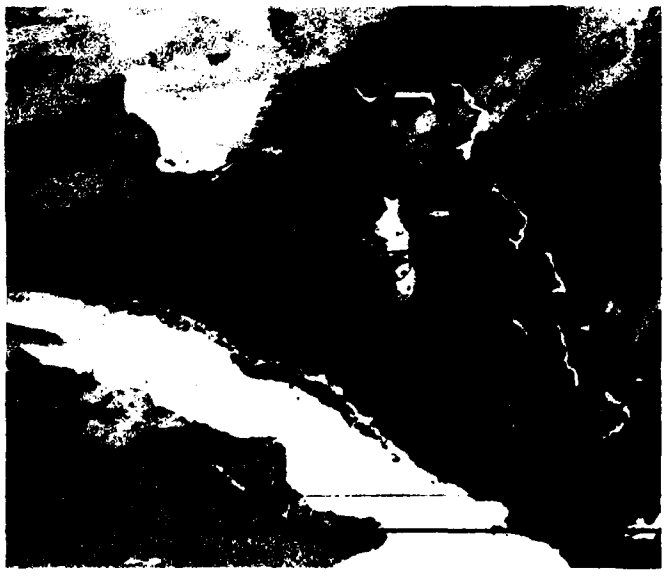

1C-9c. Ratio of reflectances from Figs. 1C-9a and 9b, 1942 GMT, 23 February 1986.

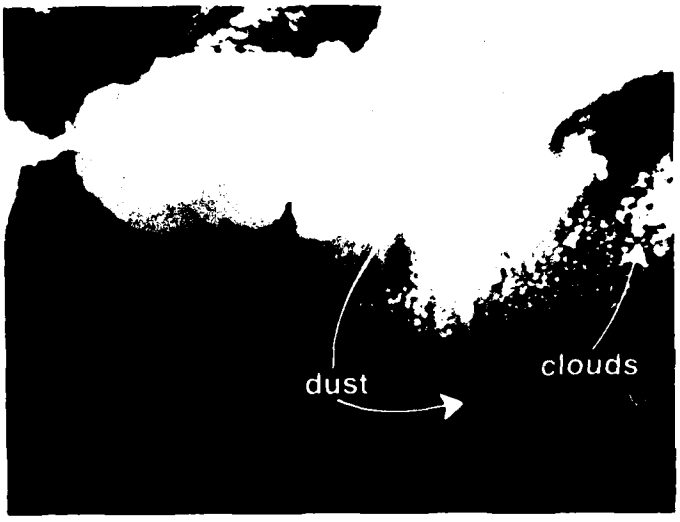

1C-10c. NOAA-9 Channel 4 (10.8 μm), 1444 GMT, 24 June 1986.

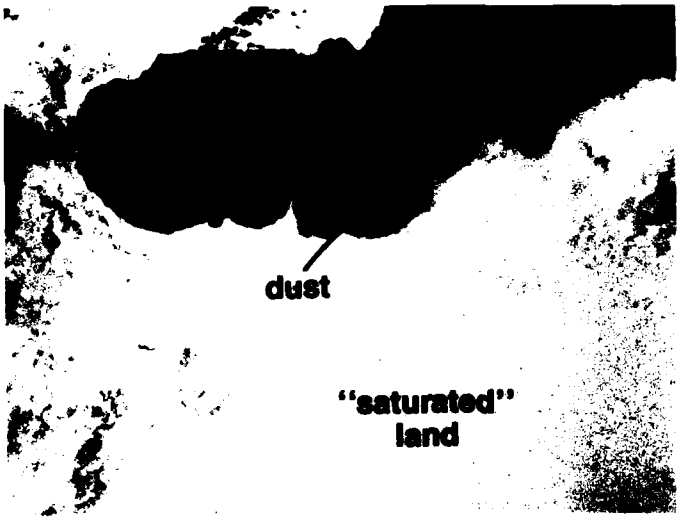

1C-10d. NOAA-9 Channel 3 (3.7 μm), 1444 GMT, 24 June 1986.

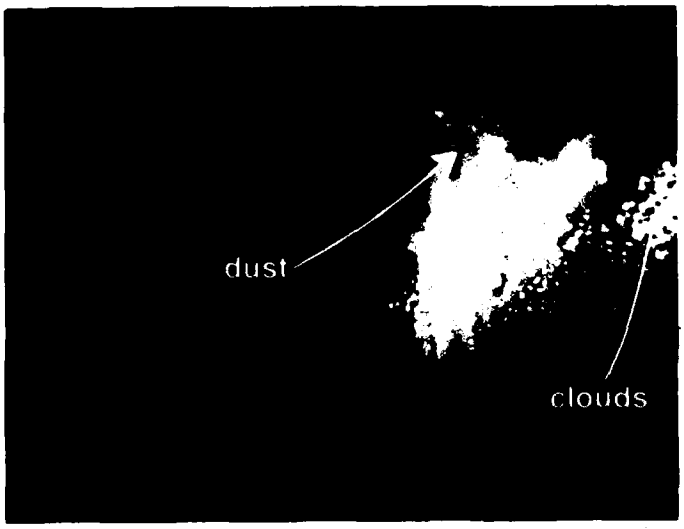

1C-10e. Brightness temperature difference based on Figs. 1C-10d and 10c (Channel 3 and Channel 4), 1444 GMT, 24 June 1986.

5. Dust over the Western Mediterranean

Dust is discussed extensively in NTAG, Vol. 5, but the multispectral capabilities of the AVHRR offer some additional analysis tools. Figures 1C-10a–10c show a duststorm sweeping dust from North Africa across the Mediterranean. In Fig. 1C-10a (Channel 2) dust contrasts well with the dark sea surface so that dust areas are fairly well identified over the ocean. However, it is more difficult to detect dust over land. This absence of contrast occurs because the underlying land has reflective properties similar to the dust itself. In the desert region producing the dust, the Channel 1 image (Fig. 1C-10b) has an appearance similar to Channel 2. The similar appearance of the two channels occurs over all regions that are free of significant growing vegetation. By contrast, the Channel 1 image (Fig. 1C-10b) is much darker than the Channel 2 image (Fig. 1C-10a) over the vegetated regions of southern Spain and extreme northern Africa.

In Fig. 1C-10c (Channel 4 infrared) the cool dust contrasts well with the hot land surface but poorly against the relatively cool sea surface. The enhanced contrast over land occurs because the elevated dust is cooler than the heated land surface. Over the ocean, however, the elevated dust has a temperature similar to the underlying sea surface. Therefore, the contrast is poor. Figure 1C-10d (Channel 3) is unique in that it shows both emitted thermal radiation (such as in Channel 4) and reflective solar radiation (as in Channels 1 and 2). Unfortunately, while the Channel 3 image portrays dust effectively over water, the land areas are saturated. Saturation can be identified by the very bright, uniform appearance. An effective way to image dust over both land and sea is to subtract Channel 4 from Channel 3, as in Fig. 1C-10e.

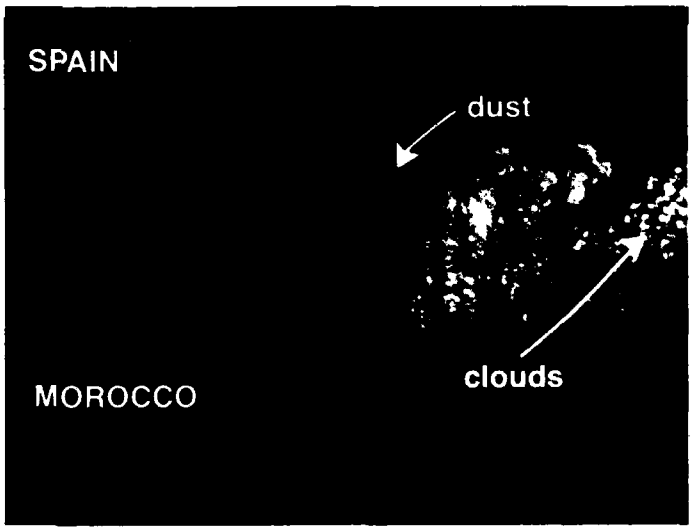

1C-10a. NOAA-9 Channel 2 (0.86 μm), 1444 GMT, 24 June 1986.

1C-10b. NOAA-9 Channel 1 (0.63 μm), 1444 GMT, 24 June 1986.

6. Summer Shamal over the Persian Gulf

Figures 1C-11a–11d show a dust storm resulting from the summer shamal (for general discussion, see NTAG, Vol. 5, Part 1, Sec. 1E, Case 3). The Channel 1 image (Fig. 1C-11a) shows the dust relatively poorly over the bright land surface regions of the Tigris and Euphrates Valley north of the Persian Gulf. Dust shows up better over the darker surface of the gulf. The Channel 4 image (Fig. 1C-11b) shows the elevated, relatively cool dust well over the heated land area but poorly against the cool sea surface. The reflective desert land (Fig. 1C-11c) nearly saturates the sensor in Channel 3, causing the desert and overlying dust to appear nearly white. Over the water, on the other hand, the Channel 3 image gives a superior depiction of dust compared to the images of the other two channels. Figure 1C-11d, a difference image of Channels 3 and 4, is an excellent depiction of dust over both land and sea.

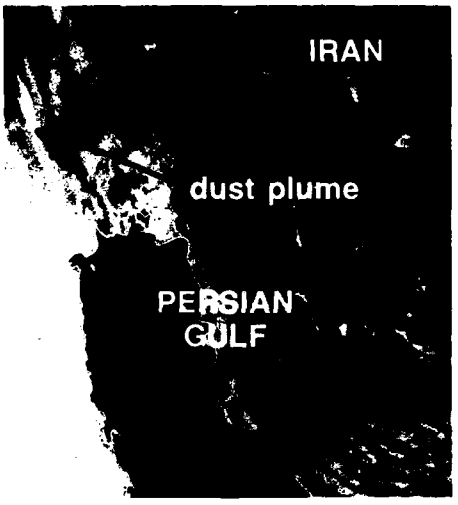

1C-11a. NOAA-9 Channel 1 (0.63 μm), 1037 GMT, 28 June 1986.

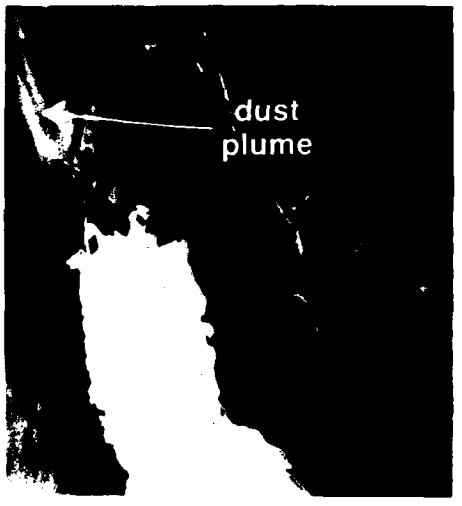

1C-11b. NOAA-9 Channel 4 (10.8 μm), 1037 GMT, 28 June 1986.

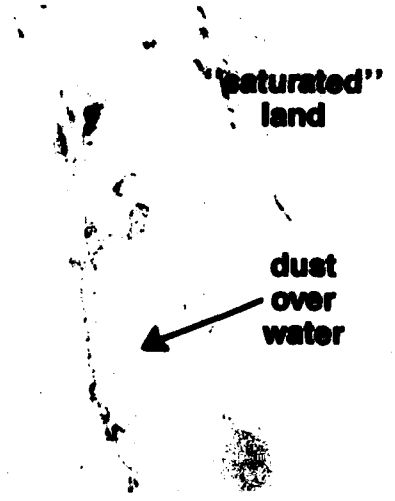

1C-11c. NOAA-9 Channel 3 (3.7 μm), 1037 GMT, 28 June 1986.

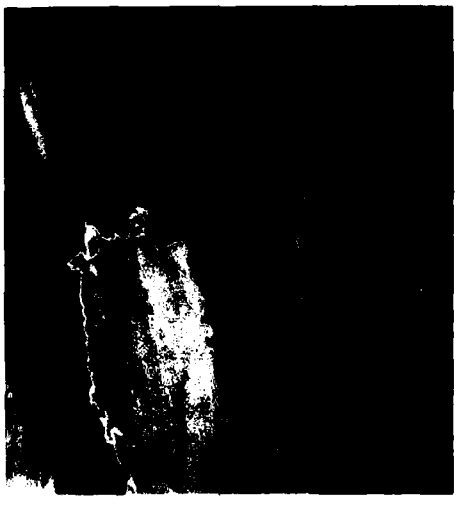

1C-11d. Brightness temperature difference based on Figs. 1C-11c and 11b (Channel 3 and Channel 4), 1037 GMT, 28 June 1986.

8. Low Cloud Detection over Elevated Terrain

On 29 June 1986, NOAA-9 imaged northern Iran and the southern Caspian Sea. The nearly vertical striations in the Channel 3 image (Fig. 1C-12c) are the characteristic Channel 3 noise. The low cloud in the southern portion of the image stands out well over water, but poorly over land. Identification of low cloud is particularly difficult around the mountainous terrain of northern Iran, where the temperature variations caused by uneven terrain blend in with the cloud tops. The Channel 4 image is similarly difficult to interpret (Fig. 1C-13a).

A brightness temperature difference image between Channels 3 and 4 (Fig. 1C-13b) resolves these problems. Low clouds are associated with high differences and stand out well against the surface, which is associated with small differences. In particular, the low cloud now can easily be distinguished from the mountains in northern Iran.

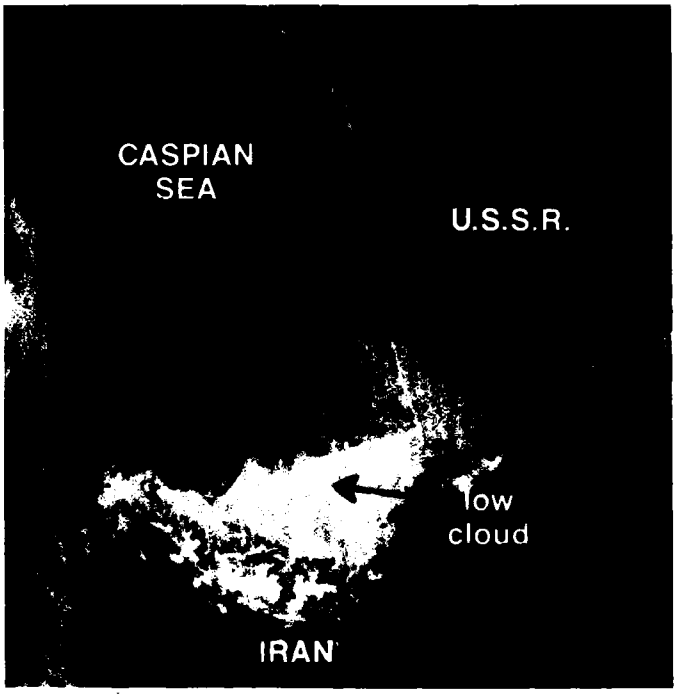

1C-12c. NOAA-9 Channel 3 (3.7 μm), 2304 GMT, 29 June 1986.

7. Comparison of Low and High Clouds in Channels 3 and 4

Images at 3.7 μm are particularly good at detecting low cloud at night. For example, a Channel 3 image (Fig. 1C-12a) reveals low, relatively warm cloud well over Yucatan. However, a Channel 4 image (Fig. 1C-12b) does not show this cloudiness nearly as well. Note, too, that cirrus is much more transparent in the Channel 3 image than in the Channel 4 image. Over the ocean areas, the cirrus in the Channel 3 image (Fig. 1C-12a) is so thin that lower stratocumulus clouds can be seen. In the Channel 4 image (Fig. 1C-12b) this cirrus is more opaque such that lower cloudiness is difficult to detect.

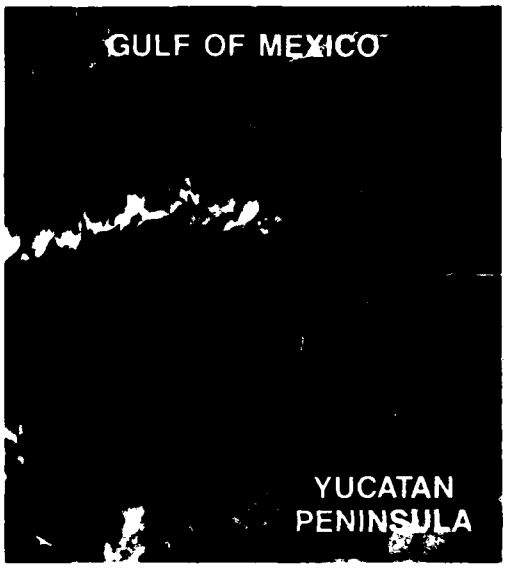

1C-12a. NOAA-11 Channel 3 (3.7 μm), 0757 GMT, 14 May 1989.

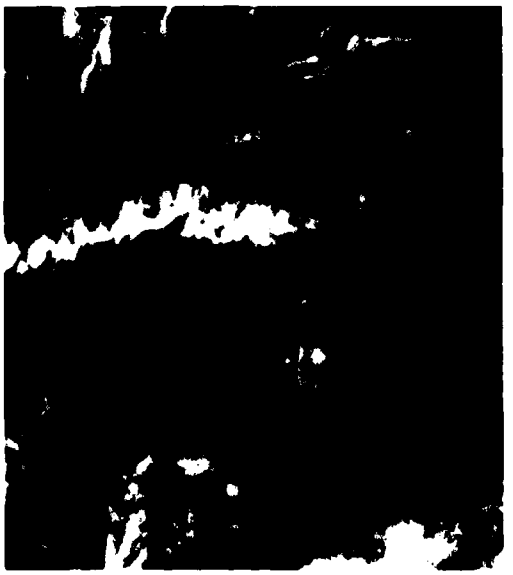

1C-12b. NOAA-11 Channel 4 (10.8 μm), 0757 GMT, 14 May 1989.

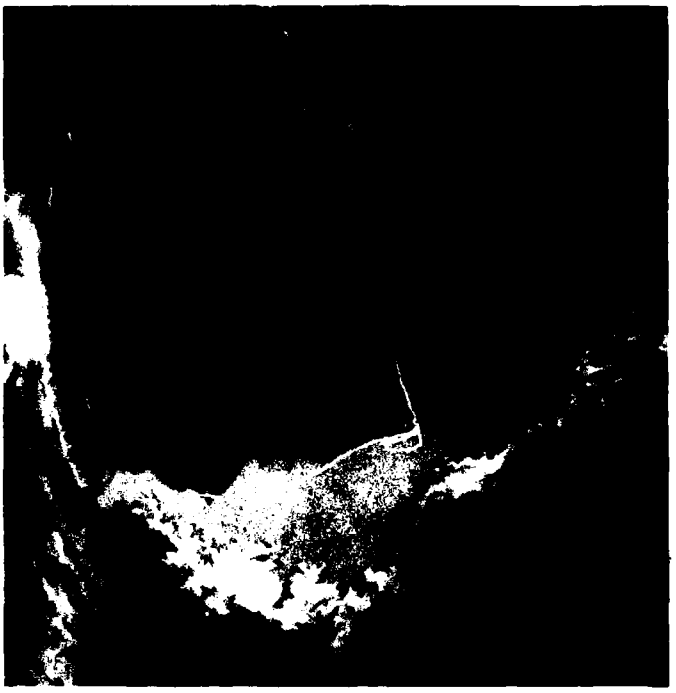

1C-13a. NOAA-9 Channel 4 (10.8 μm), 2304 GMT, 29 June 1986.

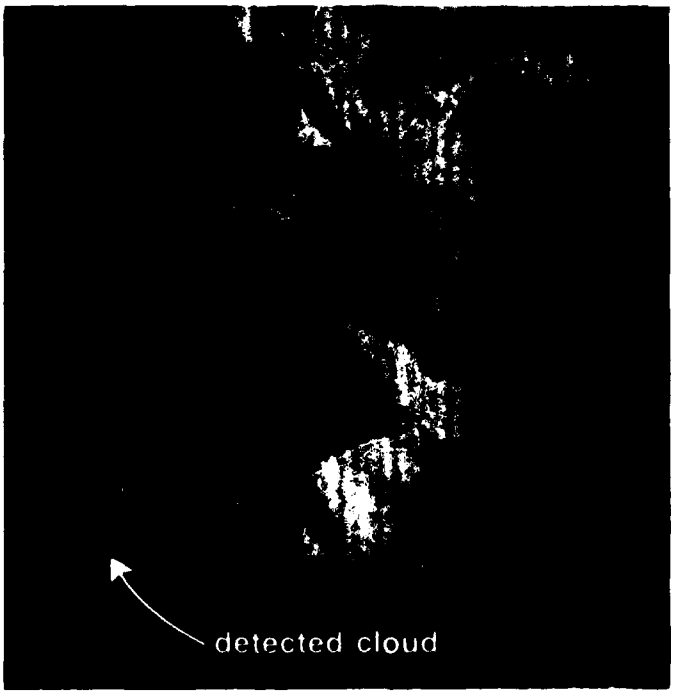

1C-13b. Brightness temperature difference based on Figs. 1C-12a and 13a (Channel 3 and Channel 4), 2304 GMT, 29 June 1986.

9. Detection of Fog and Stratus over Florida

Figure 1C-14a is a Channel 3 winter scene over Florida. Although it is possible to distinguish cloud from water off the Florida coast, it is difficult to distinguish cloud from the peninsula itself. Detection of low cloud using a Channel 4 image is nearly impossible (Fig. 1C-14b). The difference image (Fig. 1C-14c) distinguishes cloud from the surface with remarkable clarity. Gradients of sea surface temperature are also more clearly revealed in the difference image.

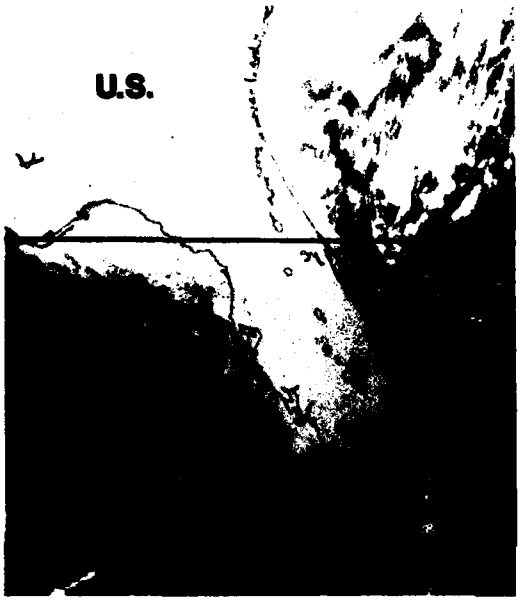

1C-14a. NOAA-9 Channel 3 (3.7 μm), 0836 GMT, 24 January 1986.

1C-14b. NOAA-9 Channel 4 (10.8 μm), 0836 GMT, 24 January 1986.

1C-14c. Brightness temperature difference based on Figs. 1C-14a and 14b (Channel 3 and Channel 4), 0836 GMT, 24 January 1986.

10. Anomalous Cloud Lines in Nighttime Infrared Imagery

Anomalous cloud lines are narrow, linear features that appear in the stable marine atmosphere. They are produced by the interaction of ship effluents with the moist marine environment (NTAG, Vol. 2, Sec. 1C). Anomalous cloud lines appear in Channel 3 off British Columbia (Fig. 1C-15a). In Channel 4 (Fig. 1C-15b), however, little trace of the cloud lines is evident. Also, in Channel 3 it is easier than in Channel 4 to distinguish the boundary between the stratus in the eastern two-thirds of the scene and the clear region to the west. Notice the characteristic noise that appears in the Channel 3 image (Fig. 1C-15a). This noise seriously degrades the ability to examine variations in sea surface termperature in the clear regions.

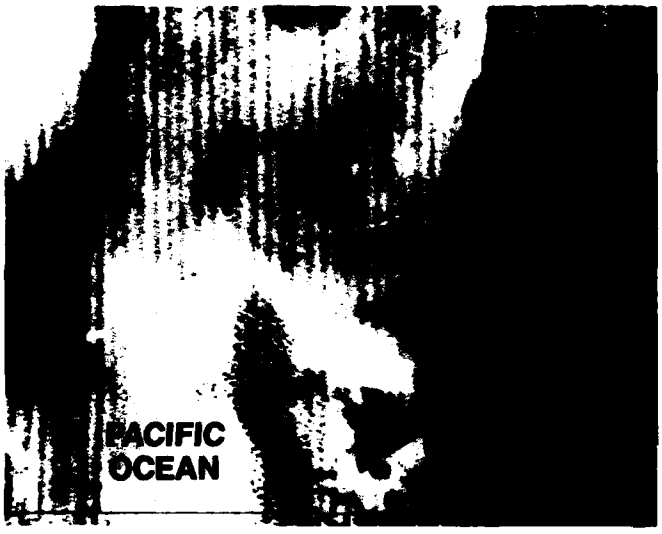

1C-15a. NOAA-9 Channel 3 (3.7 μm), 1157 GMT, 17 December 1985.

1C-15b. NOAA-9 Channel 4 (10.8 μm), 1157 GMT, 17 December 1985.

11. Anomalous Cloud Lines in the Eastern Pacific

On the nighttime Channel 3 image (Fig. 1C-16a), anomalous cloud lines appear distinctly against a darker background. On the Channel 4 image (Fig. 1C-16b) on the other hand, these lines appear much less distinctly. In fact, on the Channel 4 image the tip of one cloud line is not detectable in the vicinity of a strong sea surface temperature gradient. In the Channel 3 image (Fig. 1C-16a) the tip of this cloud line appears distinctly.

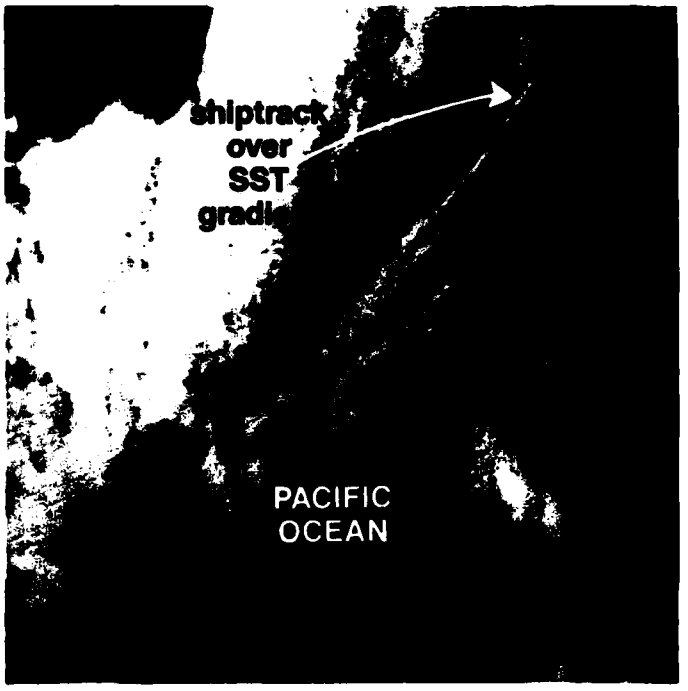

1C-16a. NOAA-10 Channel 3 (3.7 μm), 0304 GMT, 18 October 1989.

1C-16b. NOAA-10 Channel 4 (10.8 μm), 0304 GMT, 18 October 1989.

12. Daytime Anomalous Cloud Lines off the Oregon Coast

During the daytime, anomalous cloud lines in the Channel 3 image are particularly reflective of solar radiation compared to surrounding cloud or ocean features. The enhanced reflectivity occurs because the anomalous cloud lines are composed of numerous but very small cloud droplets. This unique cloud property arises from the large concentrations of cloud condensation nuclei emitted by ships. Figures 1C-17a–17c show an example of anomalous cloud lines off the Oregon coast. The Channel 3 image (Fig. 1C-17a) shows the effect better than the Channel 2 image (Fig. 1C-17b) or Channel 4 image (Fig. 1C-17c).

1C-17a. NOAA-9 Channel 3 (3.7 μm), 2314 GMT, 13 July 1987.

1C-17b. NOAA-9 Channel 2 (0.86 μm), 2314 GMT, 13 July 1987.

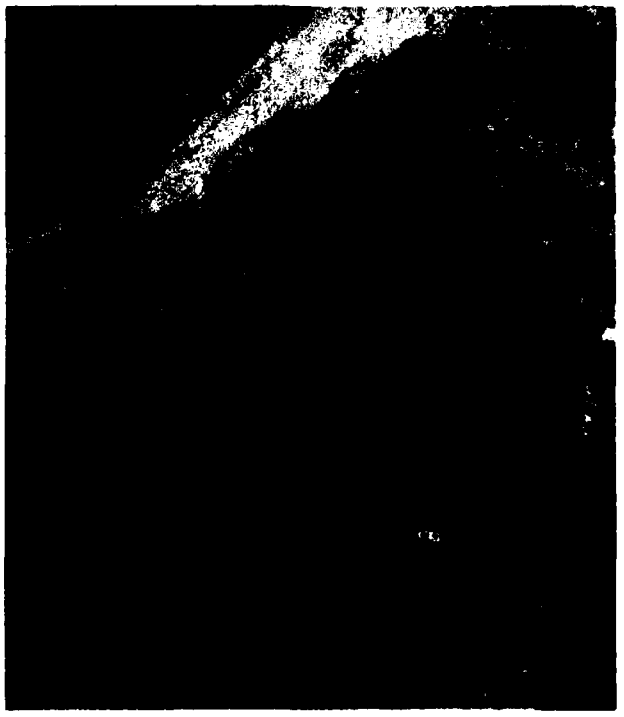

1C-17c. NOAA-9 Channel 4 (10.8 μm), 2314 GMT, 13 July 1987.

13. Degradation of Nighttime Channel 3 in Cold Regions

Nighttime images of Channel 3 often become degraded over land regions covered with ice and snow. Notice the lack of detail in Fig. 1C-18a, a Channel 3 image of a very cold scene. This effect occurs because very cold land surfaces emit very little energy at the Channel 3 wavelength (3.7 μm). Thus, its ability to distinguish variations in surface temperature is greatly diminished. It is the lack of sufficient radiance that is mainly responsible for the degradation, not the sensor itself. Figure 1C-18b is a Channel 4 image of the same scene, containing improved detail. Notice that the characteristic noise of the Channel 3 image (vertical lines on Fig. 1C-18a) is more prominent over the colder regions (brighter gray shades) of the image. Over such cold scenes it is often not feasible to use nighttime Channel 3 for detection of low cloud. Daytime Channel 3 images, on the other hand, are often extremely useful in frigid polar regions. The explanation for the improvement during the daytime is that solar reflection helps raise the overall energy reaching the satellite and partially compensates for the absence of thermal emission from the surface.

1C-18a. NOAA-10 Channel 3 (3.7 μm), 0118 GMT, 16 December 1986.

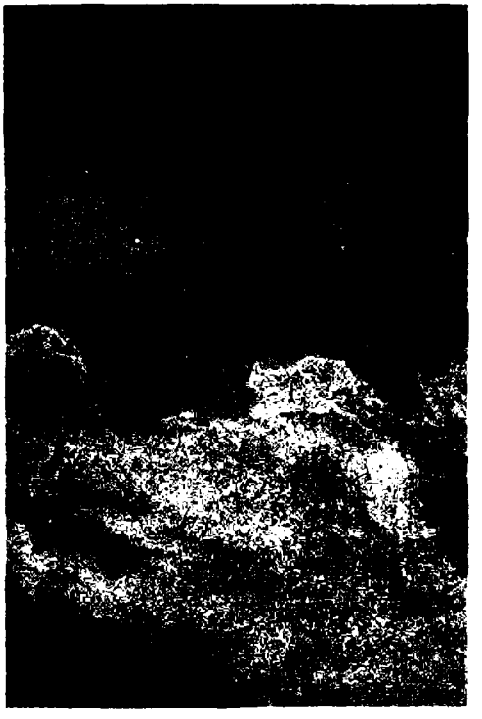

1C-18b. NOAA-10 Channel 4 (10.8 μm), 0118 GMT, 16 December 1986.

14. Thermal Hotspots in the Persian Gulf

Channel 3 has a special capability to detect tiny hotspots, including factory exhaust stacks, gas flare stacks, wildfires, and agricultural burning. It should be possible to observe battlefield fires using this channel if clouds do not obscure the scene. The hotspots observed can be much smaller than the approximate 1-km spatial resolution of the satellite, though it is not possible to determine precisely where the fire lies within the pixel.

Hotspots resulting from gas flares are persistent features on nighttime Channel 3 images of the Persian Gulf region (Fig. 1C-19a). They appear over both land and sea. Being very tiny, hotspots often fail to be detected on images of large areas. Thus the ability to detect hotspots depends on the analyst's ability to expand and enhance imagery on an interactive workstation.

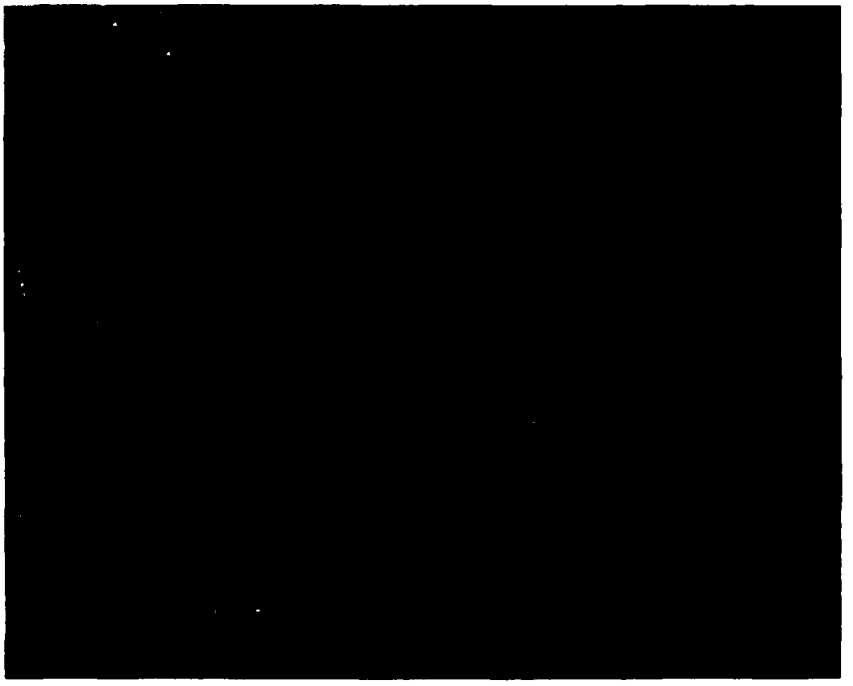

1C-19a. NOAA-9 Channel 3 (3.7 μm), 2304 GMT, 28 June 1986.

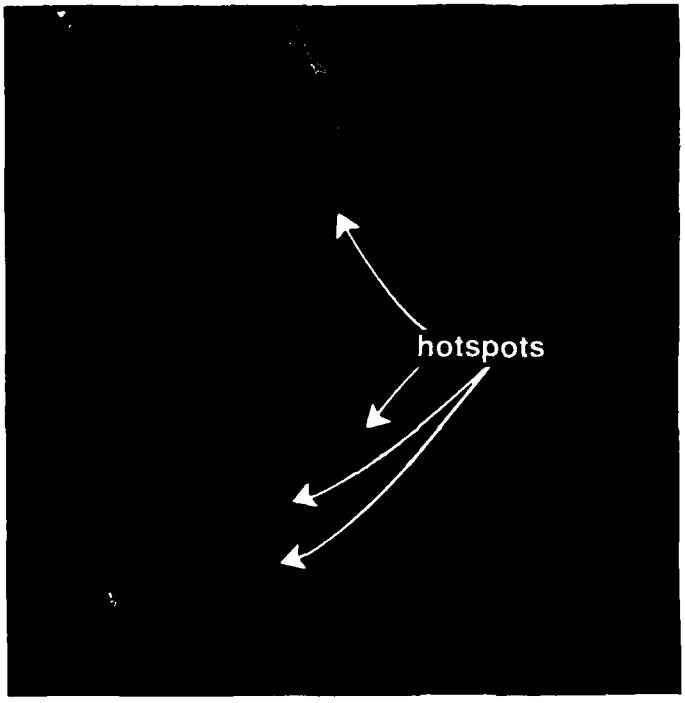

1C-20b. NOAA-10 Channel 3 (3.7 μm), 0304 GMT, 18 October 1989.

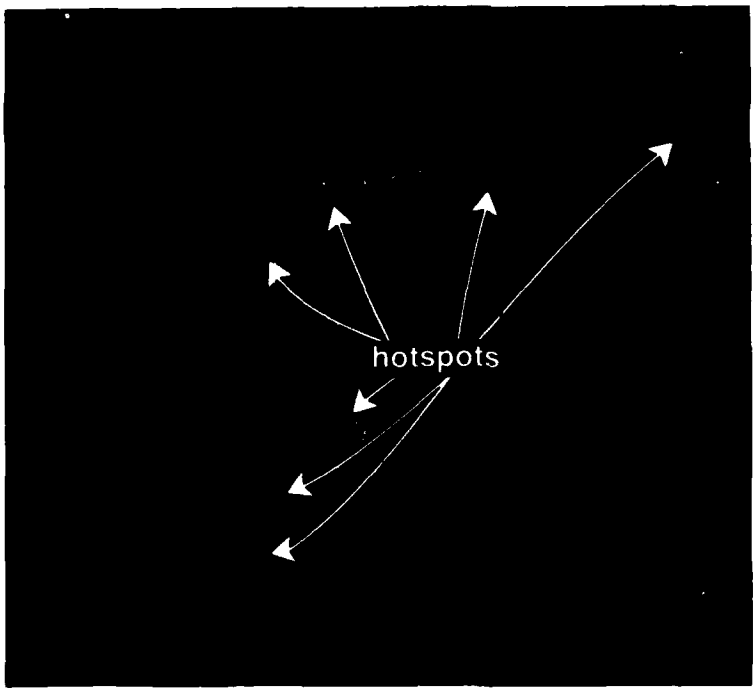

1C-20c. Brightness temperature difference based on Figs. 1C-20b and 20a (Channel 3 and Channel 4), 0304 GMT, 18 October 1989.

15. Hotspots Arising from an Earthquake

A major earthquake occurred in central California at 0004 GMT on 18 October 1989. NOAA-10 imaged the scene approximately 3 hours later. The Channel 4 image (Fig. 1C-20a) shows no trace of the resulting fires. The Channel 3 image (Fig. 1C-20b), on the other hand, shows numerous bright dots corresponding to high temperature sources. The most noteworthy among these is a fire on the northern coast of San Francisco (in the marina district). This dot represents the burning of a number of adjacent apartment buildings. Fires resulting from the earthquake also occurred in the town of Watsonville and in the Santa Cruz Mountains near the epicenter. A number of hotspots developed that were not related to the earthquake directly. For example, some of the dots show the hot stacks from factories or power plants.

In Fig. 1C-20b some hotspots are difficult to distinguish from hilly terrain. A brightness temperature difference image between Channel 3 and Channel 4 shows the hotspots less ambiguously (Fig. 1C-20c). However, this difference image also eliminates helpful geographic landmarks such as valleys and ridges. Two hotspots appear well offshore (Figs. 1C-20b and 20c); these are probably caused by hot stacks aboard ships. Nevertheless, the general ability of this sensor to detect stacks aboard ships has not been proven and should not be considered reliable pending further research.

1C-20a. NOAA-10 Channel 4 (10.8 μm), 0304 GMT, 18 October 1989.

Difference images (such as Fig. 1C-21c) can also show fire movement or growth over a 24-hour period. Figure 1C-21d is an expanded image of Fig. 1C-21c centered on Yellowstone Lake. To show changes in position in fire location from one day to the next, Fig. 1C-21d and the corresponding difference image from the following morning, Fig. 1C-21e, were coregistered, then subtracted from one another. Figure 1C-21f shows the 24-hour difference between the two images. Black shows the positions of the fires on the first night, and white shows the positions on the second night. Thus, the analyst can determine the growth or movement of the fires.

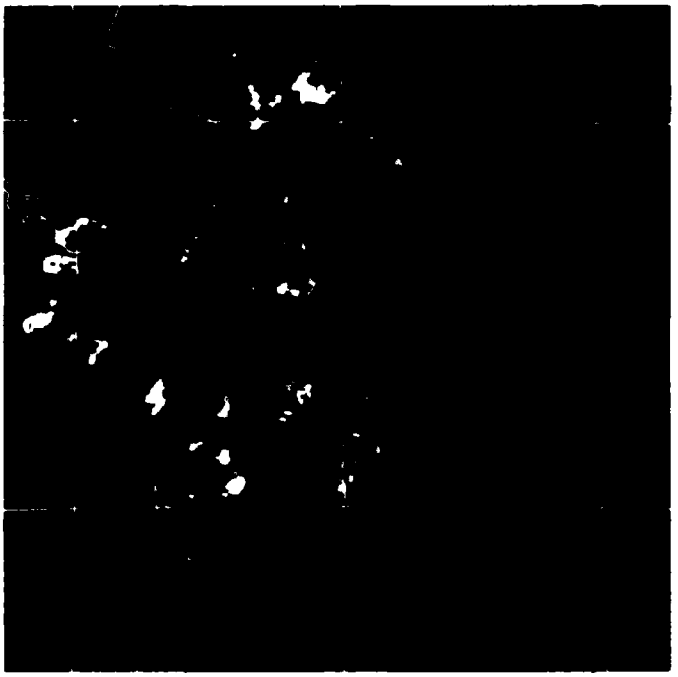

1C-21e. Difference image as in Fig. 1C-21d, but imaged at 1147 GMT, 3 September 1988.

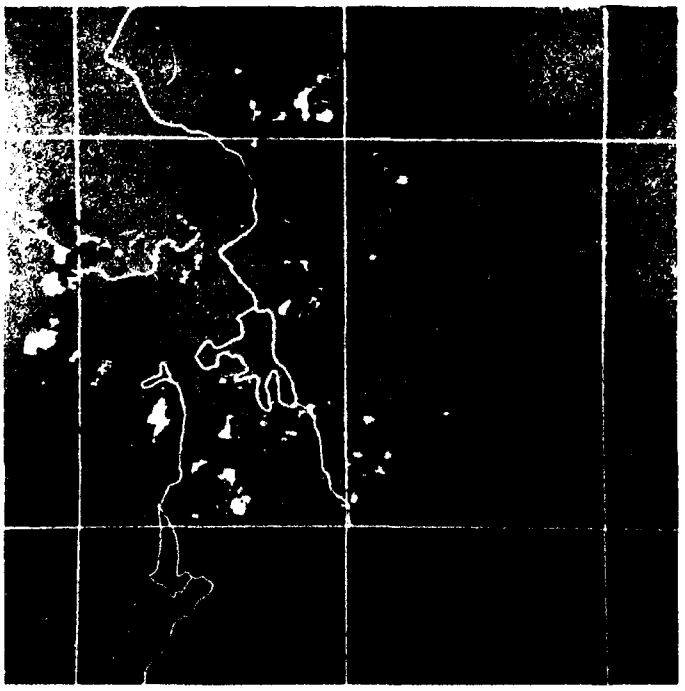

1C-21f. Twenty-four hour "change" image, based on the difference of Figs. 1C-21d and 21e.

16. Detection of Forest Fires

On a predawn image taken on 2 September 1988, a Channel 4 image (Fig. 1C-21a) shows little evidence of fire around the edges of Yellowstone Lake. A Channel 3 image (Fig. 1C-21b), on the other hand, shows the fires as white spots against a darker background. A difference image (Fig. 1C-21c) eliminates conflicting thermal signals resulting from the elevated terrain, revealing the hotspots vividly. For example, several fires are apparent in the southern region of Fig. 1C-21c that could not plainly be seen in Fig. 1C-21b.

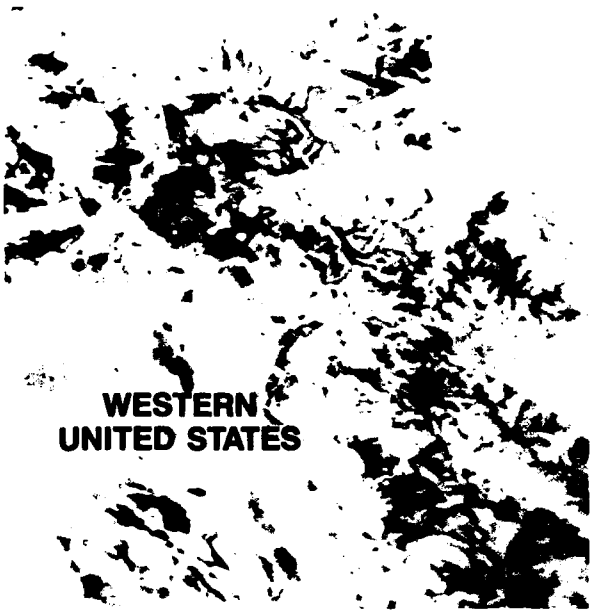

1C-21a. NOAA-9 Channel 4 (10.8 μm), 1158 GMT, 2 September 1988.

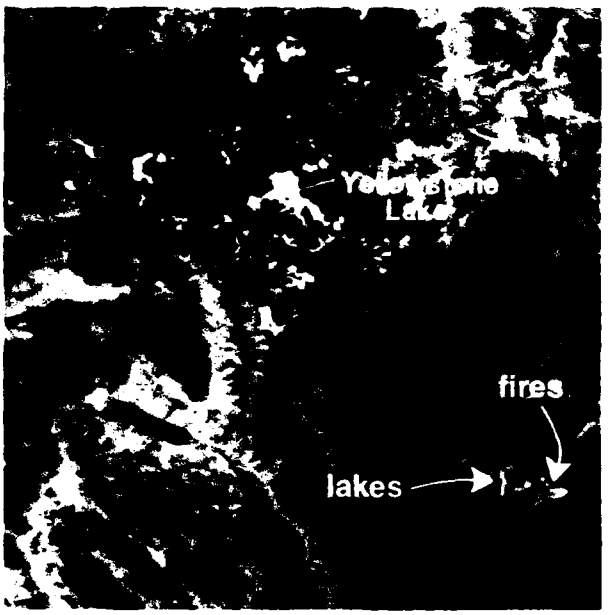

1C-21b. NOAA-9 Channel 3 (3.7 μm), 1158 GMT, 2 September 1988.

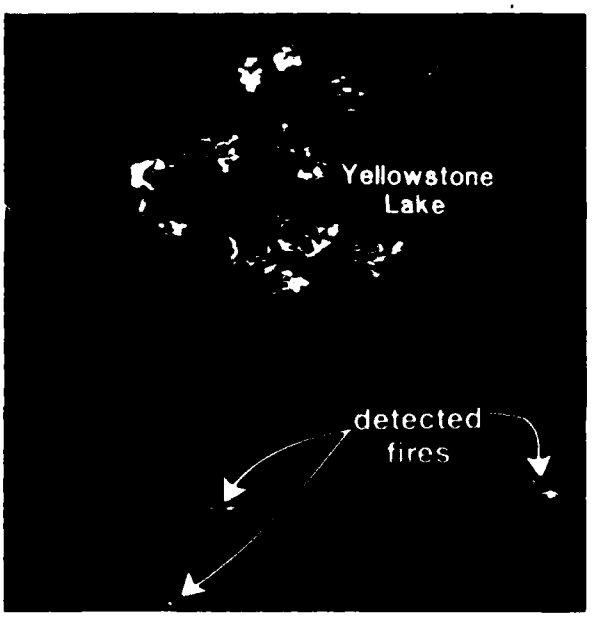

1C-21c. Brightness temperature difference based on Figs. 1C-21b and 21a (Channel 3 and Channel 4), 1158 GMT, 2 September 1988.

1C-21d. Blowup of Fig. 1C-21c, 1158 GMT, 2 September 1988.

17. Identification of an Aircraft Accident

More skill is required to analyze hotspots during the daytime than at night. The increased difficulty occurs because daylight solar reflection from clouds or other land features can mask hotspots. Figures 1C-22a, 1C-23a, and 1C-23b represent a daytime scene over southern California during a period of warm offshore winds, a "Santa Ana" condition. Figure 1C-22a is a Channel 3 (negative) image of extreme southern California and northern Mexico. Considerable smoke appears in the image because of recent brush fires. A bright spot (annotated) marks the site of a recent military training mission crash. The size of the signature suggests a large burning area; however, the actual burn area is much smaller. The size discrepancy occurs because the intense heat of the relatively tiny fire saturates the response over several adjacent pixels. A Channel 2 image (Fig. 1C-23a) and a Channel 4 image (Fig. 1C-23b) show no trace of the fire. Thus, Channel 3 is useful to locate the position of downed aircraft when other information is absent.

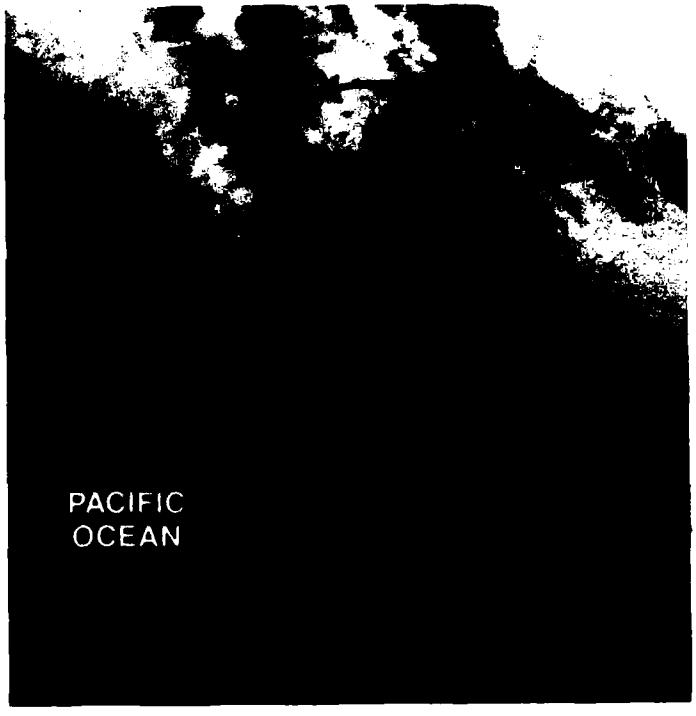

1C-22a. NOAA-11 Channel 3 (3.7 μm), 2139 GMT, 30 November 1989.

18. Identification of Pollution Within Water Clouds

Channel 3 images can distinguish clouds with continental drop size distributions from those with marine distributions. Figures 1C-23c and 23d show a stratus cover over the Los Angeles basin and offshore waters. In the Channel 2 image (Fig. 1C-23c), the brightness of the stratus cover is fairly uniform. In particular, the stratus cover has an equal brightness over the basin as over the offshore waters. In the Channel 3 image (Fig. 1C-23d) on the other hand, marked variations in reflectivity occur over the cloud deck. In particular, tiny bright spots over the Los Angeles basin indicate point sources of pollution. Also, the Channel 3 image (Fig. 1C-23d) shows a dividing line between relatively polluted cloud (relatively small droplets) over and just off the southern California coast and relatively unpolluted cloud (large droplets in smaller concentrations) offshore.

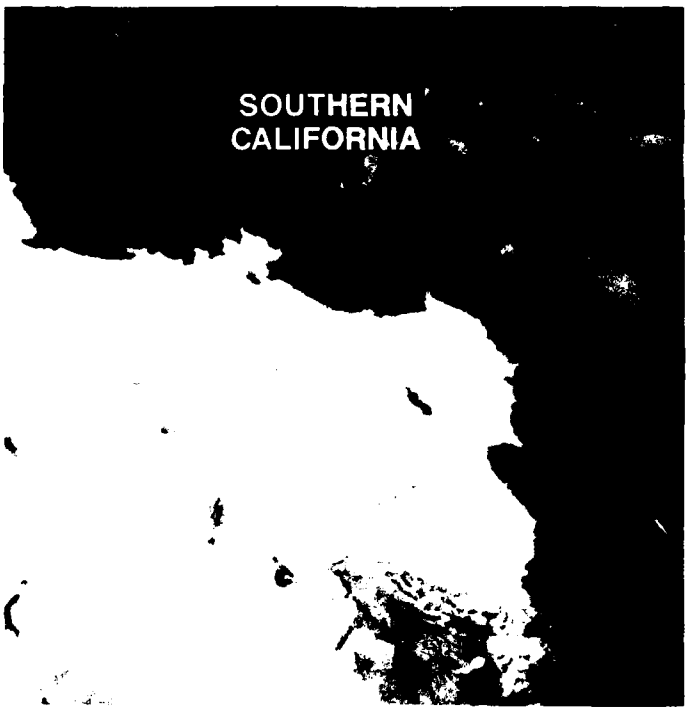

1C-23c. NOAA-10 Channel 2 (0.86 μm), 1550 GMT, 30 June 1987.

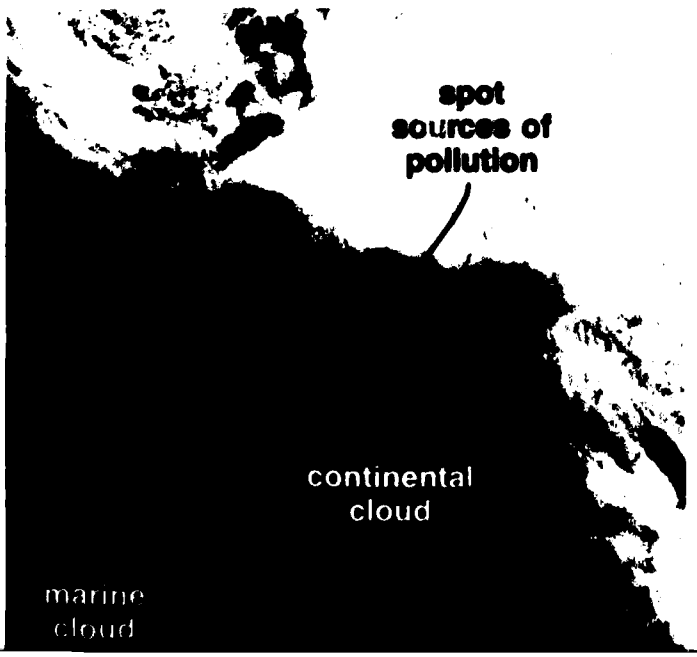

1C-23d. NOAA-10 Channel 3 (3.7 μm), 1550 GMT, 30 June 1987.

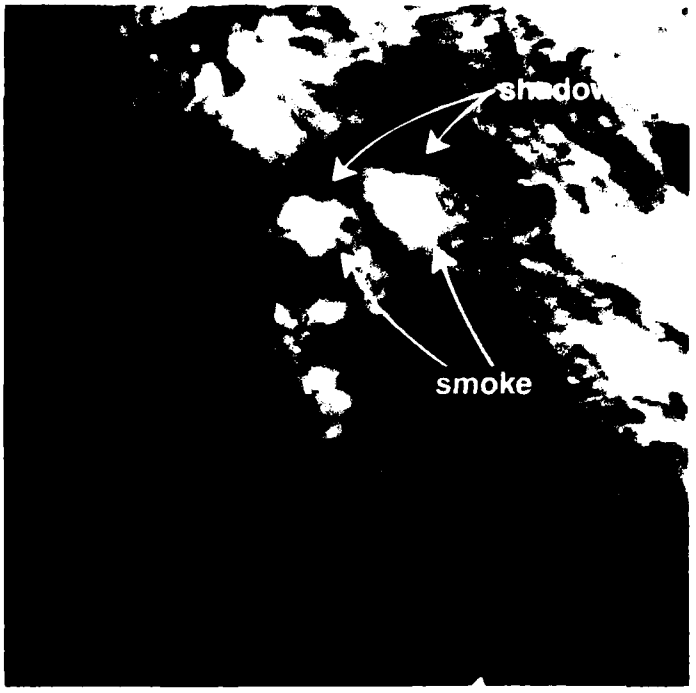

1C-23a. NOAA-11 Channel 2 (0.86 μm), 2139 GMT, 30 November 1989.

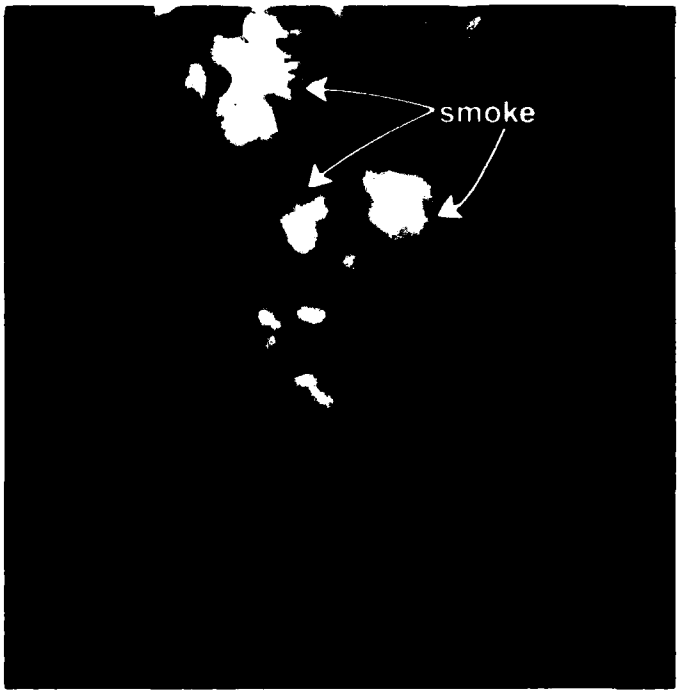

1C-23b. NOAA-11 Channel 4 (10.8 μm), 2139 GMT, 30 November 1989.

19. Stratus off Central California

Channels 2 and 4 (Figs. 1C-24a and 24b) show a nearly unbroken, rather uniform sheet of stratus over the offshore waters and over the coastal valleys. The cloud deck in the Channel 3 image (Fig. 1C-25a), on the other hand, shows considerable variation. This absence of uniformity is caused by variations in drop size distribution and cloud thickness. Over the coastal valleys the low cloud tends to blend in with surrounding surface features, making detection of cloud boundaries difficult. A difference image (3 minus 4), shown in Fig. 1C-25b, sharpens the boundaries of the stratus over the coastal valleys. The bright gray shades of the onshore cloudiness in Fig. 1C-25b suggest a continental type cloud characterized by high concentrations of relatively small water droplets.

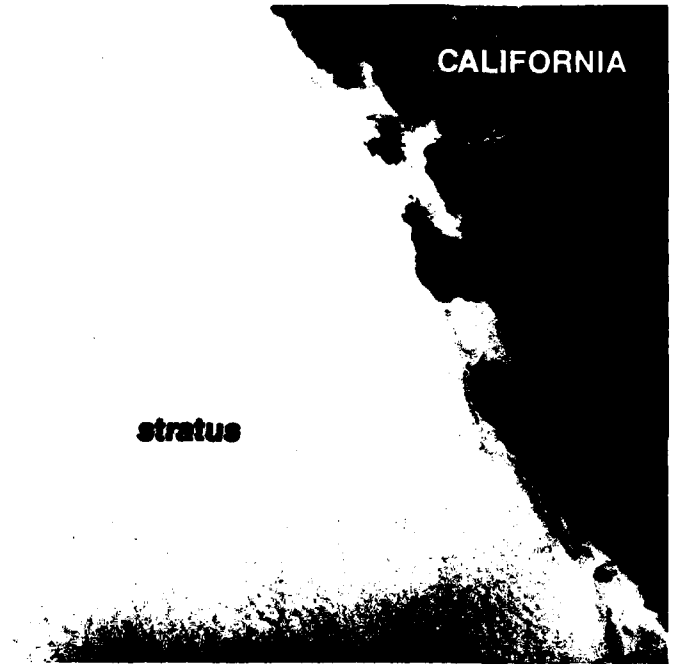

1C-24a. NOAA-10 Channel 2 (0.86 μm), 1547 GMT, 14 July 1987.

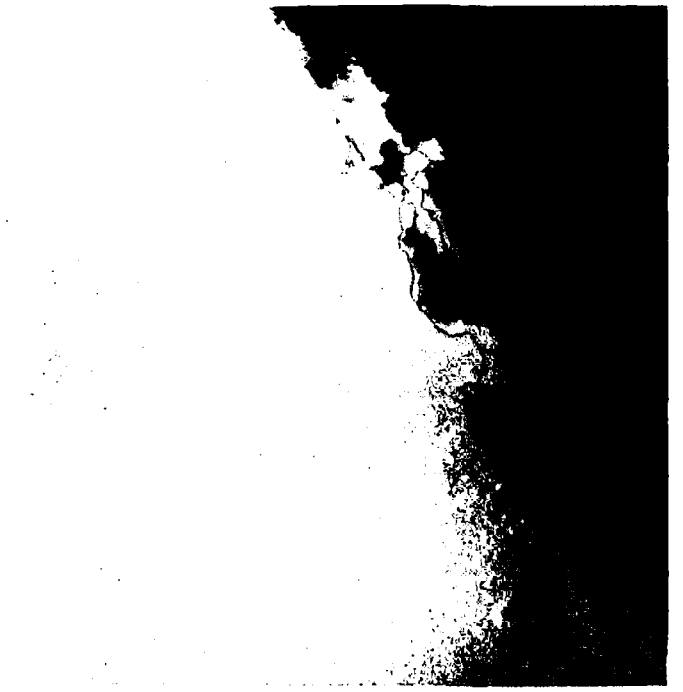

1C-24b. NOAA-10 Channel 4 (10.8 μm), 1547 GMT,

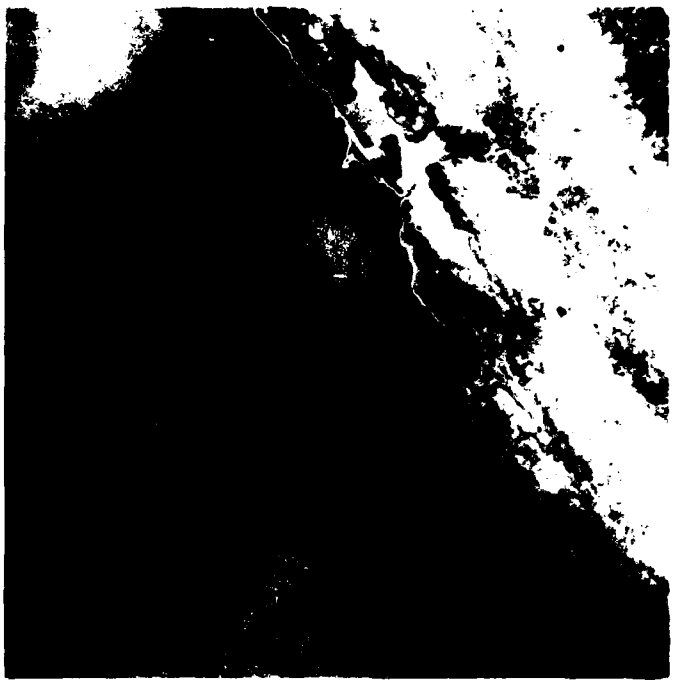

1C-25a. NOAA-10 Channel 3 (3.7 μm), 1547 GMT, 14 July 1987.

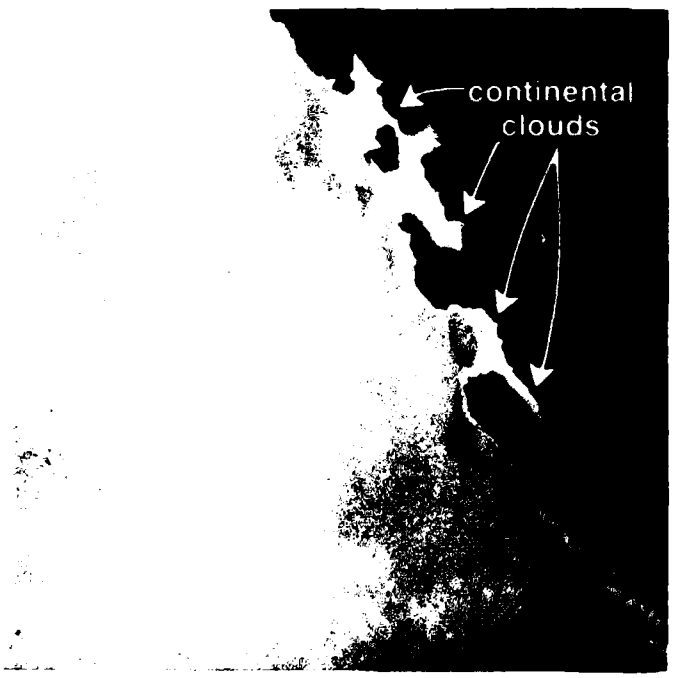

1C-25b. Brightness temperature difference image based on Figs. 1C-25a and 24b (Channel 3 and Channel 4), 1547 GMT, 14 July 1987.

20. Identification of Water Cloud over Ice

During the daytime, AVHRR imagery offers distinct advantages in the identification of cloud over ice and snow. The Channel 2 image (Fig. 1C-26a) shows the eastern edge of Greenland, including the coastal ice sheet. A faint suggestion of cloud is evident over the ice sheet, but it is difficult to distinguish cloud from ice. A Channel 3 negative image (Fig. 1C-27a) shows these clouds distinctly as white against a dark background. This effect occurs because in Channel 3 low water clouds are more reflective of solar radiation than the underlying frozen surface. Thus, even thin low clouds stand out well against the background. On the other hand, Channel 4 (Fig. 1C-27b) is very insensitive to thin cloud and thus "sees through" the clouds that were reflective in Channel 3. In fact, Channel 4 reveals the ice fissures below the cloud.

1C-26a. NOAA-10 Channel 2 (0.86 μm), 1000 GMT, 27 March 1987.

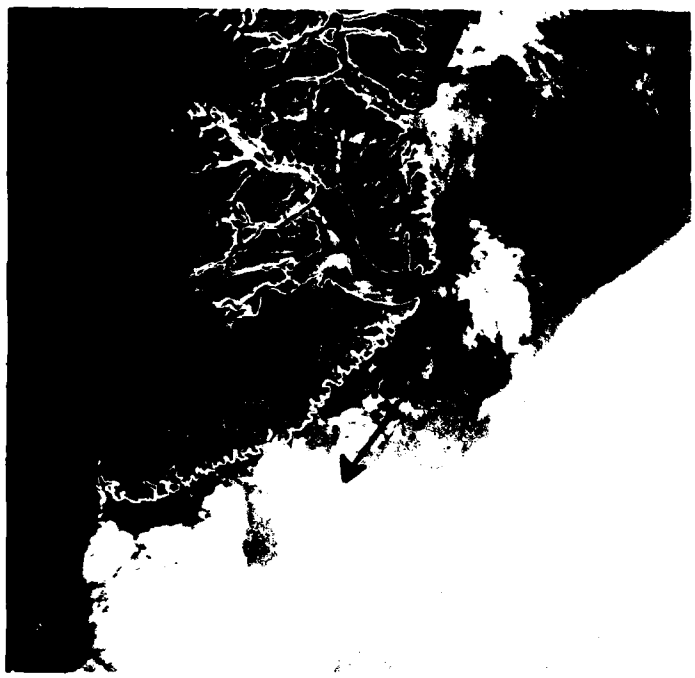

1C-27a. NOAA-10 Channel 3 (3.7 μm), 1000 GMT, 27 March 1987.

1C-27b. NOAA-10 Channel 4 (10.8 μm), 1000 GMT, 27 March 1987.

21. Identification of Contrails from Channels 4 and 5

The Channel 4 image (Fig. 1C-28a) shows the central valley of California. The cirrus in the image is so thin that energy from the Earth's surface passes through. Thus the cirrus appears in relatively dark (warm) gray shades and in some places cannot be distinguished easily from the surface background. The image produced from the Channel 5 image (Fig. 1C-29a) is nearly identical.

The brightness temperature difference between the two channels (Fig. 1C-29b) reveals regions of thin cirrus (bright white) better than either of the raw channels (Figs. 1C-28a and 29a). Of particular interest are the contrails in Fig. 1C-29b. These were barely detectable in the raw images. The contrails show up well because they consist of very thin cirrus, which has large brightness temperature differences in the two channels.

1C-28a. NOAA-9 Channel 4 (10.8 μm), 2223 GMT, 1 May 1985.

1C-29a. NOAA-9 Channel 5 (11.8 μm), 2223 GMT, 1 May 1985.

1C-29b. Brightness temperature difference based on Figs. 1C-28a and 29a (Channel 4 and Channel 5), 2223 GMT, 1 May 1985.

1C-30b. NOAA-9 Channel 5 (11.8 μm), 0719 GMT, 13 August 1989.

1C-30c. Brightness temperature difference based on Figs. 1C-30a and 30b (Channel 4 and Channel 5), 0719 GMT, 13 August 1989.

22. Thin Cirrus Associated with a Pacific Typhoon

The Channel 4 image (Fig. 1C-30a) shows a West Pacific typhoon, which has recently moved across the Philippines. Having weakened over land, the storm's eye is mostly covered with cirrus and is difficult to identify well. The Channel 5 image (Fig. 1C-30b) has a similar appearance. The difference image (4 minus 5) (Fig. 1C-30c) shows the eye unambiguously because thin cirrus has a large positive difference in the two channels. This technique is useful for locating cirrus-covered eyes.

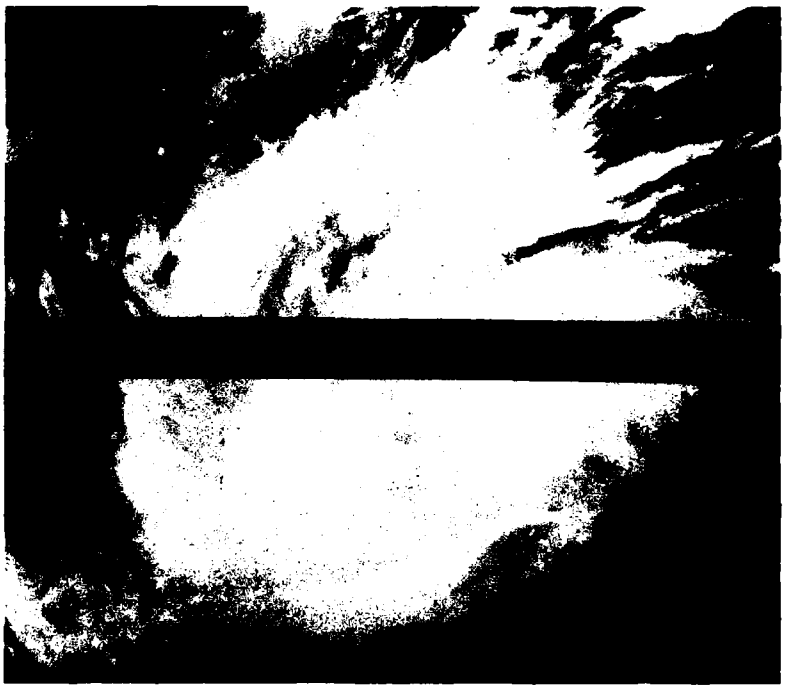

1C-30a. NOAA-9 Channel 4 (10.8 μm), 0719 GMT, 13 August 1989.

23. Multichannel Sea Surface Temperature

A large section of the eastern Pacific Ocean is shown for Channel 2 (Fig. 1C-31a), Channel 4 (Fig. 1C-31b), and Channel 5 (Fig. 1C-31c). Figure 1C-31d shows the sea surface temperature analysis based on the previous three images. The sea surface temperature algorithm used Channel 2 for cloud screening and Channels 4 and 5 for temperature estimates. In the sea surface temperature analysis (Fig. 1C-31d), the black areas represent land or regions that are cloud covered and where, therefore, sea surface temperature could not be derived. The narrow curving boundaries that appear in the image are artifacts of the cloud screening process.

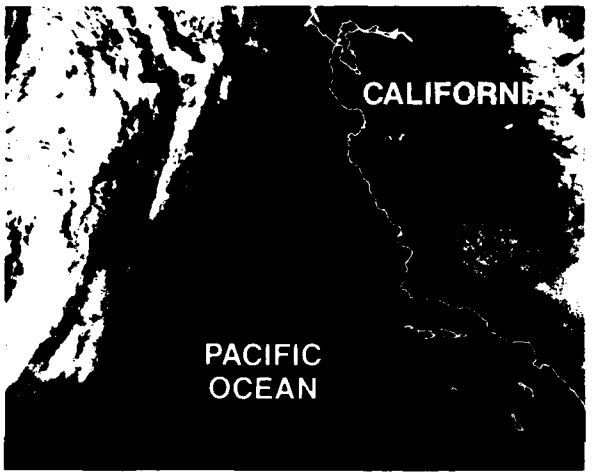

1C-31a. NOAA-11 Channel 2 (0.86 μm), 2139 GMT, 30 November 1989.

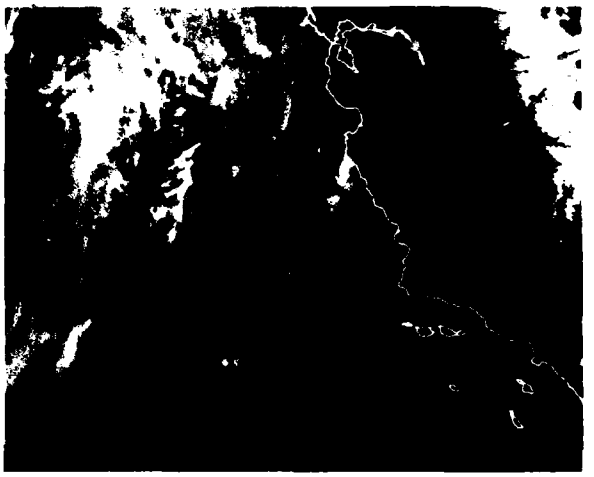

1C-31b. NOAA-11 Channel 4 (10.8 μm), 2139 GMT, 30 November 1989.

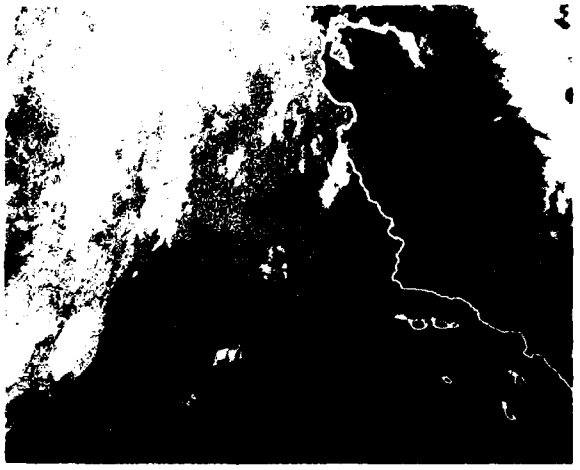

1C-31c. NOAA-11 Channel 5 (11.8 μm), 2139 GMT, 30 November 1989.

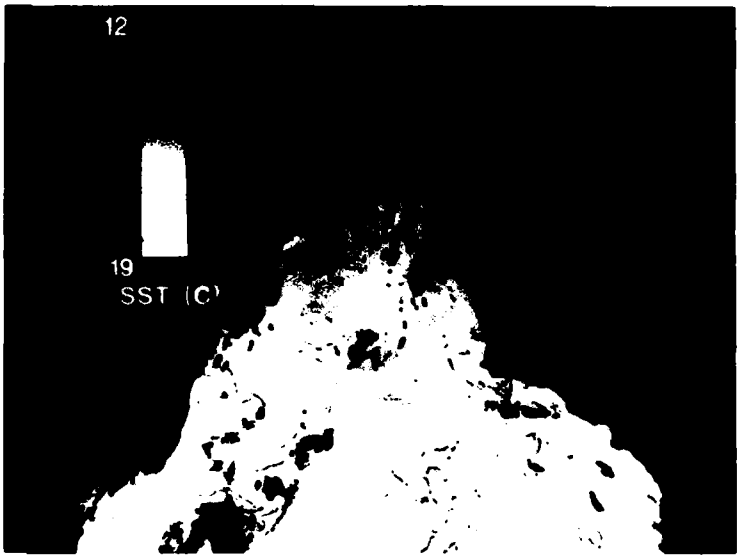

1C-31d. Sea surface temperature based on Figs 1C-31a-31c, 2139 GMT, 30 November 1989.

Meteor

Since 1969, the U.S.S.R. has been operating a polar orbiting satellite system, Meteor. Meteor 1 is the experimental phase of the system. A few of these satellites are still active near the Soviet Union, but they are not in regular service. The Meteor 2 type spacecraft are providing fairly regular service to ground receiving stations of the Automatic Picture Transmission (APT) class since 1976, with three spacecraft being active—Meteor 2-7 in an evening pass (2109 GMT descending node), Meteor 2-8 in an evening pass (1905 GMT ascending node), and Meteor 2-9 in an afternoon pass (1214 GMT ascending node). The satellites are in near-polar orbits at an altitude of 900 km with an inclination of 81°. The orbital period of revolution for Meteor 2 is approximately 102 minutes, which produces 14.1 revolutions per day.

The APT video product obtained from the Meteor 2 spacecraft is similar to that of the TIROS N series of U.S. spacecraft, in that the APT data are output at a rate of 120 lines per minute. Over the U.S.S.R., data is transmitted directly to only three ground receiving centers: Moscow, Novosibirsk, and Khabarovsk. When out of communication range, data is recorded and stored on-board until the satellite passes over one of the receiving centers, where it is processed, reduced, and sent to the hydrometeorological center in Moscow for analysis and distribution to forecast centers (Stoldt, 1973).

The following is a brief summary of current Soviet metsat activity, provided in a recent memo by Dr. Grant A. Zehr, as monitored by reports and observations by amateurs in North America and Europe:

References

Stoldt, Norman W., and Peter J. Havanac, 1973: Compendium of meteorological satellites and instrumentation, NASA, Greenbelt, Md. pp. 301-359.

Zehr, Grant A., personal communication, 6 May 1983.

Current Soviet Metsat Activity—30 April 1983

Meteor 2 series

Spacecraft in the Meteor 2 series have provided APT service over the United States on a fairly regular basis recently. It appears that Meteor 2-7, 2-8, and 2-9 are the currently active spacecraft in this series. Amateurs have received imagery from these spacecraft since about 1976.

The orbit of these spacecraft is antegrade (angle of inclination is 81.2°) and not sun-synchronous. The orbital period is about 102.3 minutes. Amateur measurements of the orbital period suggest that it is a bit longer, perhaps 102.5 minutes.

Meteor 2 satellites are now using the frequencies of 137.3 and 137.85 MHz. In the past, 137.4 MHz has also been used. At the present time there are two satellites transmitting on 137.3 MHz (Meteor 2-7 and 2-9). Meteor 2-8 is currently active on 137.85 MHz. The satellites now transmitting on 137.3 MHz have similar orbits and follow each other by about 12 hours.

The video product is similar to that of the TIROS N series of U.S. spacecraft. The scan rate is 120 lines per minute which is compatible with the TIROS N product. The video signal is carried as an amplitude modulation of the audio subcarrier (similar to TIROS N APT). The frequency of this subcarrier is near 2400 Hz, but has been measured and is clearly not exactly 2400 Hz. At times, the frequency of this subcarrier has seemed to drift. The subcarrier does seem to fit within the simple bandpass filters centered on 2400 Hz which are used by many amateurs. An important difference lies in the fact that the subcarrier seems to disappear during the transmission of the synchronizing pulses. This means that systems which depend on locking on the 2400 Hz subcarrier will require modification to provide an alternate 2400 Hz signal. Phase lock detection systems may not work properly, either.

In contrast to the TIROS N series, there is only one product of the image received. This appears to be in the visible light spectrum, but at times some of the characteristics suggest an infrared image. The published spectrum of the visible image is 0.5 to 0.7 μm. This spectral range is similar to Channel 1 of the TIROS N series (0.55 to 0.90 μm). Amateurs have observed that the image from the Meteor 2 spacecraft tends to show a poor delineation of the land-water boundaries. This was also true of NOAA 7 when it was transmitting Channel 1 video for the visible portion of the APT signal. At this time, the NOAA 7 spacecraft has been switched to Channel 2 (0.725 to 1.1 μm) and this spectral range does provide much improved land-water contrast. Probably the published spectral range is correct for the Meteor 2 spacecraft now in service.

The Meteor 2 image does provide some advantages compared to the TIROS N image. There is excellent resolution of snow cover during the winter. Snow cover analysis is somewhat easier with the Meteor image. In addition, the resolution of the Meteor 2 image is somewhat greater (1 km) than the TIROS N APT signal (4 km).

Some amateurs have reported a very slow line rate infrared image being transmitted from these satellites during nighttime passes. I have heard this signal on several occasions, but it does not seem to be regularly available over the U.S.

Like the TIROS N APT, the Meteor image does not provide any gridding to orient the user. This fact, combined with the rather poor demarcation of the land-water boundaries, means that in some cases the

Meteor 2 image may be difficult to orient with respect to land masses or other geographical features (compared to the TIROS N image).

It must be remembered that the Meteor 2 satellites are at times switched off and may be unavailable even though the orbital predictions have been correctly prepared. In addition, the satellites appear to turn off their APT signal when the satellite passes into darkness. This may account for some unexpected results during the winter months as the satellites suddenly begin transmitting with a loud signal (being at closer range than predicted). The signal will also disappear abruptly as the spacecraft passes from light into darkness. This spacecraft characteristic complicates the gathering of data for orbital prediction.

As previously noted, these spacecraft have provided fairly regular service during the past six years. Having demonstrated the ability to be switched on and off, it is assumed that this service could be interrupted at any time.

Meteor 1 series

Spacecraft in the Meteor 1 series have been monitored by amateurs in North America on an irregular basis during the past five years. These spacecraft appear to serve a sort of experimental or testing function. They are not in regular service on a predictible basis.

These spacecraft are in a low, sun-synchronous orbit with an orbital period of about 97.5 minutes. This is a retrograde orbit with an angle of inclination of about 97°. It is believed that these spacecraft are the ones which have been heard on 137.15 MHz. Early in 1982 amateurs in the U.S. monitored similar spacecraft on 137.13 MHz. During the latter part of 1982 and early in 1983, transmissions from a Meteor 1 type spacecraft were monitored by Italian amateur radio operators. The frequency of these transmissions was 137.12 MHz. The orbital characteristics of the spacecraft on these frequencies coincide with those of the Meteor 1 series. A review of the NASA Satellite Situation Report does not suggest any other candidate which might be responsible for these transmissions. The spacecraft monitored most recently in Italy on 137.12 MHz has been identified as Meteor 1-30 using orbital data generated on an Apple II microcomputer.

The image from this series of spacecraft is also transmitted as an APT signal. The video is carried as an amplitude modulated audio subcarrier, similar to the TIROS N APT signal. The line rate for this image is 240 lines per minute. The synchronization segment of the scan line contains a four digit number and a gray scale. The significance of these numbers has not been learned.

The image from the Meteor 1 spacecraft shows panoramic distortion near the edge of the image. This contrasts with the TIROS N image which has a corrected image to eliminate panoramic distortion. The Meteor 2 image has little or no panoramic distortion.

The Meteor 1 spacecraft provide the best resolution of any APT signal yet available. Because of this, the satellites have been favorites among the amateur community.

Unfortunately, this satellite does not transmit regularly over North America. Signals were received in February and March of 1982 by at least six amateurs in the U.S. and Canada. The frequency was 137.13 MHz although some amateurs felt the correct frequency was 137.14 MHz. The satellite was observed in a north to south sun-synchronous orbit passing over North America with an overhead pass at about 10:30 a.m. local time. It was frequently transmitting an APT signal on Saturday mornings (local time).

Like the Meteor 2 series, no grid lines are available to orient the user with respect to land masses. This is not a serious handicap in the case of Meteor 1, however, since the imagery provides superior resolution of land-water boundaries. It is usually easy to orient the image with respect to land masses.